Deltares

Scenario studies on potential ecosystem effects in future offshore wind farms in the North Sea

Scenario studies on potential ecosystem effects in future offshore wind farms in the North Sea

Author(s)
Firmijn Zijl
Stendert Laan
Leo Leummens
Tammo Zijlker
Thijs van Kessel
Vincent van Zelst
Luka Jaksic
Lauriane Vilmin
Lisa Schneider
Luca van Duren

Scenario studies on potential ecosystem effects in future offshore wind farms in the North Sea

Opdrachtgever	Rijkswaterstaat Water, Verkeer en Leefomgeving
Contactpersoon	mevrouw I. van Splunder
Referenties	
Trefwoorden	Offshore wind; ecosystem effects; scenarios, Wozep,

Documentgegevens	
Versie	0.4
Datum	23-06-2023
Projectnummer	11208071-001
Document ID	11208071-001-ZKS-0010
Pagina's	84
Classificatie	
Status	final

Auteur(s)		
	Firmijn Zijl	
	Stendert Laan	
	Leo Leummens	
	Tammo Zijlker	
	Thijs van Kessel	
	Vincent van Zelst	
	Luka Jaksic	
	Lauriane Vilmin	
	Lisa Schneider	
	Luca van Duren	

Gebruik van deze tabel is voor de controle van de juiste uitvoering door Deltares van de opdracht. Ieder ander klantgebruik en externe verspreiding is niet toegestaan.

Doc. Versie	Auteur	Controle	Akkoord
0.1	Firmijn Zijl	Peter Herman	Toon Segeren
	Stendert Laan		
	Leo Leummens		
	Tammo Zijlker		
	Thijs van Kessel		
	Vincent van Zelst		
	Luka Jaksic		
	Lauriane Vilmin		
	Lisa Schneider		
	Luca van Duren		

Summary

Wozep (the *Wind Op Zee Ecologisch Programma*) is an integrated research programme to reduce the knowledge gaps regarding the possible negative environmental effects of offshore wind farms (OWFs) on the North Sea.

In a first study published in 2021 it was shown that ecosystem effects of large-scale offshore wind farms can be profound (Van Duren et al. 2021). These effects are due to interactions of the wind turbines with the ambient flow, resulting in changed currents, stratification, changes in fine sediment dynamics and consequently changes in primary production. The 2021 study was the first project where the full range of the DCSM-FM model with fine sediment and water quality and ecology modelling were used in an applied project. The modelling suite showed its potential, but in this first exercise there were also a few teething problems highlighted. Many of these were solved in a follow-up study in 2022 (Van Kessel et al. 2022). The current report details further improvements in parameterisation of certain parameters, significantly improving model performance.

The first modelling study (Van Duren et al. 2021) had identified a potential decrease of fine sediment transport to the Wadden Sea. This was with the first version of the model that showed a significant bias in absolute suspended particulate matter (SPM) concentrations. This effect was now further investigated with the latest version of the model. The present study confirmed the decrease in mud fluxes towards the Wadden Sea. It appears that the changes in alongshore transports are a consequence of the larger scale changes in hydrodynamics of the Rhine region of freshwater influence (ROFI), affected by the combined presence of wind farms in the southern North Sea.

The main part of the current study comprises the results of two new scenarios. One is relatively close to the expectations of wind farm locations in the Dutch North Sea around 2040, the second one is a more extreme upscaling scenario, including wind farms that may not be developed due to user conflicts and a few areas that are currently not in the set of official wind search areas. The new scenarios did not give rise to significant changes in the way we currently think different parts of the North Sea will respond to the presence of wind farms. However, particularly the use of the now fully coupled model indicated a more severe effect of increased fine sediment concentrations in the top layers of the water, resulting in more areas showing a decrease in primary production due to limited light availability. The presence of mussels on the turbine monopiles had some effect on primary production, but limited effect on chlorophyll concentrations. The impact of mussels and other grazers needs further investigation before we can draw quantitative conclusions about their impact.

Finally, the report describes planned relevant follow-up research, particularly efforts on gaining insight in the knock-on effect of changes at the base of the food web on higher trophic levels.

Content

1 Introduction

1.1 General context: Wozep

Wozep (the *Wind Op Zee Ecologisch Programma*) is an integrated research programme to reduce the knowledge gaps regarding the possible negative environmental effects of offshore wind farms (OWFs) on the North Sea.

This current report describes results of a follow-up study on ecosystem effects of offshore wind. In a first study published last year (Van Duren et al. 2021) it was shown that ecosystem effects of large-scale offshore wind can be profound. These effects are due to interactions of the wind turbines with the ambient flow, resulting in changes in currents spatio-temporal patterns, stratification, changes in fine sediment dynamics and consequently changes in primary production. This study (Van Duren et al. 2021) was the first project where the full range of the DCSM-FM model with fine sediment and water quality and ecology modelling were used in an applied project. This study was followed in 2022 with a report that tackled a number of the teething problems that were encountered in the first modelling work. The current study details results of further model improvements as well as additional scenario studies.

1.2 Approach

The general approach within the Wozep projects on ecosystem effects is two-tiered, with a bottom-up and a top-down line. The top-down approach estimates the vulnerability of several species (birds, marine mammals) with a high conservation status for changes in environmental conditions that can be caused by large-scale development scenarios for offshore wind. This has resulted in recommendations to tackle these questions in future with Individual Based Models (Van der Meer and Aarts 2021).
The bottom-up approach project applies a state-of-the-art suite of numerical models to assess potential changes in hydrodynamics, sediment dynamics, light attenuation, primary production and secondary production (Zijl et al. 2021). Three scenarios were assessed:

- a reference scenario without any wind farms
- a “2020” scenario with the currently present wind farms
- a hypothetical future scenario with a large upscaling of offshore wind farms in the southern North Sea.

The first modelling study indicated that different regions of the North Sea responded differently to the implementation of offshore wind. Relaxation of stratification and changes in fine sediment dynamics caused increases or decreases in primary production, depending on depth, bed composition and stratification regime of specific areas (Van Duren et al. 2021). This was the first application of the full suite of models. In follow up work (Van Kessel et al. 2022), a number of technical issues with the model were fixed, now allowing fully coupled model runs as well as incorporating the growth of mussels on the turbine poles. In this report also significant improvements were made in the fine sediment modelling reducing the earlier bias in predicting SPM concentrations that were too low. The overall conclusions of the earlier report (Van Duren et al. 2021) did not change.

1.3 Research questions this report

getting
The bottom-up model has undergone some further improvements and calibrations. The primary aim of this part of the research is to apply the improved model to two scenarios that

contain the currently known search areas for offshore wind. In addition, a second aim was to assess the contribution of individual wind farms in the Dutch coastal zone to changes in the long-shore fine sediment transport. The latter was identified in Van Zijl et al. (2021) as a potentially important factor for transport of fine sediment to the Wadden Sea.

The two new upscaling scenarios are closer to likely future lay-outs, but still contain wind farm locations that may never be developed. The main question remains at which level of upscaling we can expect effects that are so large that we risk significant changes in the North Sea food web at ecosystem level. The new scenarios are steps towards gaining more fundamental insight in the relative impact of upscaling.

1.4 Report lay-out

Chapter 2 details further methodological changes and calibration of parameters in the SPM and ecological modelling. In Chapter 3 the impact of wind farms on transport of fine sediment along the Holland coast and ultimately towards the Wadden Sea is investigated. This chapter also aims to assess which of the wind farms in the Holland Coast contribute most to changes in transport. Chapter 4 gives the results of the two new scenario studies. The final chapter synthesises the conclusions and recommends further steps.

2 Model validation and calibration

2.1 Fine sediment dynamics

2.1.1 Background concentration

In the previous Wozep report by Van Kessel et al. (2022), background concentrations of suspended sediment were calibrated and validated. The present study makes use of a newer D-Flow FM software version (Zijl and Laan 2022) and in addition, two variables that influence the sediment dynamics are updated (*Table 2.1*). In this section it is verified that the resulting fine sediment fields remain the same.

The reason for this update is that in the newer software version root-mean-square (rms) wave height instead of significant wave height is used to compute wave-induced bed shear stress. As rms wave height is a factor of $\sqrt{2}$ smaller than significant wave height, the resulting bed shear stress is a factor 2 smaller. To compensate for this, the Nikuradse bed roughness has been increased to maintain the (calibrated) wave-induced resuspension flux at the same magnitude.

Another reason is that the coarse model grid does not provide space covering information for the fine model grid, as some areas in the Wadden Sea and Western Scheldt fall outside the coarse grid model domain but within the fine grid model domain. The way in which these missing data were supplemented has been improved by using bed composition data from detailed Wadden Sea and Western Scheldt fine sediment models.

Table 2.1 New model settings compared to Wozep midterm report by Van Kessel et al. (2022) The initial bed samples are improved in the parts of the domain that only exist in the current, fine (0.5nm) model and not the older, coarse (4nm) model schematization.

Adapted variable	**Location**	**Original value**	**New value**
Wave friction coefficient: Nikuradse ks, used in (Swart 1974)	Entire domain, spatially uniform	0.001 m	0.005 m
Bed samples: Initial mass IM1S2, IM2S2	Part of the *Wadden Sea* that only exists in the fine (0.5nm) model and not in the coarse (4nm) model	See Van Kessel et al.(2022)	Based on Dutch Wadden Sea model (Vroom et al. 2020)
	Part of the *Scheldt estuary* that only exists in the fine (0.5nm) model and not in the coarse (4nm) model		Based on ZUNO-DD (Cronin et al. 2013)

Figure 2.1, Figure 2.2 and Figure 2.3 show results with the new settings in comparison with CEFAS earth observation data (with a spatial resolution of 0.015°longtitude and 0.01°latitude. Also, the difference between the old model (with the original settings as explained in *Table 2.1*) and CEFAS data is shown. Figure 2.1 shows year-averaged SPM values, Figure 2.2 the average for June and Figure 2.3 the average for December. Based on these comparisons, it is concluded that changes in the model performance are very minor and that the model validation discussed in the midterm report (Van Kessel et al., 2022) is still valid.

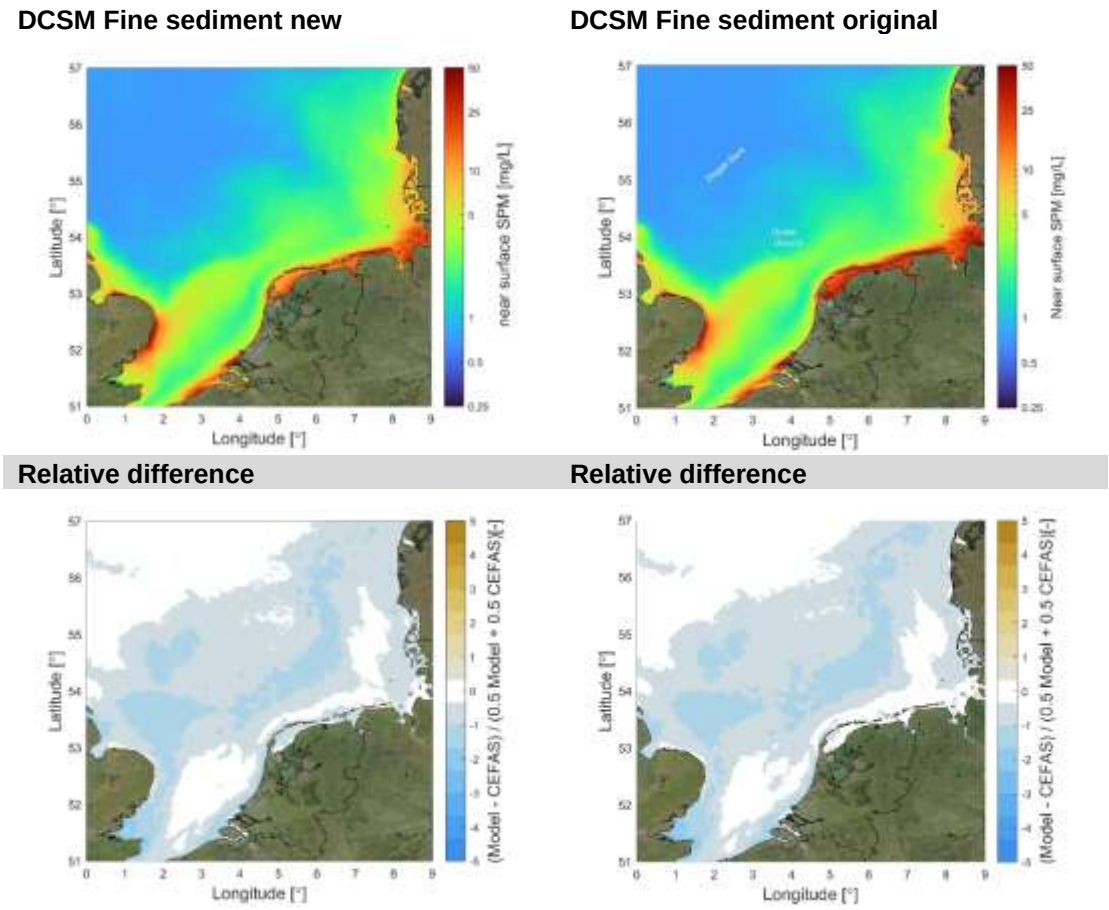

Figure 2.1 Year-averaged, modelled spatial distribution of suspended particle matter (SPM) compared to CEFAS EO data for the year 2007 Top panels: absolute modelled SPM concentration (mg/l). Bottompanels: relative difference with CEFAS data.

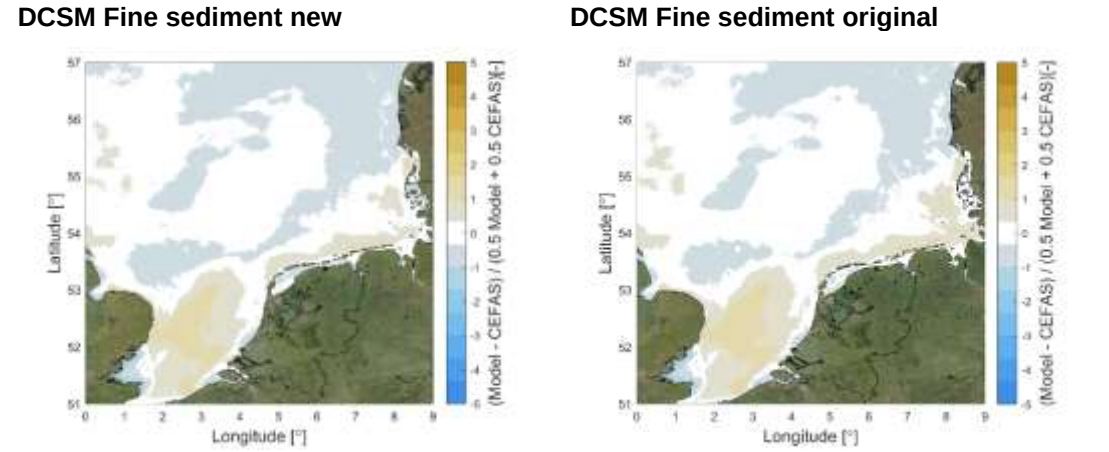

Figure 2.2 Modelled spatial distribution of suspended particle matter (SPM) compared to CEFAS EO data, average values for June 2007.

DCSM Fine sediment new **DCSM Fine sediment original**

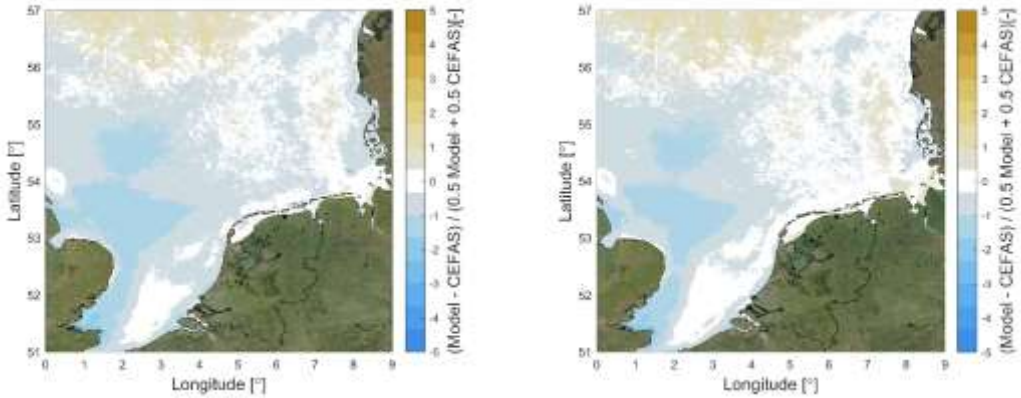

Figure 2.3 Modelled spatial distribution of suspended particle matter (SPM) compared to CEFAS EO data, average values for December 2007.

2.1.2 OWF impacts validation

For the validation of computed OWF impacts on fine sediments (and other parameters), measurements are required in- and outside OWFs. Figure 2.4 and Figure 2.5 show the locations of field measurements with ships and fixed frames in and around an OWF close to the sea border between Belgium and the Netherlands. These measurements have been carried out in June 2022 and have not yet been fully analysed. These data have not been acquired by Deltares but have kindly been provided by the Flanders Marine Institute (VLIZ) and the research project OUTFLOW (Hendriks *et al*, 2022). A short overview of these data is provided in *Table 2-2*. Only data inside the OWF have been disclosed, reference data outside the area of influence of the OWF are not yet available. Also, hydrodynamic and wave forcing data for the measurement period to steer the fine sediment model are not yet available. However, in the available years of hydrodynamic forcing, a period has been carefully selected for which tide, wind and wave conditions are similar.

What is already possible now:

- Showing and discussing observations on vertical gradients of salinity, temperature and SPM inside the OWF;
- Comparing of model results with these monitoring data: are the modelled levels and gradients consistent with the observations?

What will be possible in the future:

- Analysis of differences upstream and downstream of the OWF with regard to salinity , temperature and SPM levels and gradients;
- Direct comparison of model and observations for the same hydrodynamic forcing (i.e. for same period);
- Comparison of the modelled difference with the observed difference.

Figure 2.6 shows the observed and computed salinity, temperature and suspended sediment concentration (SSC) gradients in the OWF. Overall, there is very little stratification both in the observations and the model, but:

- Near the surface the observations show small temperature and salinity gradients, as relatively fresh surface water from the Rhine-Scheldt discharge is not yet fully mixed. The model does not capture this, possibly due to insufficient grid resolution.
- Spatial gradients are substantial, which the model cannot capture at this small scale (as all observation points fall within the same computational cell).

- Model output with high temporal resolution is not (yet) available for the same time and position as the observations, resulting in extrapolation errors.
- The optical backscatter sensor (OBS) calibration for conversion from Nephelometric Turbidity Unit (NTU) to mass concentration is not yet available. This factor has been assumed to be 2 (i.e. 1 NTU = 2 mg/l) based on earlier observations in this area, but this factor may vary in time and space.

Therefore, firm conclusions cannot yet be drawn. For a detailed comparison it is recommended to refine the model grid locally, rerun it for the period in which the field campaign took place and also include data outside OWF (when available).

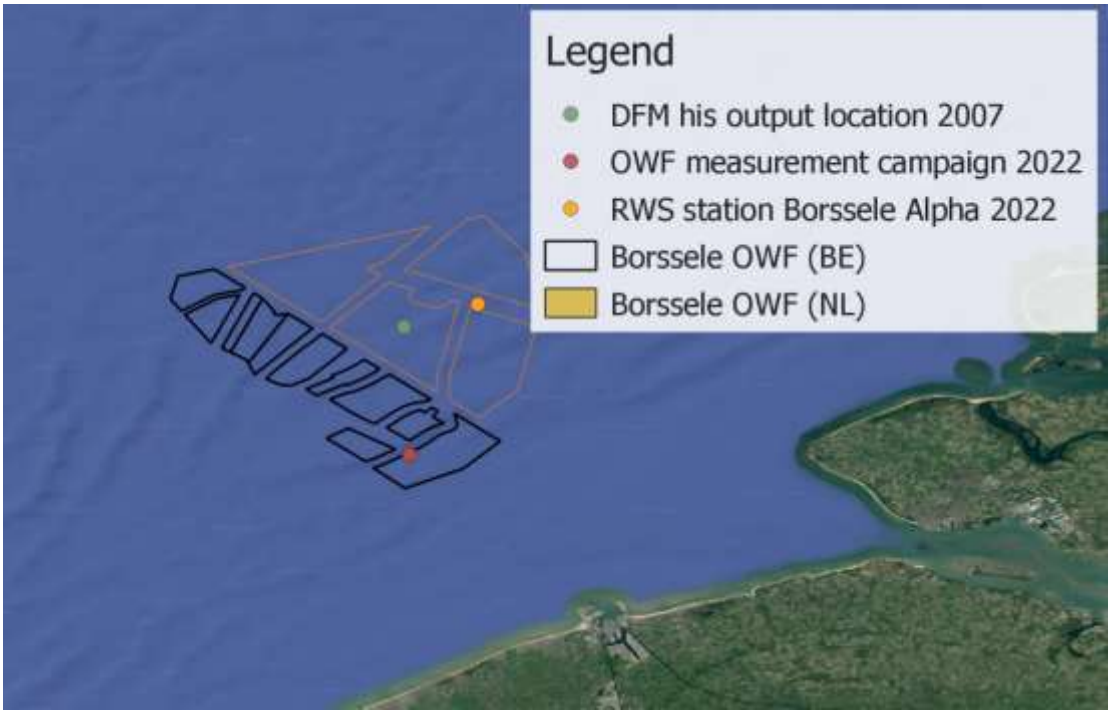

Figure 2.4 Flux measurements carried out in and around OWF at the sea border between Belgium and the Netherlands in June 2022. For a zoom in and details of OWF locations see Figure 2.5.

Table 2-2 Short overview of OWF impact field campaign in June 2022.

14hr transect (sediment budget analysis)		**Single turbine analysis (detailed wake analysis).**		
Shipboard • **ADCP[1]** • **CTD[2] surface** • **CTD cast** • **OBS cast**	Sampling • SPM, Pigments, POC/PON[3]	Shipboard measurement (downstream monopile) • ADCP zig-zag transect • CTD surface water • CTD cast • OBS cast	Measurement frame (upstream monopile) • ADCP • CTD • Sonar Sea bed	Sampling • Sediment samples • Water samples during OBS casts

[1] Acoustic Doppler Current Profiler
[2] Conductivity, Temperature, Density
[3] Particulate Organic Carbon/Nitrogen

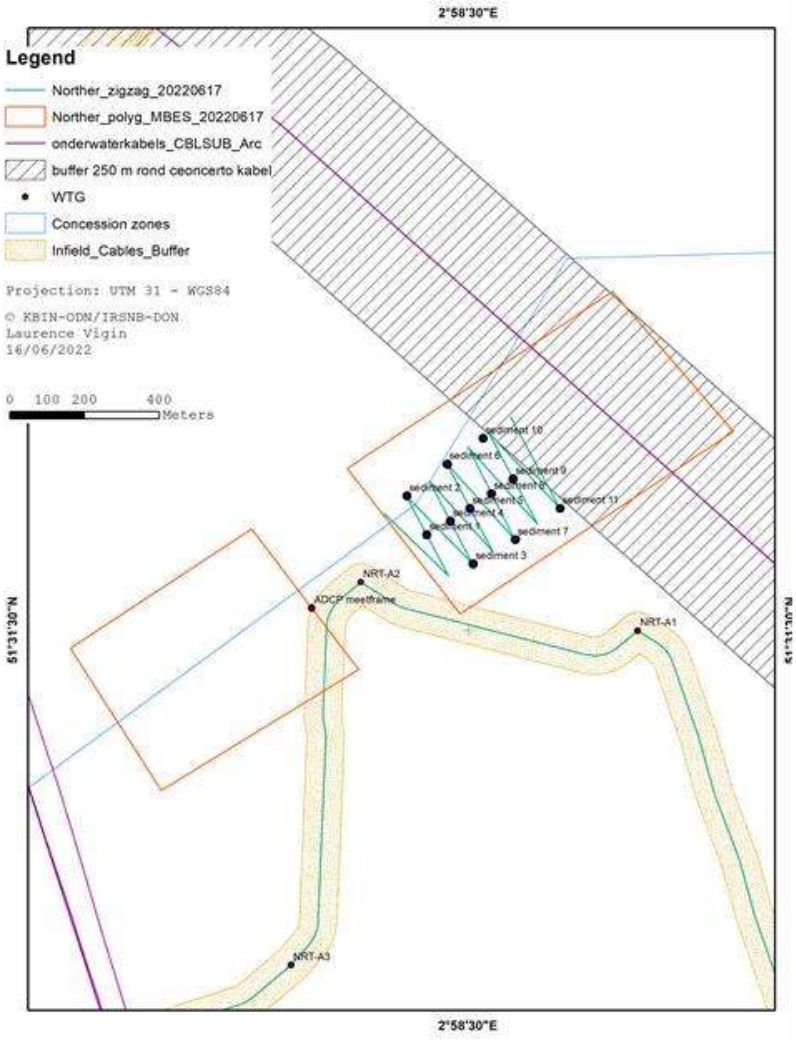

Figure 2.5 Single turbine measurements in the wake of a pile near the sea border between Belgium and the Netherlands in June 2022 (Hendriks et al. 2022).

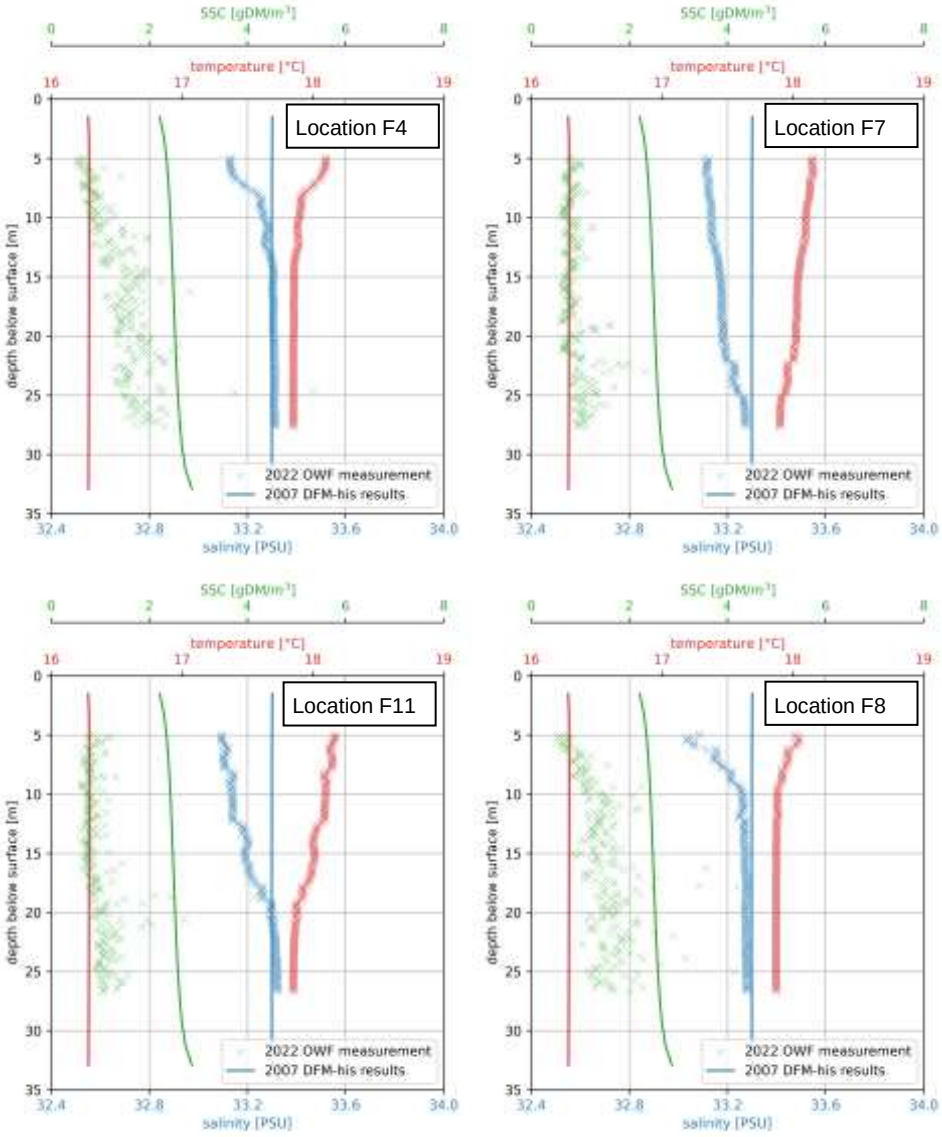

Figure 2.6 Comparison between observed (×) and computed (lines) salinity, temperature and SSC (=TIM, SPM) gradients in the OWF. Observation locations as indicated in Figure 2.5. Time of observations: 27 June 2022, 13:00 – 15:30. Model output 27 June, 2007, 15:00 (Hendriks et al. 2022).

2.2 Ecology

2.2.1 Model inspection and calibration

Even though first results of the coupled sediment-ecological model were promising (Van Kessel et al. 2022), the model needed further calibration to constitute a reliable tool for the study of ecological effects of OWFs. One of the main shortcomings of the previous version of the coupled model was that it overestimates chlorophyll-a concentrations over the entire growing season and predicted the spring bloom too early in the year.

In this report, a deeper analysis of the coupled model results was carried out, before calibrating the water quality component. This calibration phase was performed using the coarse grid to limit computation times in that phase of the work. The new setup was then

applied to the fine grid coupled sediment and water quality model and compared to the initial uncoupled water quality model. These runs were carried out for the year 2007.

As in previous reports, the model results were compared to measurements at the MWTL stations along the Walcheren (2, 20 and 70 km from the coast), Noordwijk (2, 10, 20 and 70 km), Terschelling (10, 100, 135, 175 and 235 km) and Rottumerplaat (3, 50 and 70 km) transects. Stations Walcheren 2 km, Noordwijk 2 km and Rottumerplaat 3 km are outside of the coarse model grid and are therefore not used in the model calibration phase.

2.2.1.1 Initial coupled model inspection

The full coupling of sediment, water quality and ecology processes led to an improvement of the simulated total N (TN) concentrations, most likely due to an improvement of the nutrient burial processes. The speciation of nitrogen through the year was however not fully captured by the model, with overestimated summer dissolved inorganic N (DIN) concentrations at several observation stations. This is most likely the consequence of an overestimation of nitrogen re-mineralization rates, or the lack of less labile organic matter form in the model. Other model drawbacks were that it clearly overestimated chlorophyll-a concentrations during the entire growing season at all monitoring stations, and that the spring bloom occurred too early (by ~1 month). The too high mineralization of nutrients, leading to increased available forms, could explain the overestimation of the phytoplankton biomass. However, the delay in the spring bloom might have other causes, for example linked to the effects of light climate and/or temperature on phytoplankton growth. The light climate (extinction coefficient) seems overall well represented by the model during the growing season, even though model results seem to have a lower variability than the observations (see Figure 2.7). Winter extinction values might however be underestimated, even though the number of observations to confirm this is limited.

Finally, the initial version of the coupled sediment-ecological model overestimates inorganic phosphorus (PO4) uptake and underestimates nitrogen uptake at most observation locations during the growing season, as did the uncoupled water quality model (Van Kessel et al. 2022). This is most likely linked to phytoplankton internal ratios.

To visualise the overall performance of the model for different measured water quality variables, target diagrams of chlorophyll-a, extinction, DIN, PO4, TN, O_2, particulate organic C (POC) and particulate organic N (PON) were plotted at all monitoring stations (Figure 2.2). These represent two quantitative skill metrics: the model bias (i.e. average difference between simulated and measured values) and the unbiased Root-Mean-Square Error (uRMSE). For each variable and at each station these metrics are calculated using all available measurements and the corresponding simulated values at the date of the measurements.

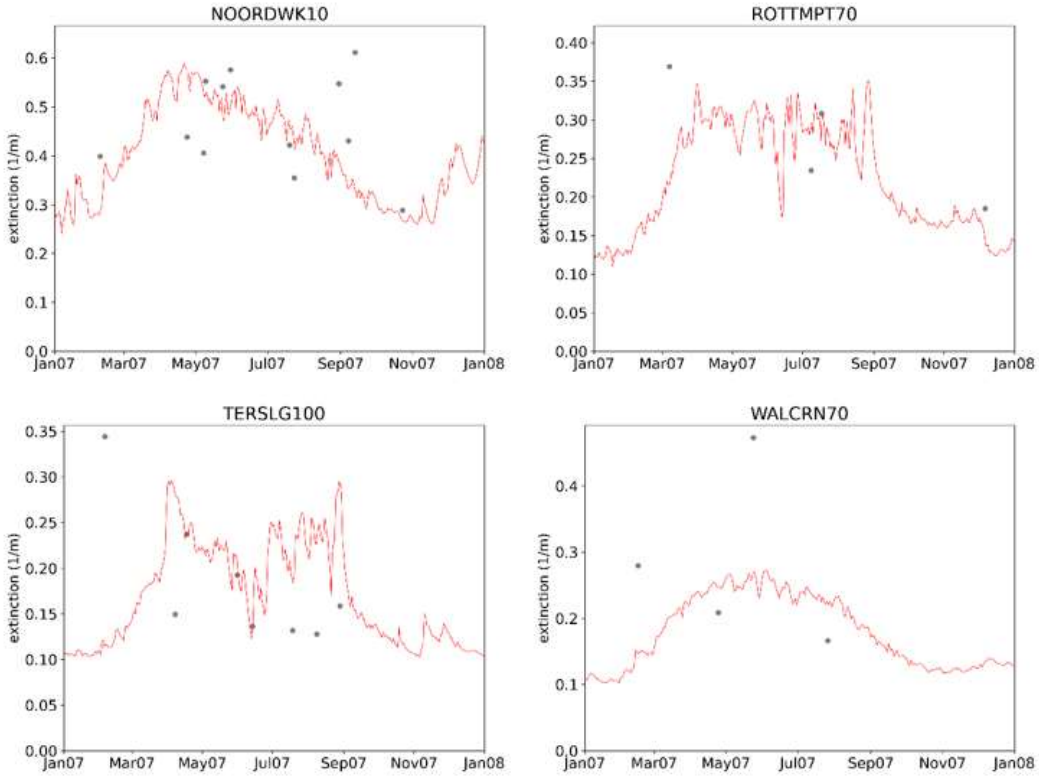

Figure 2.7 Examples of extinction model-observation comparisons at four MWTL monitoring stations for the initial coupled sediment-ecology model (Van Kessel et al. 2022). Red lines represent model results; grey dots indicate measurements.

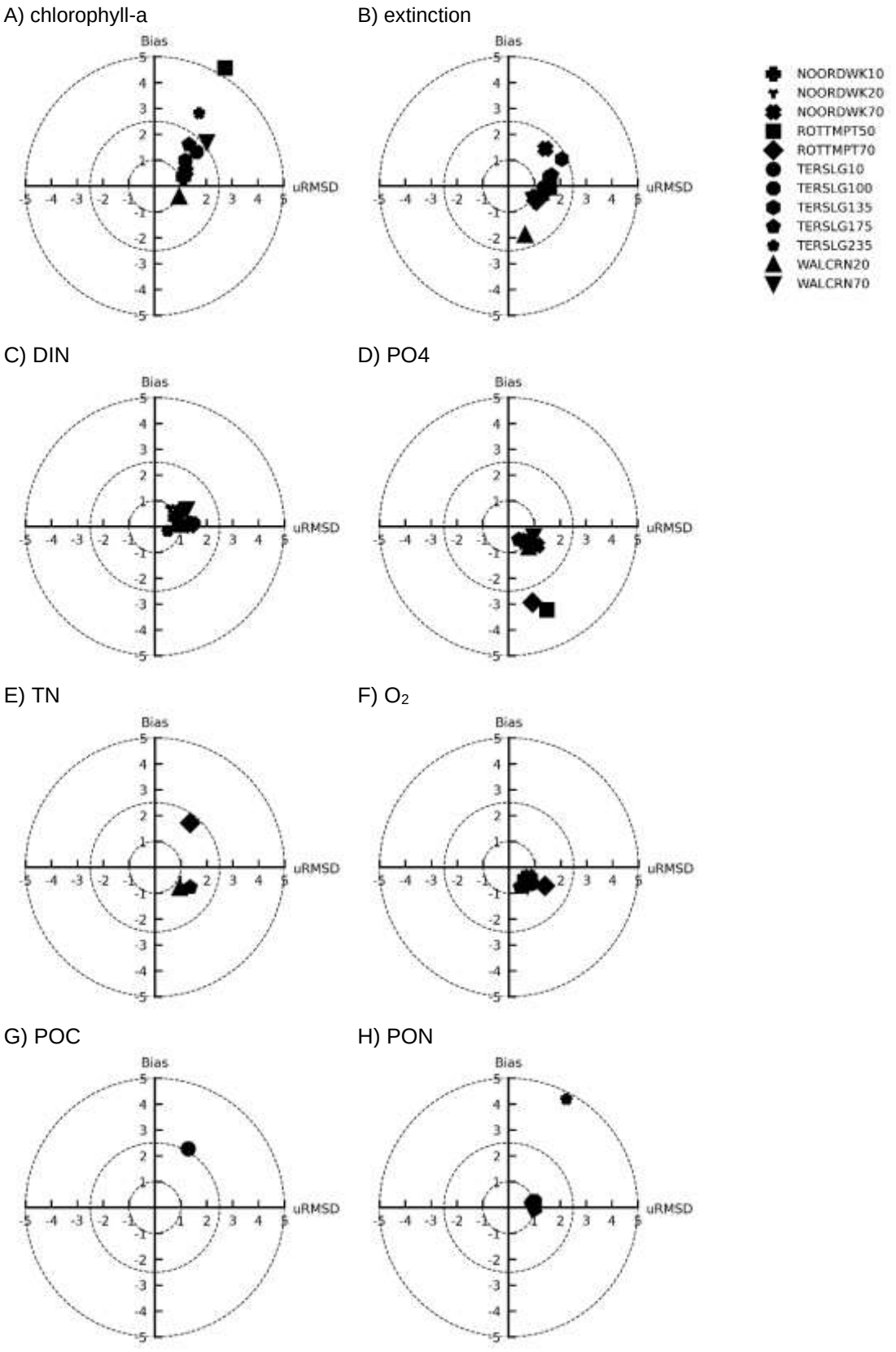

Figure 2.8 Target diagrams of A) chlorophyll-a, B) extinction, C) DIN, D) PO4, E) TN, F) O_2, G) POC and H) PON at all monitoring stations for the year 2007. Note that the marker for DIN at Rottumerplaat 50km and the markers for chlorophyll-a, DIN and POC at Rottumerplaat 70km, fall outside of the ranges of the plot.

2.2.1.2 Water quality model calibration

Based on the analysis of the initial coupled sediment-ecological model run, the calibration was carried out in 3 steps (Table 2.3):

1) addition of a dissolved, less labile, organic matter fraction,
2) modification of the temperature parameter for maximum primary production,
3) modification of phytoplankton N:C and P:C ratios.

Table 2.3 Description of the water quality calibration runs

Calibration run	Description
RunC_0	Coarse run, reported in interim report (Van Kessel et al. 2022)
RunC_1	RunC_0 with addition of dissolved organic matter
RunC_2	RunC_1 with modified temperature parameters for primary production
RunC_3	RunC_2 with modified N:C and P:C ratios is phytoplankton

For the calibration phase, we use once again target diagrams to visualise overall model performance. To limit the number of plots, for each run, we plot the overall performance of the different measured variables at all available monitoring locations on the same diagram (Figure 2.9).

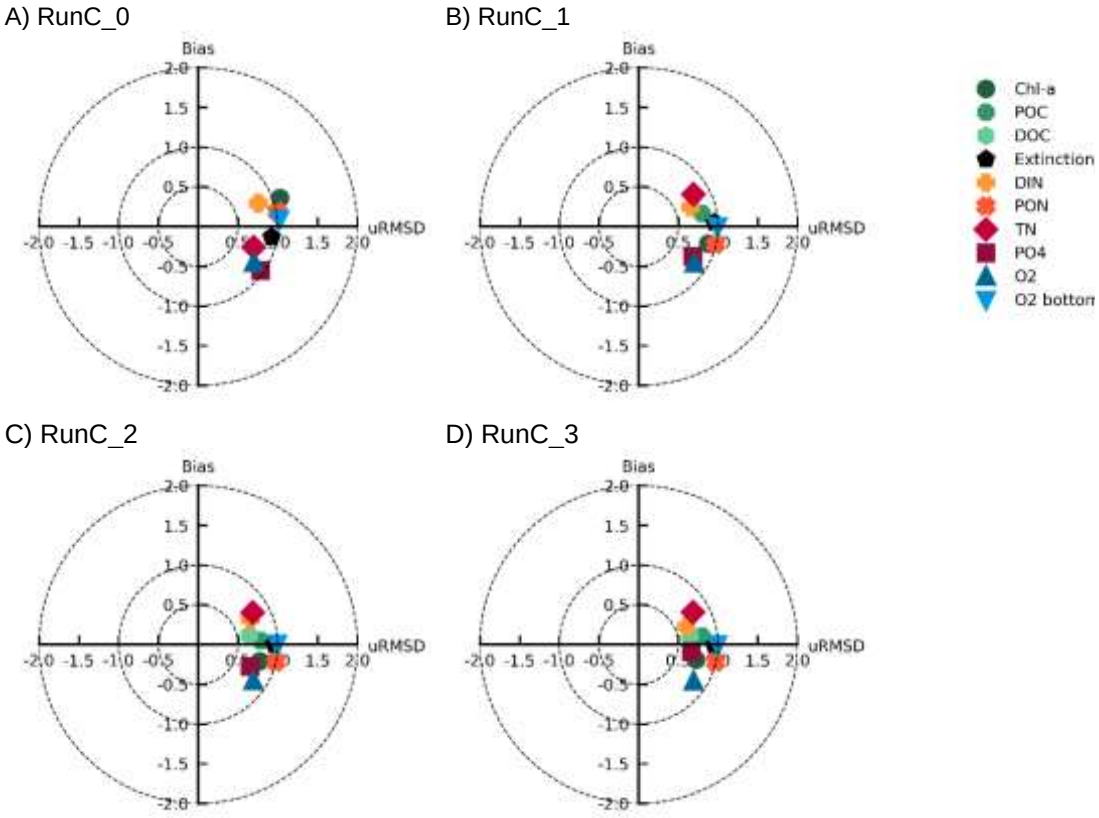

Figure 2.9 Target diagrams representing overall statistics of all available measured water quality variables for the four calibration runs: A) RunC_0, B) RunC_1, C) RunC_2 and D) RunC_3. Note that the marker for POC in RunC_0 diagram falls outside of the plot. The marker for DOC in RunC_1 diagram is behind that of TN.

Addition of a dissolved organic matter fraction

In previous versions of the model, detrital organic matter was represented by a single particulate organic matter fraction, divided into POC1, PON1 and POP1 model state variables (C, N and P content of detrital particulate organic matter, respectively). An addition dissolved, more labile, organic fraction was added to the model. This fraction is represented by three

additional model state variables: dissolved organic C, N, and P, noted DOC, DON and DOP, respectively.

DOC, DON and DOP concentrations were forced at model's offshore boundaries assuming that 91.8% of the offshore organic matter is dissolved (estimate for the waters of the shelf currents from (Agatova et al. 2008)) and using a molar C:N:P ratio of 225:19:1, corresponding to the global average export stoichiometry of semi-labile DOM below 100m estimated with the Community Earth System Model (Letscher et al. 2015).

DOC, DON and DOP concentrations in rivers are forced using the ratios of nutrient export estimates for European rivers from (Seitzinger et al. 2005). We use: DOC:POC=8:7, DON:PON=0.7:1.1, DOP:POP=0.04:0.33, DOP:DIP=0.04:0.20.

In the model, detrital particulate organic matter is now first degraded into dissolved organic matter, which is subsequently mineralized. A mineralization rate of 0.01 day^{-1} is used for dissolved organic matter. An additional extinction term is added for dissolved organic matter, using an extinction coefficient of 0.16 m^2/gC. The background extinction of visible light is reduced from 0.08 m^{-1} to 0.04 m^{-1}. Finally, the additional extinction term due to low salinity is removed. This parameterization is based on the one applied in the Massachusetts Bay eutrophication model (Deltares 2021).

This modification leads to a slowing down of the recycling of organic matter in the system, leading to less available forms of nutrients in the system. As a consequence, the overestimation in DIN is slightly reduced, but most of all, the representation of chlorophyll-a concentrations is visibly improved (Figure 2.9B compared to Figure 2.9A). POC concentrations (notably composed of living and dead phytoplankton biomass), which were overestimated by a factor ~4 in RunC_0 at stations Rottumerplaat 70 km and Terschelling 10km (outside of target diagram), are now well represented by the model.

Changes in phytoplankton temperature parameters for maximum primary production
We assume here that the discrepancies between model and observed timing of the spring bloom are linked to the temperature parameterization of maximum primary production for the simulated phytoplankton species in BLOOM. The model simulates the chlorophyll-a peak too early in the year, by approximately one month. While observed chlorophyll-a maximums occur at the different monitoring stations at the end of April/beginning of May, when the water temperature is approximately 10ºC or more, the simulated maximum occurs in March, when the water temperature is ~2ºC lower.

In BLOOM, the temperature dependency for primary production uses a linear function, parameterized by its slope and the temperature at which primary production is equal to zero (TcPMx parameter).

At the monitoring stations, the simulated spring bloom is mainly composed of marine diatoms, marine flagellates and *Phaeocystis*. Dinoflagellates occur later in the growing season. We therefore shifted the TcPMx parameter for diatoms, flagellates and *Phaeocystis* ecotypes by +2ºC.

This modification mainly changes the model performance for chlorophyll-a representation, reducing the overall uRMSE (Figure 2.9C). It also improves the performance for POC and DOC, which are produced subsequently to the death of phytoplankton.

Changes in phytoplankton internal N:C and P:C ratios

Results from previous reports showed that the model tends to overestimate dissolved inorganic P levels in the growing season at almost all monitoring stations. DIN depletion during the growing season is well reproduced at some stations (such as Terschelling 253km), while DIN uptake seems slightly underestimated at other locations (such as Walcheren 20km).

Comparing simulated and observed seasonal dynamics of DIN and PO_4, it roughly seems that reducing PO_4 uptake by 10% in the model and increasing DIN uptake by 10% would improve the model performance for the representation of inorganic nutrients in the growing season. Therefore, as a third calibration step, we reduced the P:C ratios of all phytoplankton species in the model by 10% and increased their N:C ratios by 10%.

This modification led to a reduction in the overall biases for simulated DIN and PO_4 concentrations (Figure 2.9D).

2.2.1.3 Updated coupled sediment and water quality model performance

The final setup (RunC_3) was adopted for the rest of this report and applied on the fine grid version of the model. Before further scenario applications, the model results on the fine grid were compared to MWTL observations using time-series plots (see Figure 2.10) for results along the Noordwijk and Terschelling transects) and skill metrics (Table 2.4).

Overall model results have been improved with respect to previous versions.
the timing of the modelled spring bloom has been significantly improved with respect to the initial version of the fully coupled sediment-ecology model. Nevertheless, it is still slightly on the early side. The intensity of the spring bloom seems underestimated close to the shore (e.g. Noordwijk 2km and 10km, Terschelling 10km), but is well reproduced by the model further offshore. The chlorophyll-a levels during the rest of the growing season are well reproduced by the model.

Dissolved inorganic nutrient seasonal patterns have been much improved with respect to previous versions of the model. Concentrations during both the winter period and the growing season are now well reproduced. The drop in nutrients during the spring bloom and increase at the end of the growing season are overall well captured. At some stations, however, the increase in inorganic nutrients at the end of the growing season starts too early in the model. This is for example the case for DIN at stations Terschelling 100km and 175km, and seems to be linked to the fact that modelled phytoplankton stops growing earlier in the year than what observations suggest.

Finally, near-surface dissolved oxygen concentrations are now slightly underestimated at all monitoring stations during the entire growing season. The intensity of the O_2 peak linked to the spring bloom is underestimated by the model. These discrepancies need further investigation. They might be linked to an overestimation of re-aeration in the model, that “waters out” the impact of primary production in dissolved O_2 concentrations.

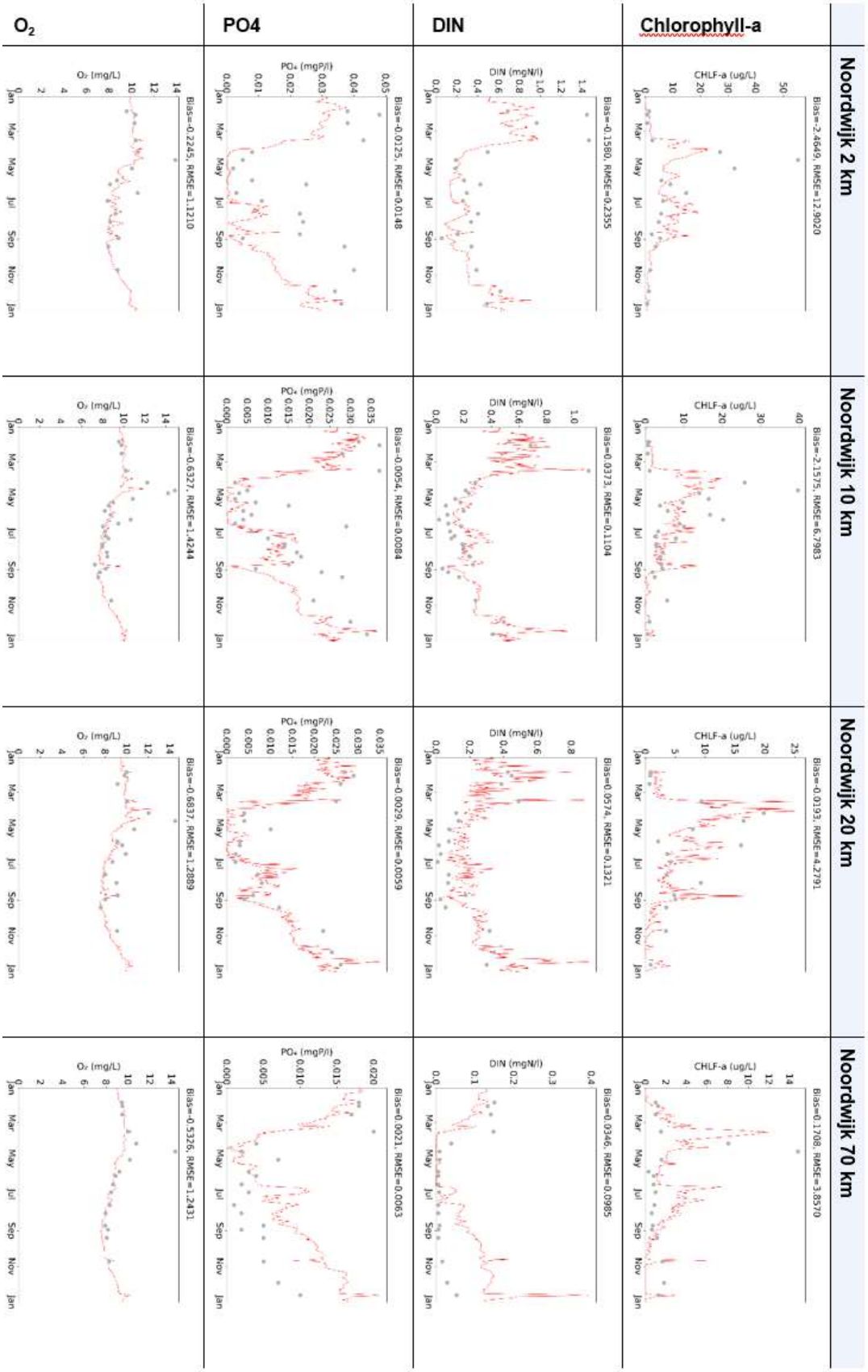

Figure 2.10 Comparison of simulated (red lines) and observed (grey dots) chlorophyll-a, DIN, PO4 and O_2 time series along the Noordwijk transect for the year 2007 for the final calibrated run (fine grid)

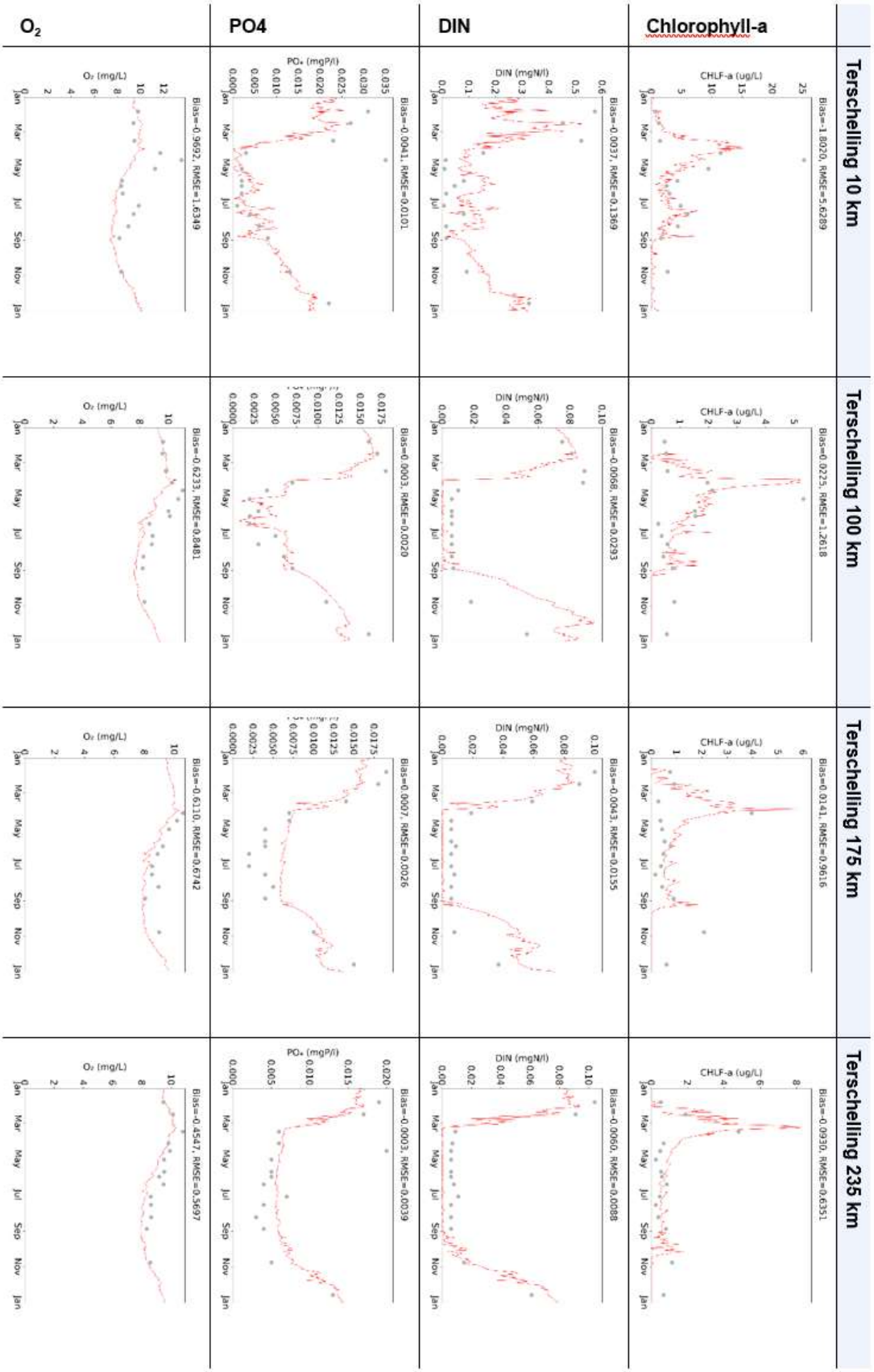

Figure 2.11 Comparison of simulated (red lines) and observed (grey dots) chlorophyll-a, DIN, PO4 and O_2 time series along the Terschelling transect for the year 2007 for the final calibrated run (fine grid)

Table 2.4 Statistical comparison of measured and simulated time series for the year 2007 for the final calibrated run (fine grid). σ_{obs}=standard deviation of observations; σ_{sim}=standard deviation of model results at sampling dates; ρ=correlation. Note that at Rottumerplaat 50 and 70, observations are only available in summer. During this period, measurements show that DIN is depleted.

	Chlorophyll a					DIN					PO4					O_2				
Stat. criterion	σ_{obs}	σ_{sim}	RMSE	Bias	ρ	σ_{obs}	σ_{sim}	RMSE	Bias	ρ	σ_{obs}	σ_{sim}	RMSE	Bias	ρ	σ_{obs}	σ_{sim}	RMSE	Bias	ρ
Unit	*µg/L*	*µg/L*	*µg/L*	*µg/L*	-	*mgN/L*	*mgN/L*	*mgN/L*	*mgN/L*	-	*mgP/L*	*mgP/L*	*mgP/L*	*mgP/L*	-	*mg/L*	*mg/L*	*mg/L*	*mg/L*	-
Walcheren 2 km	11.3	4.0	10.7	-4.2	0.52	0.26	0.16	0.13	-0.04	0.97	0.013	0.010	0.013	-0.012	0.90	2.24	1.08	1.58	-0.46	0.80
Walcheren 20 km	9.3	2.5	9.6	-6.3	0.86	0.12	0.04	0.12	0.05	0.45	0.011	0.005	0.008	-0.003	0.84	1.57	0.88	1.41	-0.81	0.69
Walcheren 70 km	1.1	1.8	2.1	-0.6	0.09	0.04	0.04	0.05	0.04	0.59	0.015	0.003	0.014	0.002	0.62	0.87	0.81	0.91	-0.62	0.69
Noordwijk 2 km	13.7	5.4	12.9	-2.5	0.38	0.38	0.25	0.24	-0.16	0.94	0.015	0.012	0.015	-0.012	0.85	1.48	0.91	1.12	-0.22	0.67
Noordwijk 10 km	8.7	4.0	6.8	-2.2	0.73	0.22	0.18	0.11	0.04	0.89	0.011	0.009	0.008	-0.005	0.83	1.84	0.98	1.42	-0.63	0.76
Noordwijk 20 km	5.7	5.0	4.3	0.0	0.69	0.16	0.16	0.13	0.06	0.73	0.010	0.009	0.006	-0.003	0.86	1.58	1.10	1.29	-0.68	0.72
Noordwijk 70 km	3.4	2.3	3.9	0.2	0.12	0.05	0.09	0.10	0.03	0.24	0.006	0.006	0.006	0.002	0.51	1.50	0.80	1.24	-0.53	0.68
Terschelling 10 km	6.2	3.1	5.6	-1.8	0.51	0.20	0.11	0.14	0.00	0.73	0.012	0.007	0.010	-0.004	0.62	1.50	0.93	1.63	-0.97	0.49
Terschelling 100 km	1.3	1.2	1.3	0.0	0.49	0.03	0.03	0.03	-0.01	0.65	0.006	0.004	0.002	0.000	0.95	0.88	0.81	0.85	-0.62	0.77
Terschelling 135 km	1.1	0.9	0.9	-0.2	0.63	0.03	0.03	0.03	-0.01	0.72	0.007	0.004	0.004	0.000	0.85	0.91	0.85	0.74	-0.51	0.81
Terschelling 175 km	0.9	0.9	1.0	0.0	0.43	0.03	0.03	0.02	0.00	0.88	0.006	0.003	0.003	0.001	0.97	0.74	0.73	0.67	-0.61	0.93
Terschelling 235 km	1.1	0.8	0.6	-0.1	0.82	0.03	0.03	0.01	-0.01	0.98	0.006	0.004	0.004	0.000	0.75	0.69	0.76	0.57	-0.45	0.89
Rottumerplaat 3 km	7.2	5.2	7.3	-4.2	0.57	0.38	0.19	0.31	-0.17	0.77	0.011	0.010	0.018	-0.014	0.38	1.44	0.94	1.36	-0.80	0.65
Rottumerplaat 50 km	1.3	1.8	2.6	0.3	-0.44	0.00	0.03	0.07	0.07	-0.24	0.001	0.003	0.002	0.000	0.50	0.48	0.44	0.42	-0.23	0.72
Rottumerplaat 70 km	0.5	3.1	3.8	1.9	-0.24	0.00	0.02	0.04	0.03	0.21	0.001	0.002	0.002	0.000	0.82	0.25	0.34	0.37	-0.31	0.82

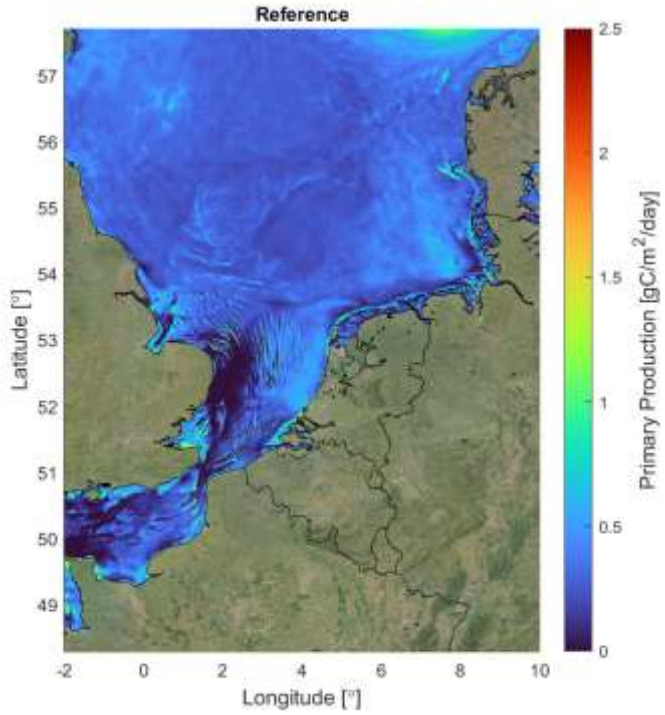

Figure 2.12 Simulated average yearly phytoplankton primary production with the calibrated fully coupled sediment-ecological model for the year 2007

The updated coupled sediment-ecological model computes phytoplankton primary production rates over the model domain that are clearly lower than its uncalibrated version and slightly lower than the initial Wozep ecological model (see results from Van Kessel et al. (2022)). The new estimates coincide better with rates estimated by (Gwee Simin 2018) for the different hydrological regions of the North Sea. Gwee Simin (2018) processed and aggregated remote sensing data to assess primary production in the North Sea and estimated average annual from ~60 gC/m/year in seasonally stratified areas (0.16 gC/m^2/day) to ~160 gC/m/year in the ROFI area (0.44 gC/m^2/day).

2.2.2 Representation of mussels

Using the conditions simulated in the calibrated model, we re-calibrated the parameters used to represent mussel dynamics, with the goal to simulate a stable yearly average biomass of mussels near the water surface at the FINO1 OWF, varying around the order of magnitude of the density observed by Krone et al. (2013) (assuming this represents the situation, where mussels have settled and reached equilibrium). The method is similar to the one applied in the latest mid-term report (Van Kessel et al., 2022). However, the previous calibration was carried out using forcing from an older version of 3D DCSM-FM including water quality, where sediment dynamics were not explicitly represented.

During the calibration, most of the physiological parameters for mussels, based on lab experiments and previous modelling studies (e.g. Troost et al., 2010), are left unchanged. Only average individual size is modified. It is at the moment not verified how realistic the new parametrization for offshore populations is. However, the method allows for the simulation of more realistic biomasses at FINO1 and allows for deriving a first estimate of the order of magnitude of additional grazing and effects on primary production linked to mussel growth on pillars.

The mussel parameters were recalibrated using a 1D-vertical (1D-V) model. The 1D-V model represents the German windfarm FINO1, located at 6.59 E and 54.01 N. This windfarm was chosen as a calibration point for mussel growth as there are in-situ biomass values available for calibration. The 1D-V model was forced with boundaries conditions that were extracted from the updated DCSM model described in the previous sections.

The mussel module in D-Water Quality is based on a Dynamic Energy Budget (DEB) approach and can simulate 1) the life cycle and growth of individual mussels (ISO-morph approach) and 2) the behaviour of a whole mussel population (V1-morph approach). Simulating single mussel individuals provides useful information on the physiological growth of mussels at a certain location. In the ISO-morph approach, the individual's death is simulated by a shrinking of the biomass (reduction of it's structural length when assimilated food is not sufficient for somatic maintenance). Simulating a mussel population provides information on how a population interacts as well as influences the ambient environment. The latter approach is the one we apply in the 3D DCSM-FM model. For the V1-morph approach the DEB formulations are simplified by assuming a constant size distribution of the population, which is parametrized using a reference length, and a mortality rate. The reference length is an important factor that determines the biomass of the population. If it is overestimated the population dies off because the maintenance needs are too high compared to the available food, while if it is too low, then maintenance needs are small and structural biomass will grow too fast.

In the different 1D-V runs, the ISO-morph biomass was initialized with 1 individual per m^2, with a structural biomass corresponding to half of the assumed size at reproduction maturity and energy reserves assumed to be equal to 1/10th of the structural biomass, as done in Van Kessel et al 2022). The V1-morph population structural biomass was initialized using a mussel density of 1000 g of mussel wet weight per 0.04 m^2 of pillar to be consistent with the observed order of magnitude of mussel biomass at FINO1 (Krone et al. 2013), as described in Van Kessel, et al. (2022).

The calibration of the mussel module was completed in 2 steps. In a first step, the 1D-V model was run with only an ISO-morph to see which size the ISO-morph mussel can reach under the provided boundary conditions. In a second step, the 1D-V model was run with different V1-morph lengths to see at which length the V1-morph population can hold its initial biomass after a yearly cycle. Figure 2.13 shows that an ISO-morph can reach a length of 3 cm, but those are then ideal conditions without any competition of other mussel individuals. That value was used as a starting value for the calibration of the V1-morph length. A mussel population with an average length of 3 cm will however not be able to survive. The calibration of the V1-morph length is shown in Figure 2.14. The length of the V1-morph mussel was decreased in intervals to 1.75 and 1.65 cm at which the mussel population was able to hold its initial biomass over a 3-year cycle. A length of 1.65 cm was chosen for the 3D model runs because a second three-year run showed that it yielded more stable initial biomass compared to a length of 1.75 over a 6-year cycle (data not shown).

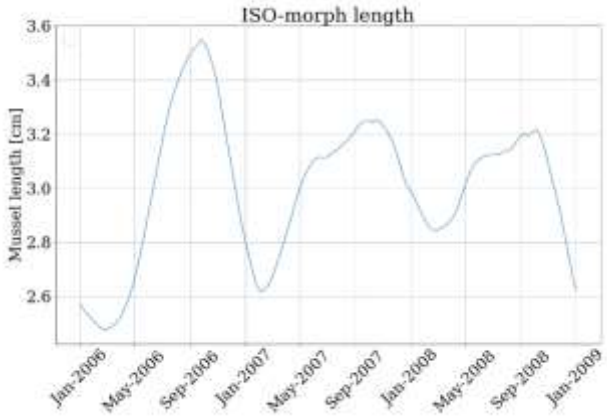

Figure 2.13 Length of a mussel individual (ISO-morph) over a three-year simulation. The plot shows that the ISO-morph length varies between 2.6 and 3.6 cm.

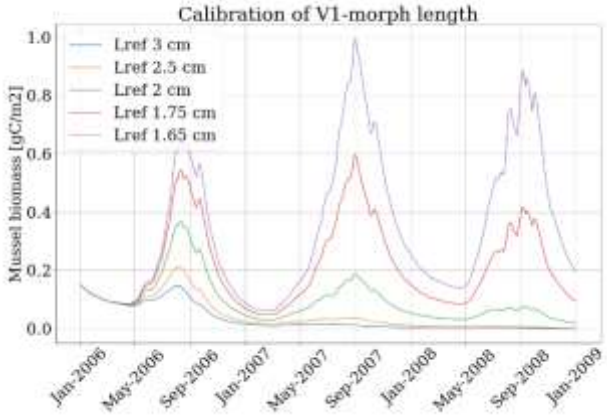

Figure 2.14 Mussel population (V1-morph) biomass for the different V1-moprh lengths. Only V1-morph populations with a reference length of 1.75 and 1.65 cm are able to hold the initial biomass over the three-year cycle.

Thus, for the 3D model runs, a V1-morph length of 1.65 cm was applied. In the 3D runs, structural mussel biomass was initialized near the sea-surface in all OWF areas at 1000 g of wet weight per 0.04 m^2 of pillar as well. The value was translated to g C per surface area of seabed, using the model pillar densities and diameter values of the different OWFs and assuming that the population grows over the top 5 m under the sea surface.
The steps completed here are only the first in a series of calibration steps that will be looked at in the coming year with the aim of improving our system understanding of mussel growth on pillars; next steps are proposed in the discussion section (section 5.4).

2.2.3 Rerun of “2020 scenario” with the updated model

For comparison with results from previous Wozep reports, the “OWF 2020” report was re-run using the newly calibrated coupled sediment-ecological model. This scenario was run without simulating the presence of mussels on pillars and with mussels on pillars, using the updated parameters described in section 4.1. The 2007 calibrated run, without any OWF, is used as reference.

The difference maps between simulated yearly average phytoplankton primary production for the “OWF 2020” scenario compared to the run with no OWF are plotted in Figure 2.15. This allows for comparing the simulated effects of OWFs on changes in phytoplankton primary

production with those estimated with previous versions of the model (Zijl et al. 2021, Van Kessel et al. 2022). The same is done for chlorophyll-a (Figure 2.16).

The difference between simulated phytoplankton primary production in the North Sea with and without the presence of OWFs for the scenario “OWF 2020” is, as in previous reports, quite “patchy” (Figure 2.15). For this scenario, using the updated calibrated coupled sediment-ecological model, primary production is mostly reduced directly within the OWFs. This is most likely the case, because in these scenarios, OWFs are located in non-stratified areas, where increased resuspension of sediments (i.e. decreased light availability) is the main driver for changes in primary production. With previous versions of the model (3D DCSM-FM with water quality processes with forced sediments from Zijl et al., 2021 and initial coupled sediment-water quality version from Van Kessel et al., 2022), results however showed more areas with increased primary production due to the presence of OWFs. This was for example the case for the OWFs in the Dogger Bank.

The results for the differences in near-surface chlorophyll-a concentrations within OWFs as compared to without for scenario “OWF 2020” also slightly differs from results with previous model versions. Directly within OWFs, estimated chlorophyll-a concentrations are lower than without the presence of OWFs (Figure 2.16). The sharpest differences occur in Borssele and the Southern German Bight. It seems that downstream from OWF areas, chlorophyll-a can increase compared to the reference case, most likely due to lower nutrient consumption upstream (within OWFs). These results differ slightly from those calculated with the uncalibrated coupled sediment-ecological model from Van Kessel et al (2022) which estimated an increase in chlorophyll-a in the Dogger Bank OWFs and Northern German Bight.

The effect of mussel growth on pillars within OWFs for the “OWF 2020” scenario, using the calibrated sediment-ecological model and updated parameterization for mussels, is barely visible (data not shown).

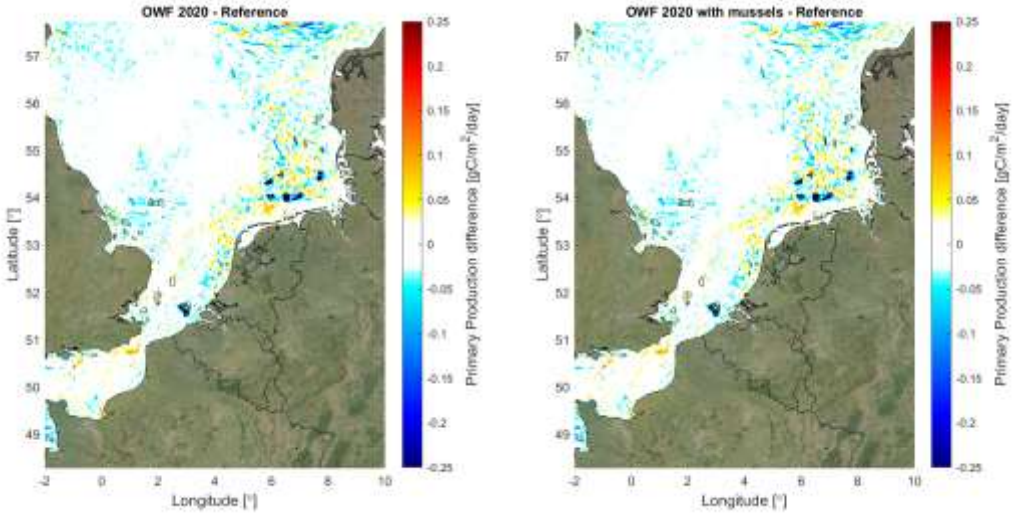

Figure 2.15 Difference in the yearly average primary production simulated for scenario OWF 2020 without (left) and with (right) mussel growth on pillars with respect to the “Reference” run.

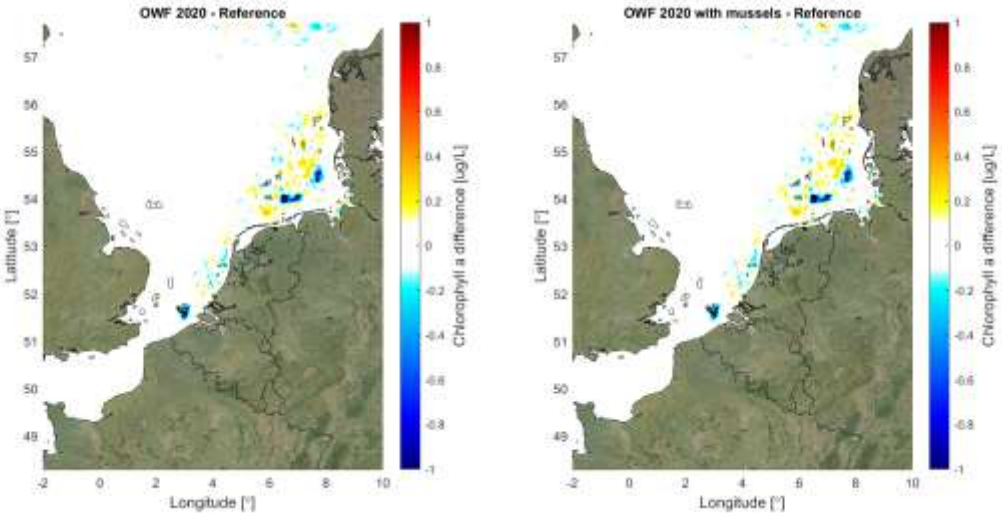

Figure 2.16 Difference in the yearly average near-surface chlorophyll-a concentrations simulated for scenario OWF 2020 without (left) and with (right) mussel growth on pillars with respect to the "Reference" run.

3 Analyses of fine sediment transport along the Holland coast

3.1 Introduction

In (Zijl et al. 2021) a ~10% decrease in the SPM flux at Texel transect (see Figure 3.1) was computed for the OWF2050 scenario. This asked for further analysis which is discussed herein.

The OWF2050 scenario (see for further explanations about the background of this scenario Van Duren et al. 2021) was remade with the new DCSM Fine hydrodynamic and sediment model (herein named SC3A) and a modified OWF2050 scenario was added in which some of the nearshore wind farms planned along the North-Holland coastline have been removed (SC3B;indicated with bold black contour lines in Figure 3.2). This makes a distinction possible between the impact of all OWFs combined on the nearshore SPM flux and the impact of OWFs closest to the coast. To support the analysis, output was generated in more transects as indicated in Figure 3.1, now also including Egmond and Callantsoog transects between Noordwijk and Texel transects.

Figure 3.1 Cross-sections used for longshore sediment transport analysis. *Arrow indicates positive direction.*

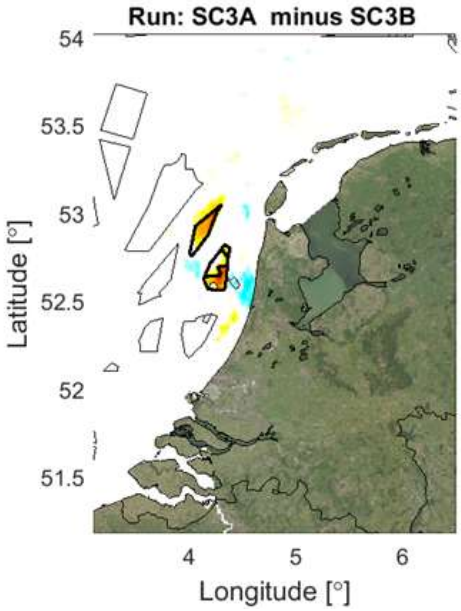

Figure 3.2 Difference between OWF2050 (SC3A) and modified OWF2050 (SC3B) scenario. In SC3B the wind farms indicated with bold black contour lines closest to the North Holland coastline have been removed.

3.2 Changes in alongshore sediment transport

Figure 3.3 shows the absolute alongshore SPM fluxes for the reference scenario, the absolute difference between SC3B and the reference and the absolute difference between SC3A and SC3B. Additionally, Figure 3.4 shows the relative difference between SC3B - reference and SC3A – SC3B.

Consistent with previous results, a ~10% decrease in the SPM flux through Callantsoog transect is computed, ~8% (i.e. 4/5th) of which is caused by the wind farms in SC3B (see light blue line in Figure 3.4) and an additional 2% (i.e. 1/5th) by the farms shown in bold in Figure 3.2. Starting at Hoek van Holland transect via Noordwijk and Egmond towards Callantsoog, the relative OWF impacts gradually increase, as the Rhine ROFI interacts with the OWFs, resulting in more mixing and less stratification.

Effects of OWFs on the Rhine ROFI on bed shear stress, salinity gradients and SPM levels are discussed in the next subsections. These results provide an explanation for the computed reduction in alongshore sediment transport.

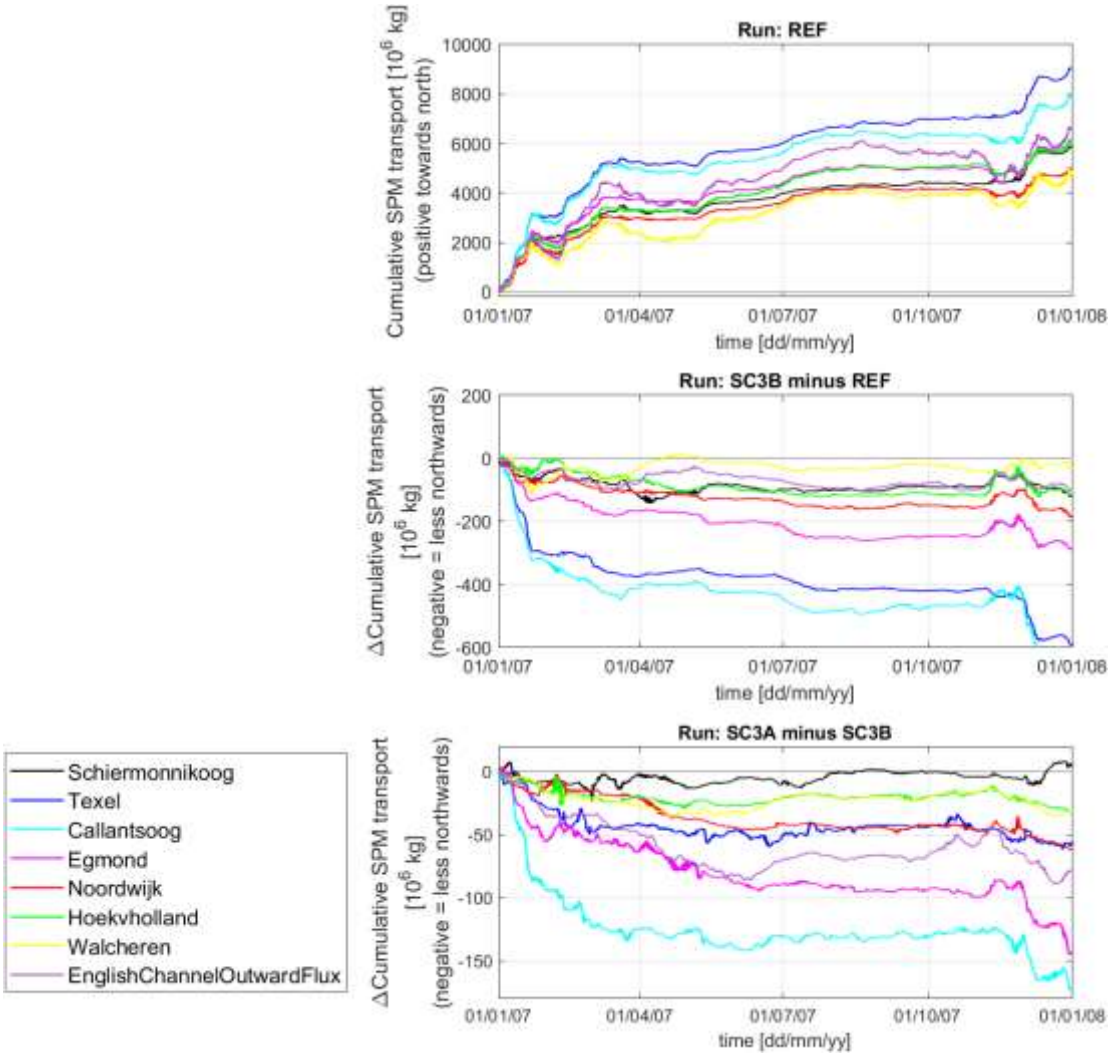

Figure 3.3 Absolute changes in longshore, residual transport of suspended particle matter (SMP) for scenarios 3B and 3A. Top panel shows cumulative, longshore SPM transport [10^6 kg] in the simulation without wind farms (northwards = positive). The different, coloured lines correspond to cross-sections in Figure 3.1. Middle panel shows the increase (positive) or decrease (negative) in northwards, longshore transport when wind farms are added according to scenario 3B. Bottom panel shows the increase (positive) or decrease (negative) in northwards, longshore transport when wind farm Hollandse Kust Noord is upscaled in surface area compared to scenario 3B (i.e. scenario 3A).

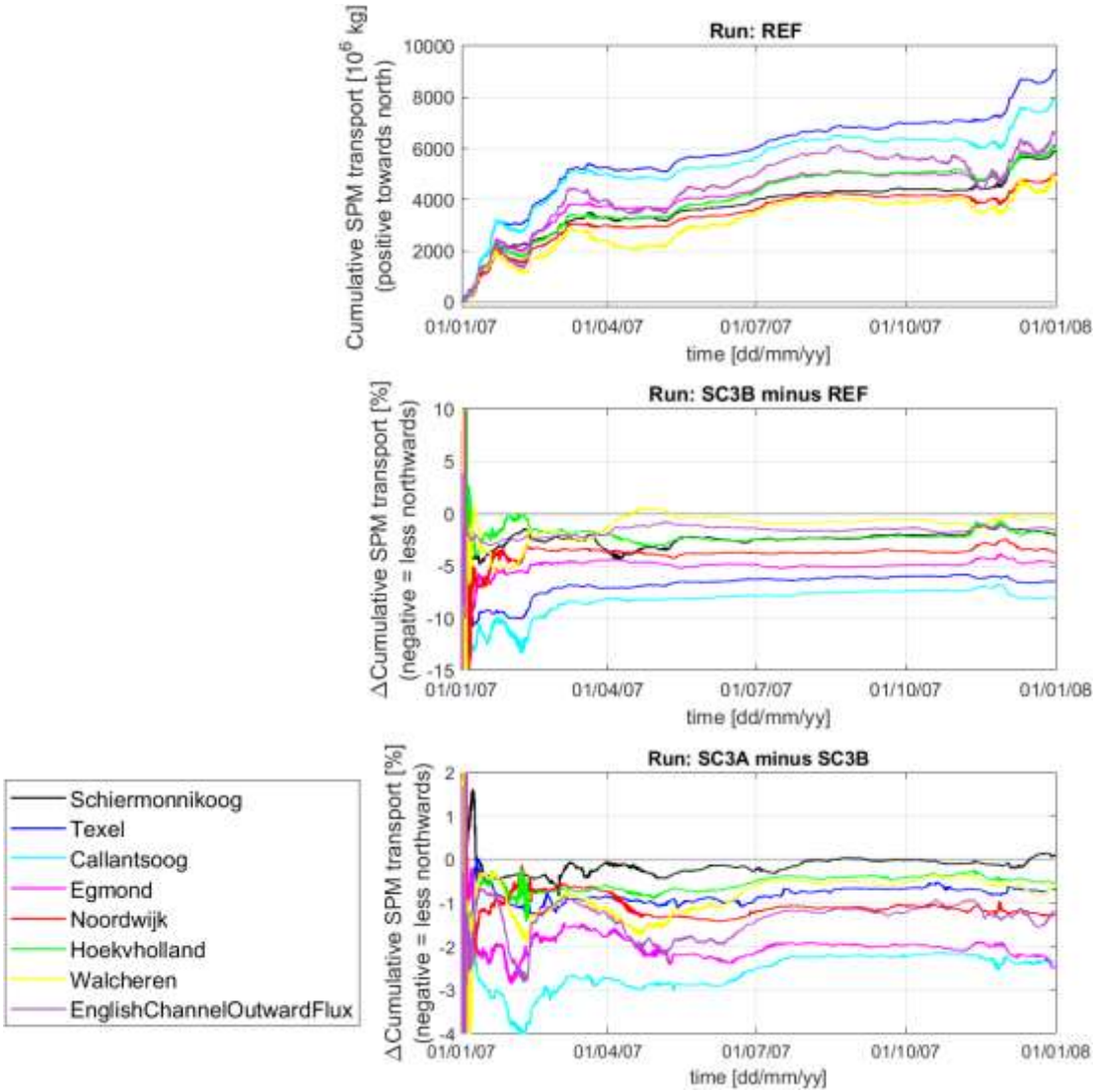

Figure 3.4 Percentual changes in longshore, residual transport of suspended particle matter (SMP) for scenarios 3B and 3A. Top panel shows cumulative, longshore SPM transport [10^6 kg] in the simulation without wind farms. The different, coloured lines correspond to cross-sections in **Figure 3.1**. *Middle panel shows the increase (positive) or decrease (negative) in northwards, longshore transport [%] when wind farms are added according to scenario 3B. Bottom panel shows the increase (positive) or decrease (negative) in northwards, longshore transport [%] when wind farm Hollandse Kust Noord is upscaled in surface area compared to scenario 3B (i.e. scenario 3A).*

3.3 Hydrodynamic changes

Figure 3.5 shows the year average bed shear stress for the reference scenario and the differences with scenarios SC3B and SC3A. Although inside most OWFs a slight increase in bed shear stress is computed, outside the OWFs a slight decrease is computed, overall resulting in a minor decrease of resuspension. The overall decrease in bed shear stress is likely related to the decrease in M2-amplitude along the Dutch coast as will be discussed in Section 4.2.

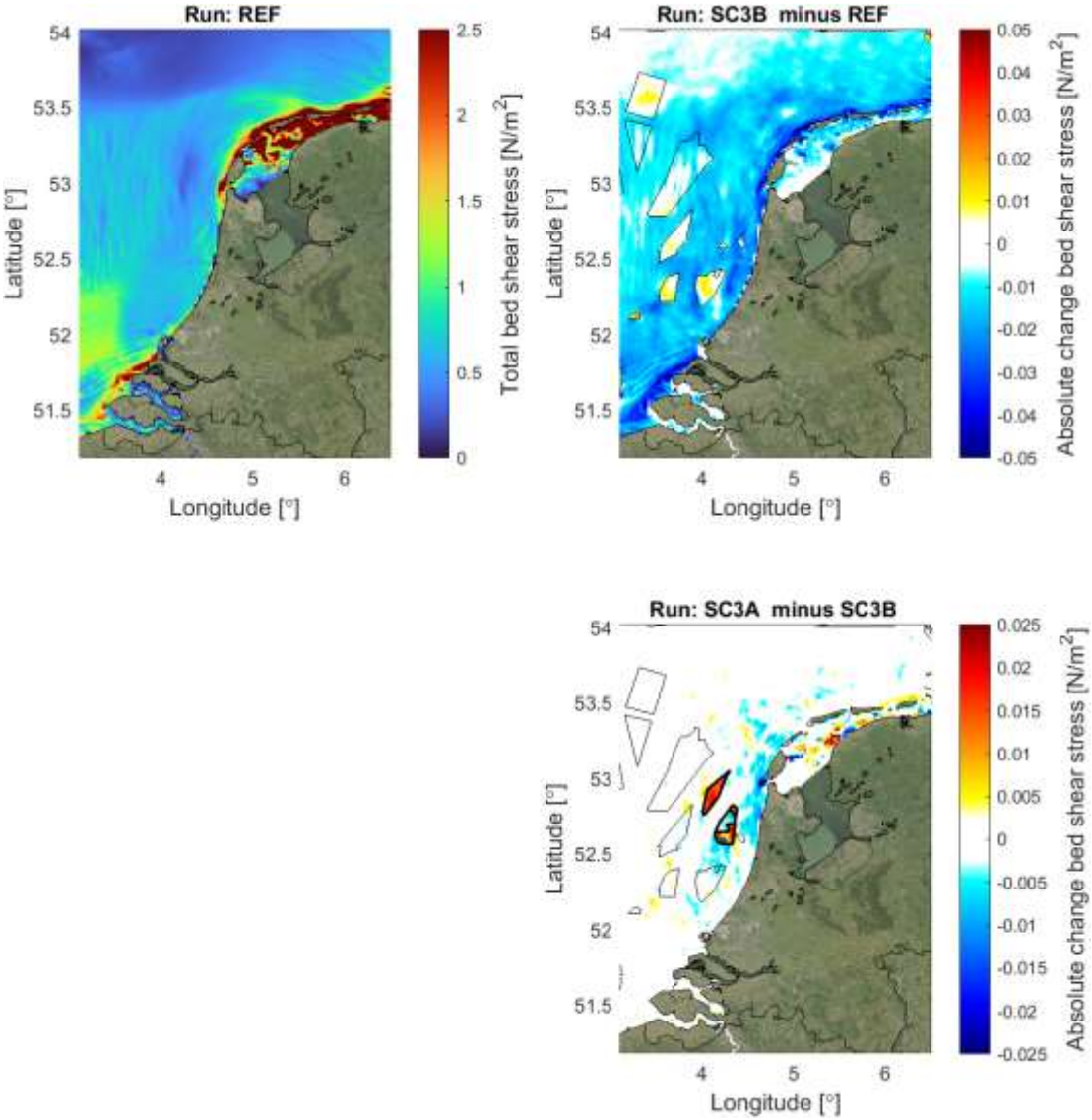

Figure 3.5 Year-average bed shear stress changes (2007) for two future wind farm scenarios with(out) OWFs "Hollandse Kust Noord" and "Hollandse Kust West". Upper-left panel shows the total bed shear stress [N/m^2] in the simulation without wind farms (average of 2007, including the effect of waves). Upper-right panel shows the bed shear stress change [N/m^2] when the wind farms of scenario 3B are added. Thin black contours indicate the wind farms in scenario 3B. Bottom-right panel shows the bed shear stress change [N/m^2] for scenario 3A compared to scenario 3B. The additional wind farms compared to scenario 3B are indicated with thick black contours.

Figure 3.6 shows the year-average near-bed salinity for the reference scenario and the differences with scenarios SC3B and SC3A. Overall the OWFs result in a decrease of the near-bed salinity of up to 0.2 ppt (locally more inside wind farms). This may be explained by additional mixing, bringing more (relatively) fresh water from the surface down.

Figure 3.7 shows the same type of results as Figure 3.6, but on near-surface salinity. Again, a small decrease of the salinity (with about 0.1 ppt) is computed in the nearshore, maybe related to a reduction of the nearshore residual currents inside the OWFs (see Section 4.2) that may increase the residence time of freshwater in the ROFI and reduce overall salinity. Inside nearshore OWFs a small increase is computed that may be explained by additional mixing, bringing more saline water up from the bottom.

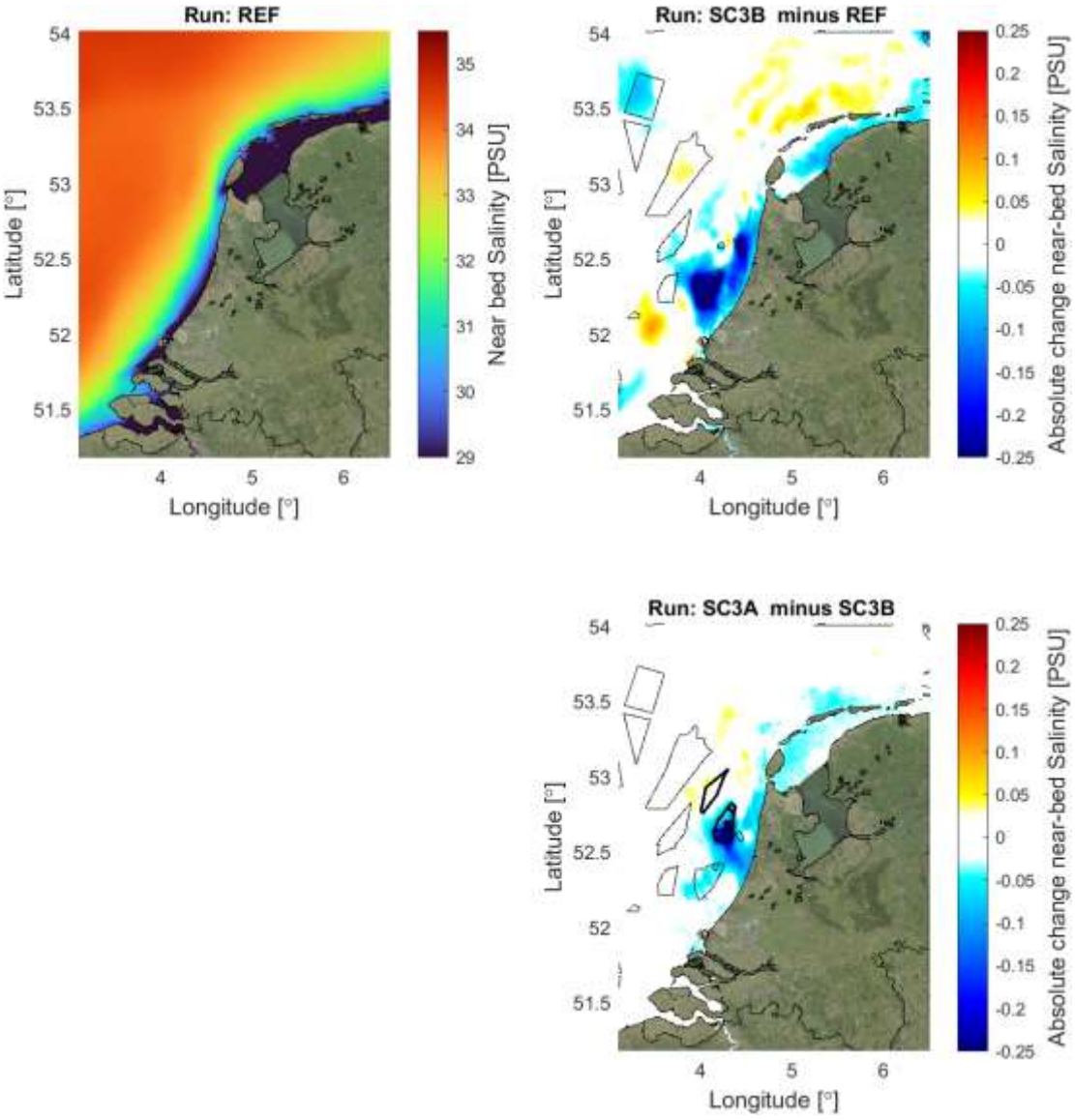

Figure 3.6 Changes in year-average, near-bed salinity for two future wind farm scenarios with(out) OWFs "Hollandse Kust Noord" and "Hollandse Kust West". Upper-left panel shows the near-bed salinity [PSU] (average of 2007) in the simulation without wind farms. Upper-right panel shows changes in near-bed salinity [%] when the wind farms of scenario 3B are added. Thin black contours indicate the wind farms in scenario 3B. Bottom-right panel shows the change in near-bed salinity [%] for scenario 3A compared to scenario 3B. The additional wind farms compared to scenario 3B are indicated with thick black contours.

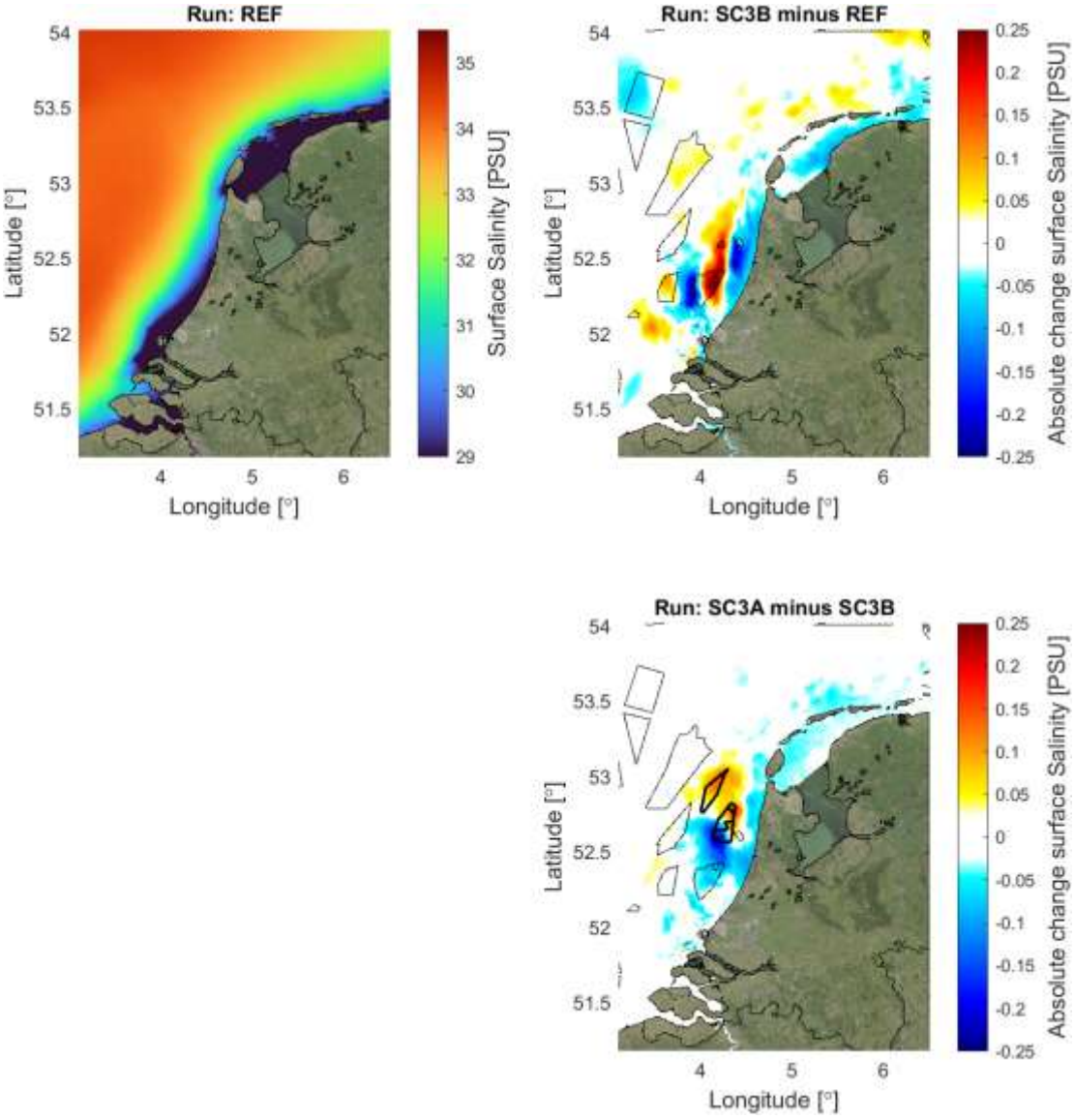

Figure 3.7 Changes in year-average, surface salinity for two future wind farm scenarios with(out) OWFs "Hollandse Kust Noord" and "Hollandse Kust West". Upper-left panel shows the surface salinity [PSU] in the simulation without wind farms (average of 2007). Upper-right panel shows the change in surface salinity [%] when the wind farms of scenario 3B are added. Thin black contours indicate the wind farms in scenario 3B. Bottom-right panel shows the change in surface salinity [%] for scenario 3A compared to scenario 3B. The additional wind farms compared to scenario 3B are indicated with thick black contours.

Figure 3.8 shows the resulting salinity stratification which slightly decreased, notably within nearshore OWFs and their vicinity. This can be explained by additional mixing inside the OWFs. As stratification in combination with cross-shore salinity gradients contributes to the onshore near-bed residual flux of water and SPM, and to nearshore trapping of SPM in the ROFI, a small reduction of the nearshore SPM concentration may be expected.

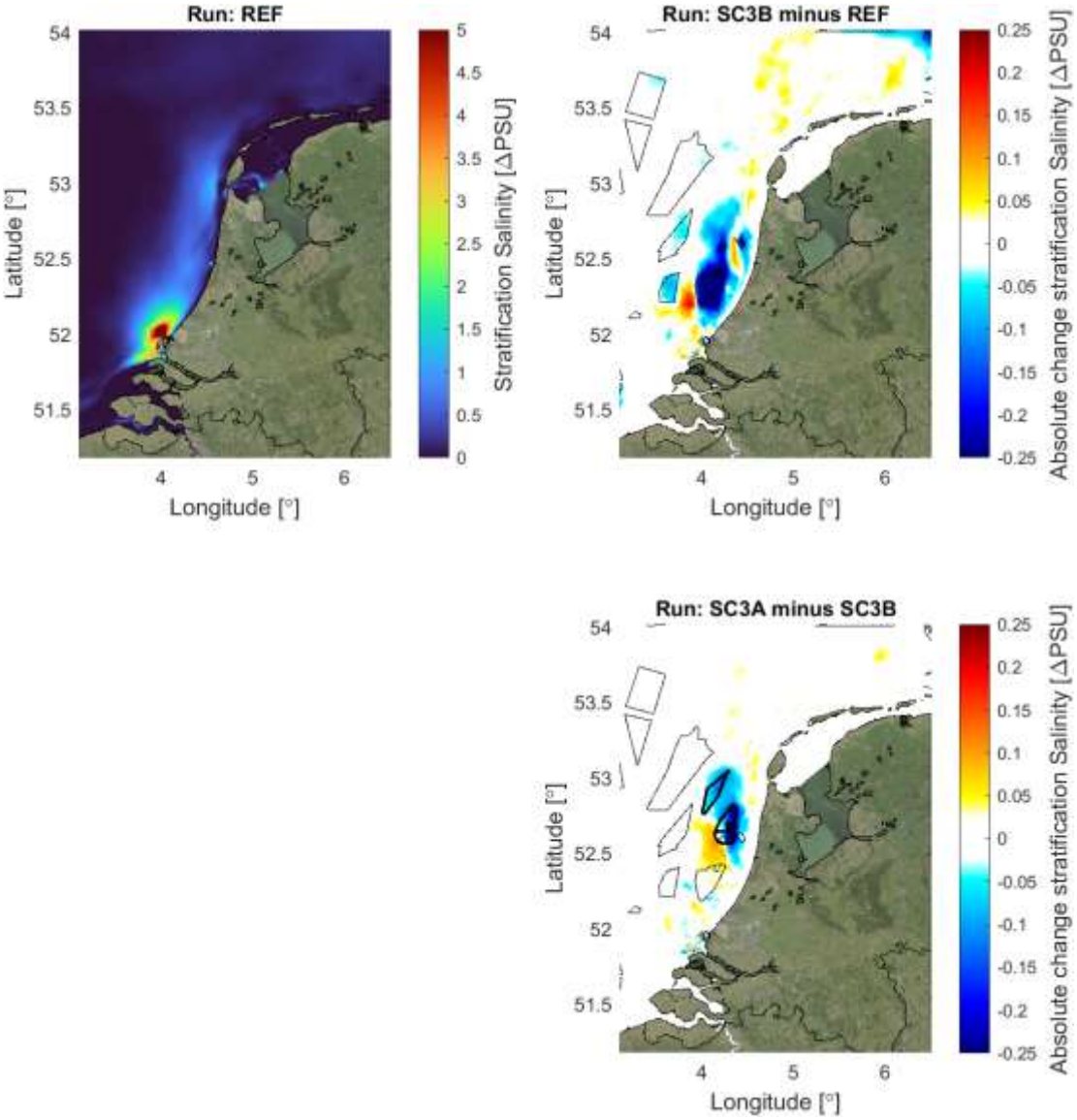

Figure 3.8 Changes in year-average salinity stratification for two future wind farm scenarios with(out) OWFs "Hollandse Kust Noord" and "Hollandse Kust West". Upper-left panel shows the difference in salinity [PSU] between the near-bottom and surface layers for the simulation without wind farms (average of 2007). This parameter is used as a proxi for the salinity stratification. Upper-right panel shows the change in stratification [%] when the wind farms of scenario 3B are added. Thin black contours indicate the wind farms in scenario 3B. Bottom-right panel shows the change in stratification [%] for scenario 3A compared to scenario 3B. The additional wind farms compared to scenario 3B are indicated with thick black contours.

3.4 Changes in fine sediment dynamics

Figure 3.9 shows the year-average near-bed SPM concentration for the reference scenario and the differences with scenarios SC3B and SC3A. Figure 3.10 shows the same for near-surface SPM. Indeed, a nearshore reduction in SPM concentration is computed of about 5% near the bed (a bit less near the surface). A combination of a small reduction in resuspension by the small decrease in bed shear stress and a small reduction in the stratification and onshore near-bed residual water and sediment flux are the most likely causes for his reduction in SPM levels. This will also result in a reduction of the alongshore sediment flux as discussed in Section 3.2. A local decrease in residual currents may further reduce the sediment flux.

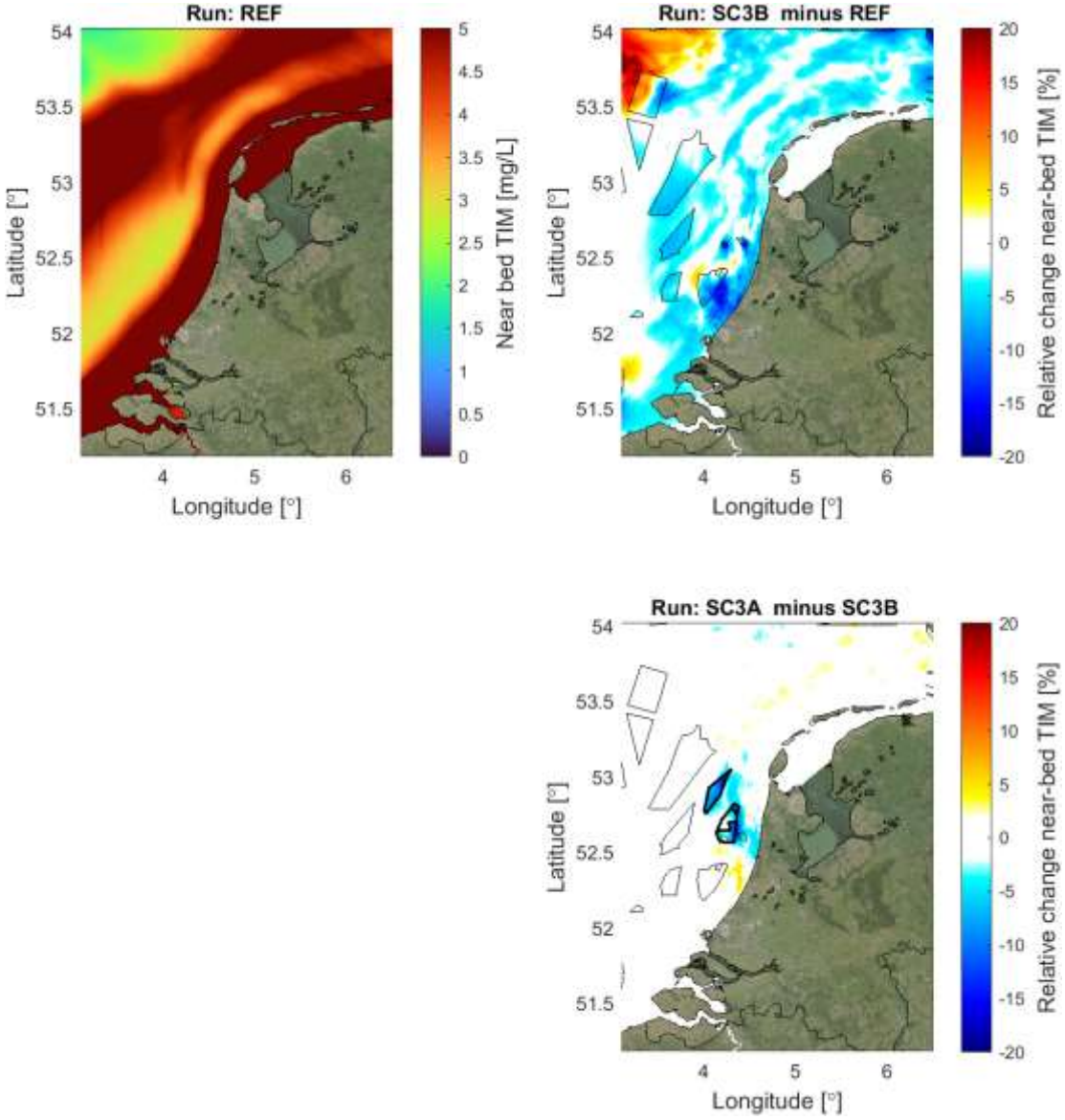

Figure 3.9 Changes in year-average, near-bed total inorganic matter (TIM = SPM) for two future wind farm scenarios with(out) OWFs "Hollandse Kust Noord" and "Hollandse Kust West". Upper-left panel shows the near-bed TIM [mg/L] (average of 2007) in the simulation without wind farms. Upper-right panel shows changes in near-bed TIM [%] when the wind farms of scenario 3B are added. Thin black contours indicate the wind farms in scenario 3B. Bottom-right panel shows the change in near-bed TIM [%] for scenario 3A compared to scenario 3B. The additional wind farms compared to scenario 3B are indicated with thick black contours.

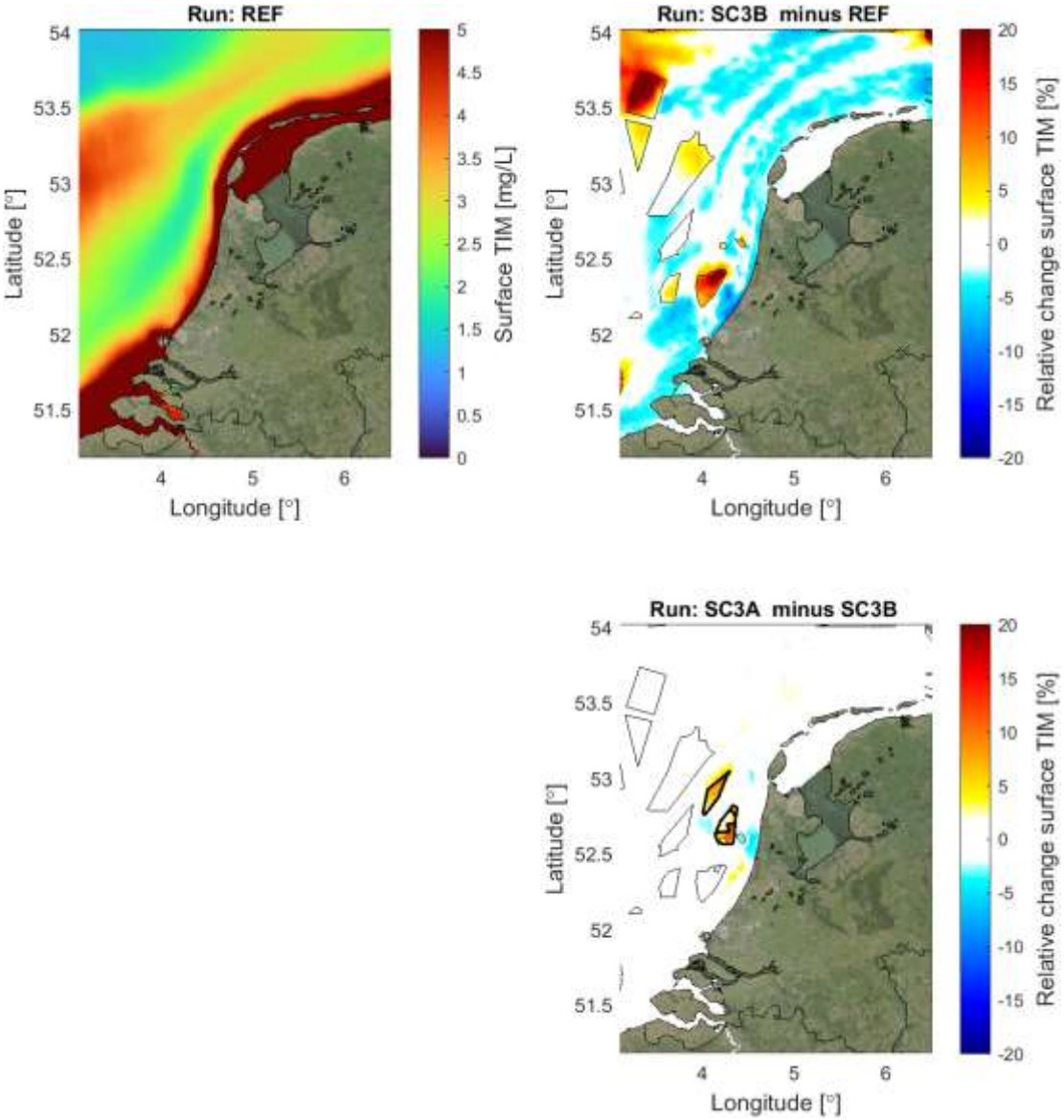

Figure 3.10 Changes in year-average, surface total inorganic matter (TIM = SPM) for two future wind farm scenarios with(out) OWFs "Hollandse Kust Noord" and "Hollandse Kust West". Upper-left panel shows the surface TIM [mg/L] in the simulation without wind farms (average of 2007). Upper-right panel shows the change in surface TIM [%] when the wind farms of scenario 3B are added. Thin black contours indicate the wind farms in scenario 3B. Bottom-right panel shows the change in surface TIM [%] for scenario 3A compared to scenario 3B. The additional wind farms compared to scenario 3B are indicated with thick black contours.

4 Upscaling scenario

4.1 Scenario description and parameterization of OWFs

Within the Wozep project on ecosystem effects of large-scale offshore wind farms two future offshore wind farms are chosen to assess, using the modelling suite that has been developed over the past couple of years. The scenarios are closely linked to the current search areas to offshore wind that Rijkswaterstaat and the Ministry of Economic Affairs and Climate (EZK) are currently working with. It takes into account the aim of the government to speed up the development of generating offshore wind energy on the North Sea to realise 21 GW offshore wind capacity by 2030 (Ministerie Economische Zaken en Klimaat, 2022)

4.1.1 Hypothetical upscaling scenario from previous study

The previous large upscaling scenario (Zijl et al. 2021) was based on projections of the offshore wind sector and assumed a total of 60 GW in the Dutch EEZ in 2050. It included the wind farms that were operational in 2020, with the associated surface areas and energy densities and assumed an energy density of 8 MW / km^2 for future farms. The scenario took into account the location of international shipping lanes and Natura-2000 areas, but no other human activities in the North Sea.

4.1.2 Aim of the new scenarios

Fundamental aim of Wozep is to assess at what level of upscaling ecosystem effects are so large that this may cause serious risks to ecosystem functioning and thus jeopardize legally protected marine species and habitats. . The current study aims to get more insight in the effect of upscaling. The previous study only had one realistic 2020 scenario and a large upscaling scenario. In the current set there is again one fairly extreme scenario (in terms of capacity larger than the one in the previous study) and also one that is more intermediate.

4.1.3 New scenarios

The scenarios below were discussed and agreed in a workshop held on the 24th of October 2022 with representatives from RWS and the Ministry of EZK. There is no certainty that these scenarios will be developed in the future as they are presented here. Also, in the current scenarios we distributed turbines over the area in a way that is unlikely to be realistic in terms of shipping corridors etc. In the new scenarios the currently operational wind farms and those under construction are included with realistic capacities. The scenario for development of OWFs in countries outside the Netherlands was kept constant and was based on the latest information of Rijkswaterstaat.

4.1.4 Farm locations

4.1.4.1 Scenario 1

This scenario (Figure 4.1A) is a ‘currently most likely’ scenario for 2040 for the placement of offshore windfarms on the Dutch EEZ. It is based on the already published lay-out of search areas and the current capacities for each wind farm as assumed by the government. From the known search areas, some wind farms, or some parts of wind farms are not included in the scenario because there are known conflicts with other uses, e.g. aggregate mining, military exercise areas, or very close proximity to shipping lanes. E.g. in this scenario only the eastern part of Lagelander Noord is included, with 2 GW of wind capacity. This scenario adds up to a total capacity of 50.2 GW.

4.1.4.2 Scenario 2

This scenario (Figure 4.1B) is a very extreme upscaling scenario that is aiming for more than 70 GW in offshore wind power generation in the Dutch EEZ. This scenario includes some areas which are not in the currently published set of search areas. This one does include turbines in some of the search areas that were previously excluded due to other uses. This scenario adds up to a total capacity of 76.2 GW.

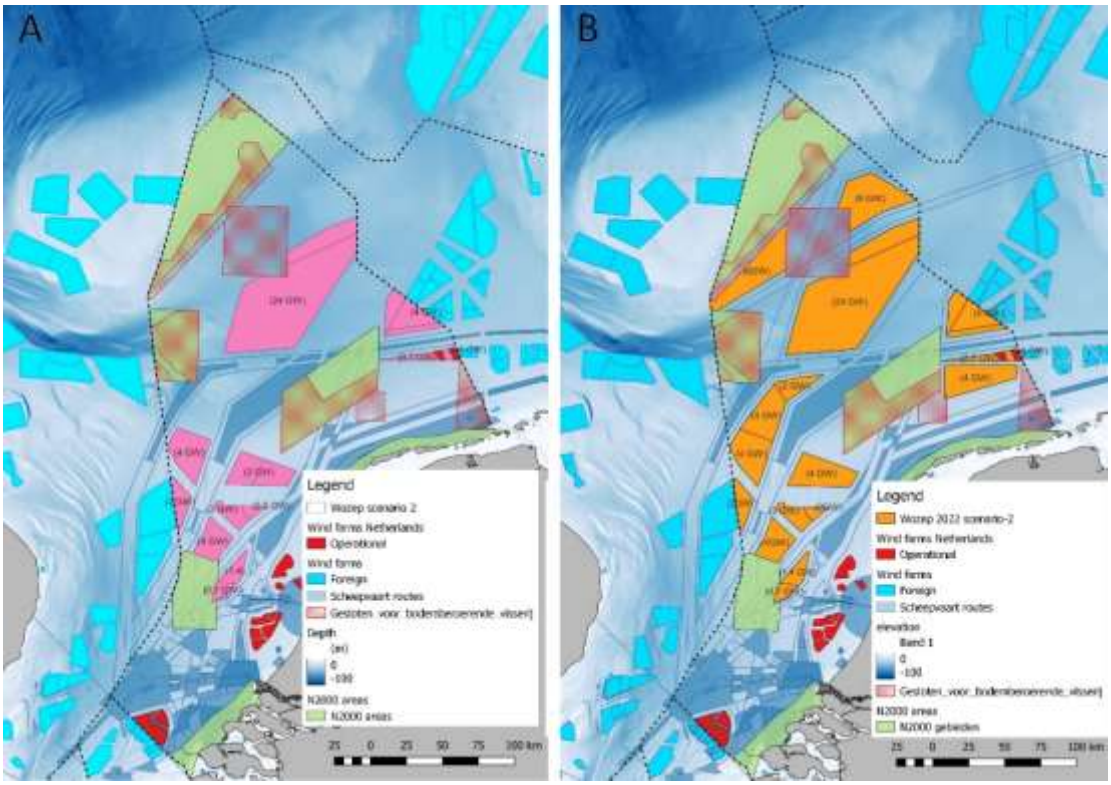

Figure 4.1 A: lay-out scenario 1 and B: lay-out scenario 2. Both with indicated capacity per search area

4.1.5 Turbine dimensions

The operational wind farms in the model have the same parameterization as used in the Wozep study in 2020. All wind turbines are assumed to have a monopile foundation. Wind farms built before 2020 have a density of 3.15 piles/km² and a pile diameter of 5 m. Existing wind farms built after 2020 have a density of 0.85 piles/km² and a pile diameter of 8 m. For all Dutch future wind turbines, we have assumed a capacity of 15 MW. These are schematized with pile diameters of 12 m. The density is calculated based on the expected number of turbines within the wind farm. Wind farms outside of the Dutch EEZ are included with pile diameters of 12 m and a density of 0.67 piles/km².

4.2 Hydrodynamic model

This section describes the parameterisation of wind farms in scenarios 1 and 2 and shows the results of the hydrodynamical modelling of the scenarios. The hydrodynamic model that was used for this analysis is equal to the one used for the 2021 Wozep study (Zijl et al., 2021). We refer to this report for further details on the hydrodynamic model and its validation.

Compared to the 2021 report, model calculations were done with a more recent D-Flow FM executable. Since Deltares has updated the operating system on its computational cluster, it is no longer possible to use the same D-HYDRO software version as was used earlier. Before this executable was applied, it was checked that a required change in software and hardware used did not significantly impact the model quality and output compared to the earlier Wozep computations and the original model validation (Zijl and Laan 2022).

4.2.1 Parameterization of wind farms

This section describes the parameterization of OWFs in the hydrodynamic model for the two scenarios. The method of parameterization has not changed and corresponds to the previous 2021 Wozep study (Zijl et al, 2021). Locations of offshore wind farms are specified in the model through a polygon along its boundaries. In each computational cell within this polygon, the appropriate sink and source terms in the momentum and turbulent kinetic energy equations are computed considering the pile density (number of piles per unit of area) and the mean pile diameter. In addition, the wind speed is reduced by 10% in the specified area.

Figure 4.2 shows the stem density of OWFs for both scenarios. The following stem densities were used:

- Dutch OWFs constructed before 2020: 3.15 piles/km^2.
- Dutch OWFs constructed after 2020: 0.85 piles/km^2.
- Foreign OWFs, 0.670 piles/km^2, conforming to the parameterization in (Zijl et al, 2021).
- Future scenario OWFs: densities calculated from power output per wind farm and assumed power of 15MW per turbine. If no information was available, 0.670 piles/km^2 was used.

Figure 4.3 shows the stem diameter used for OWFs in both scenarios. The following stem diameters were used:

- Dutch OWFs constructed before 2020: a pile diameter of 5 m was used.
- Dutch OWFs constructed after 2020: a pile diameter of 8 m was used.
- Foreign OWFs and scenario OWFs: a pile diameter of 12 m was used.

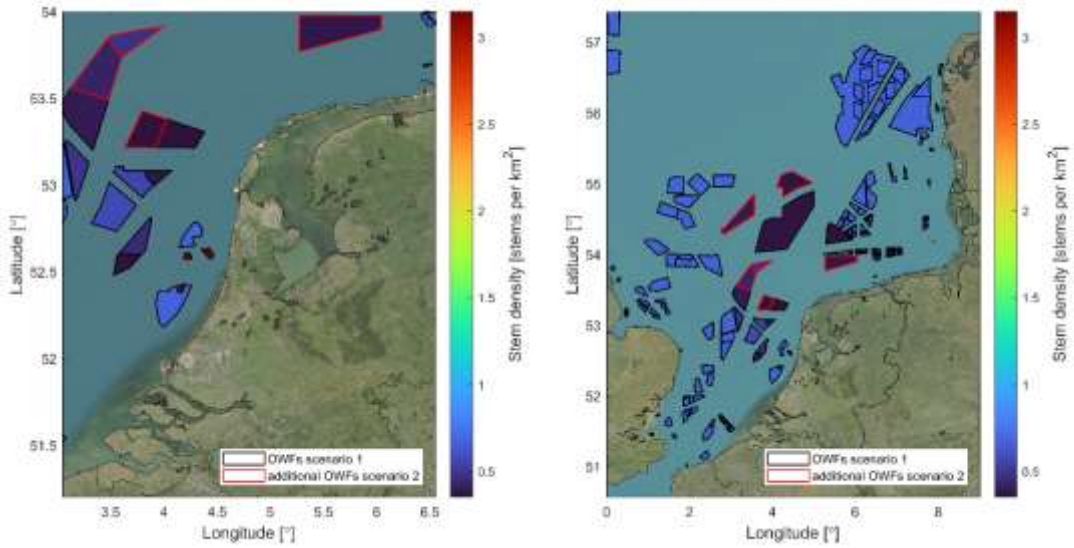

Figure 4.2 Stem density of OWFs around the Dutch coast (left) and in the southern North Sea (right). Areas with red circumference denote additional OWFs in scenario 2.

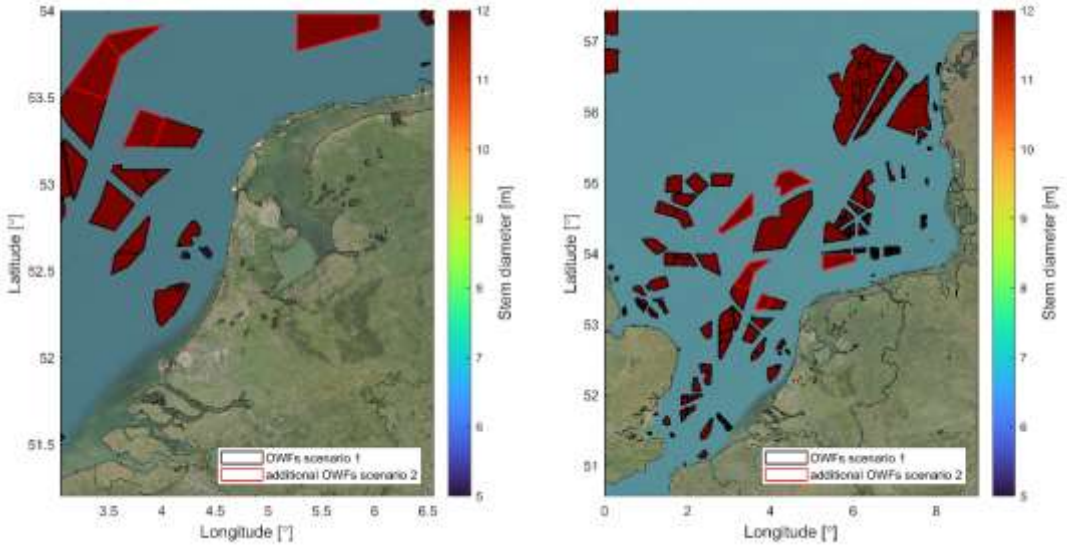

Figure 4.3 Stem diameter of OWFs around the Dutch coast (left) and in the southern North Sea (right). Areas with red circumference denote additional OWFs in scenario 2.

4.2.2 Results

The hydrodynamic impact of offshore wind farms (OWFs) will be assessed and presented in the following sections. Changes induced by OWFs for the following parameters will be reported:

- Sea surface temperature
- Temperature stratification
- Sea surface salinity
- Salinity stratification
- M2 tidal amplitude and phase
- Residual currents

The model version used contains 20 equidistant sigma layers throughout the full domain, independent of the local water depth. Where surface or bed values are used, these are taken from the layer highest or lowest in the water column, respectively. This concerns the results for salinity, temperature and residual currents. Water levels (including the M2 tide) and bed shear stress due to currents are two-dimensional quantities, without a vertical component. Note that salinity stratification is defined as the bottom value minus the surface layer value, whereas temperature stratification is defined as the surface value minus the bottom layer value. In both cases, a resulting positive value contributes to stable density stratification. Relative changes are only shown in the areas where absolute changes are within the visible range of the plotted colourmap to avoid indications of large relative changes that are not relevant (i.e. if the absolute change is less than the visible range in figures with absolute changes).

For each reported parameter the mean over an entire simulated year (2007) is calculated, using the ‘Fourier’ module of D-HYDRO. This module calculates the mean values over all simulated timesteps by means of statistical analysis during the model simulation. This allows for an accurate and at the same time storage-efficient model result since it removes the need to write 3D output at a very high temporal interval for post-processing after the simulation. Furthermore, the ‘Fourier’ module allows for a simple tidal analysis. Based on the number of cycles within the analysis time frame, as well as the prescribed nodal amplification factor and astronomical argument, an approximation of the spatial field of the M2 tidal amplitude and phase are calculated during the computation.

Effects of the addition of wind farms to the domain are calculated by taking the difference between a simulation without and a simulation with wind farms.

4.2.2.1 Results reference scenario (no OWFs)

In the reference scenario, the effect of offshore wind farms is neglected entirely, including that of the wind farms already present. The results of this scenario give an overview of the occurring spatial patterns in the North Sea.

Temperature and salinity

Below, the reference situation is presented in terms of the annual mean sea surface temperature and salinity in 2007 as well as the stratification thereof. In these figures, the amount of salinity stratification is determined by subtracting the annual mean value in the top model layer from that in the bottom model layer (and vice versa for temperature stratification).

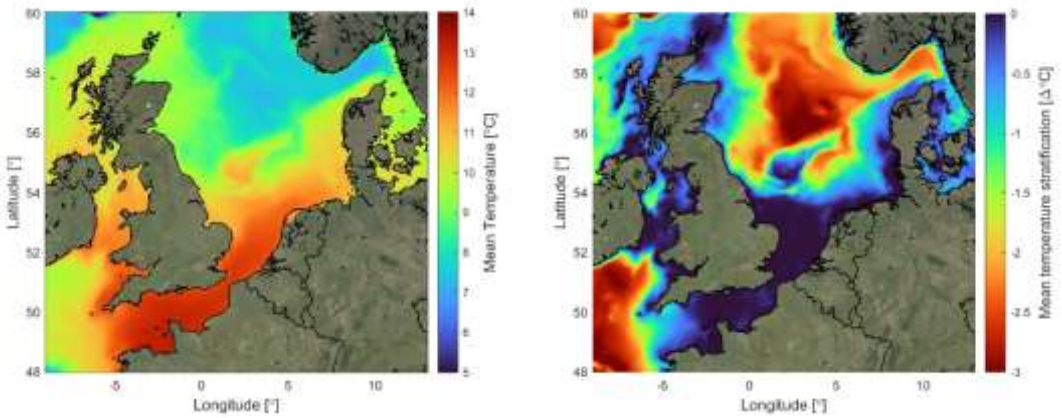

Figure 4.4 Annual mean of sea surface temperature (left) and vertical temperature difference (right) in 2007.

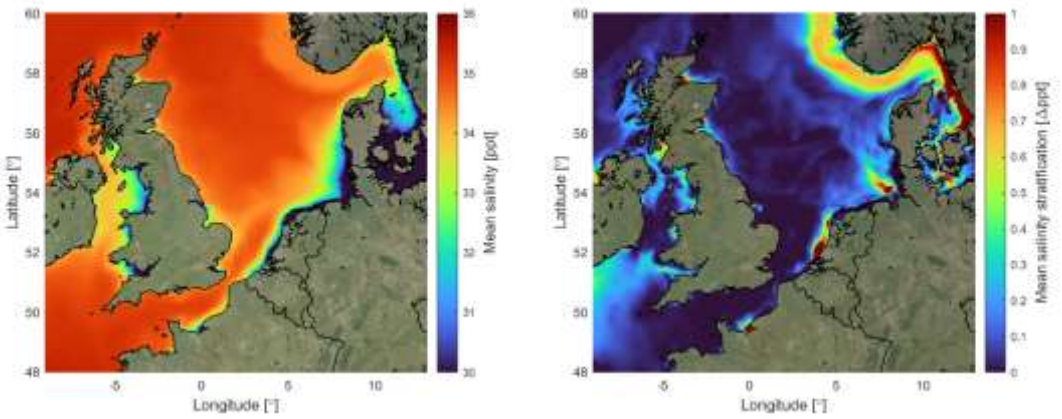

Figure 4.5 Annual mean of sea surface salinity (left) and vertical salinity difference (right) in 2007.

The overall pattern of the stratification is in line with the expected spatial variation (Van Leeuwen et al. 2015). A permanently mixed area is present in the southern part of the North Sea, between the United Kingdom and the Netherlands. The central North Sea shows a large area with temperature stratification. As expected, temperature stratification (and to some extent salinity stratification) is distinctly reduced in the shallower waters of the Dogger Bank, while mean surface temperatures are higher. Along the coast, temperature stratification is weaker due to vigorous tidal mixing, but the effect of the ROFIs attaching to the coast is visible in the salinity stratification.

Residual current patterns

In Figure 4.6 the magnitude of the annual mean (residual) currents at the surface and bottom are presented for the year 2007. These show the residual circulation at the surface roughly following a counterclockwise pattern, with residual current at the bottom much lower than at the surface. As expected, the residual transport through the English Channel is in the direction of the North Sea.

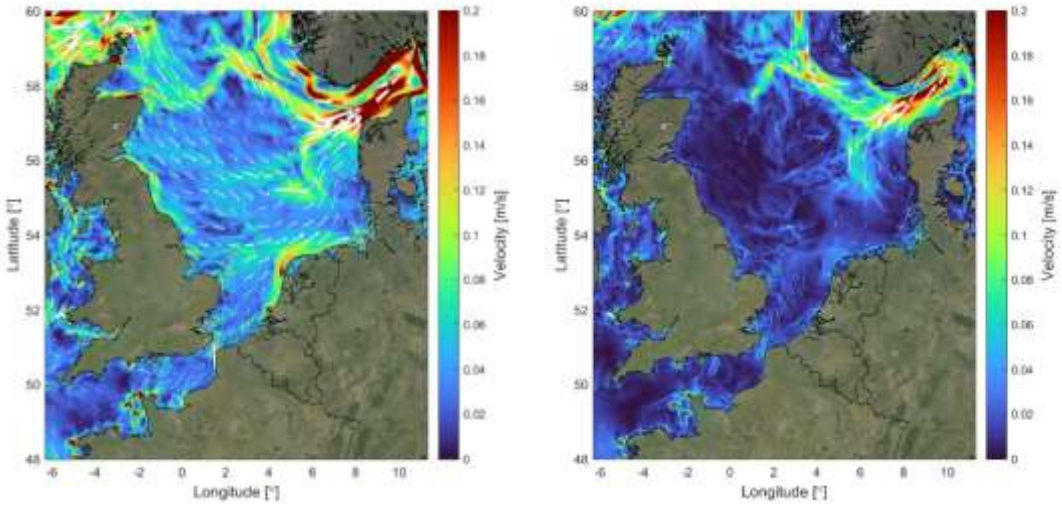

Figure 4.6 Annual mean velocity magnitude (2007) at the surface (left) and bottom (right) model layers.

M2 tide

The semi-diurnal lunar M2 tide is the main tidal constituent in most parts of the North Sea. The computed amplitude and phase thereof are presented in Figure 4.7. These figures show the M2 tide behaving as a Kelvin wave, travelling in a counterclockwise direction through the North Sea and with generally higher amplitudes along the coast. Also visible are the two complete amphidromic systems present in the North Sea, one at a latitude of 52.5° and the other further east near 55-56° latitude[4]. In addition, there is a degenerate amphidromic system[5] near the southern coast of Norway.

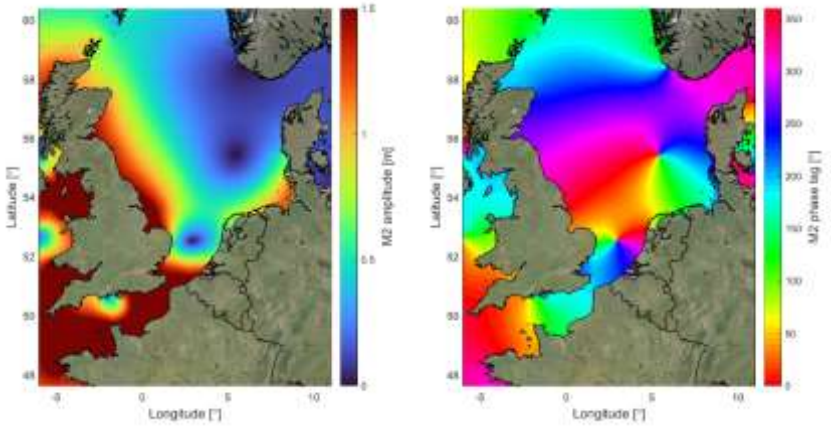

Figure 4.7 Computed M2 amplitude (left) and phase (right).

[4] An amphidromic system consists of a wave rotating around an amphidromic point, which is a point with zero amplitude for the tidal component considered (in this case M2).

[5] 'Degenerate' refers to the fact that the amphidromic point has shifted on land. The tidal wave still travels around this 'virtual' point.

4.2.2.2 Results of Scenario 1 compared to the reference scenario

In this section, the results of Scenario 1 are presented. A comparison is made to the reference scenario without any offshore wind farms.

Temperature and salinity

In Figure 4.8 the change in the annual mean of the sea surface temperature and sea surface salinity is presented. The largest changes in surface temperature can be observed in and around the band of 54° – 55° latitude, with decreases of up to 0.5 °C, but also some temperature increases around the OWFs. Increases of up to 0.2-0.3 °C can also be seen within the OWFs off the Danish coast. The largest impact on sea surface salinity can be found in the region of the Rhine region of freshwater influence (ROFI).

In Figure 4.9 the change in the annual mean of the vertical temperature difference is shown. There, a larger impact than in the surface values is present, which implies that the lower part of the water column is more affected, due to enhanced vertical mixing. The largest differences are again present in the OWFs in and around the band of 54° – 55° latitude and off the Danish coast, with decreases in the mean vertical temperature difference of more than 0.5 °C in large areas. In a relative sense, the change in average temperature stratification can be more than 60% in many of the OWFs, especially in the northern part of the North Sea.

In Figure 4.10 the change in the annual mean of the vertical salinity difference is shown. The largest differences are present in the OWFs north of the Netherlands and the Rhine ROFI, with decreases in mean vertical salinity difference of up to 0.5 psu in the latter area. In a relative sense, this implies a reduction in salinity stratification of more than 60% in some areas.

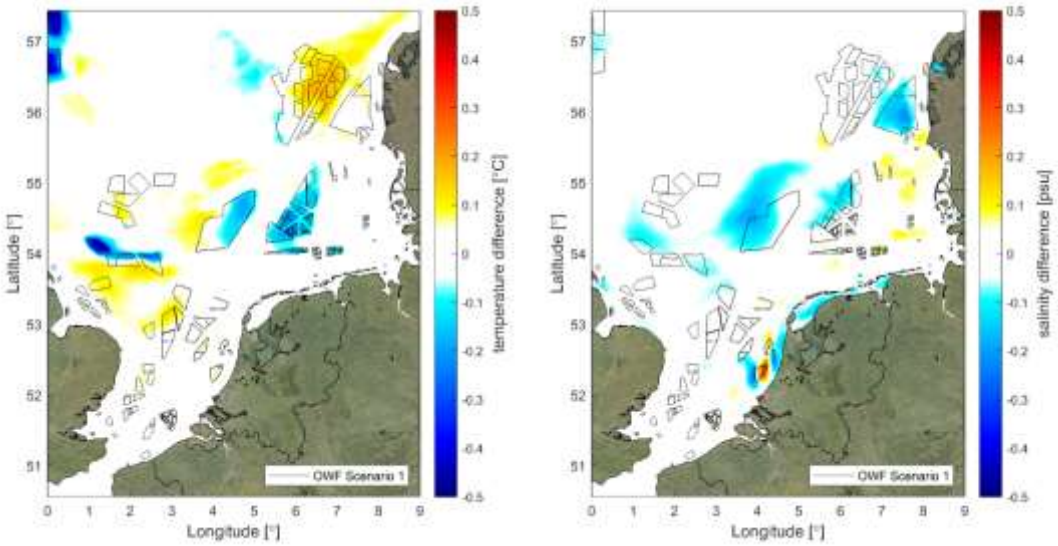

Figure 4.8 Change in the annual mean of sea surface temperature (left) and sea surface salinity (right) – scenario 1 (only absolute changes are shown as these are the most relevant for these parameters.

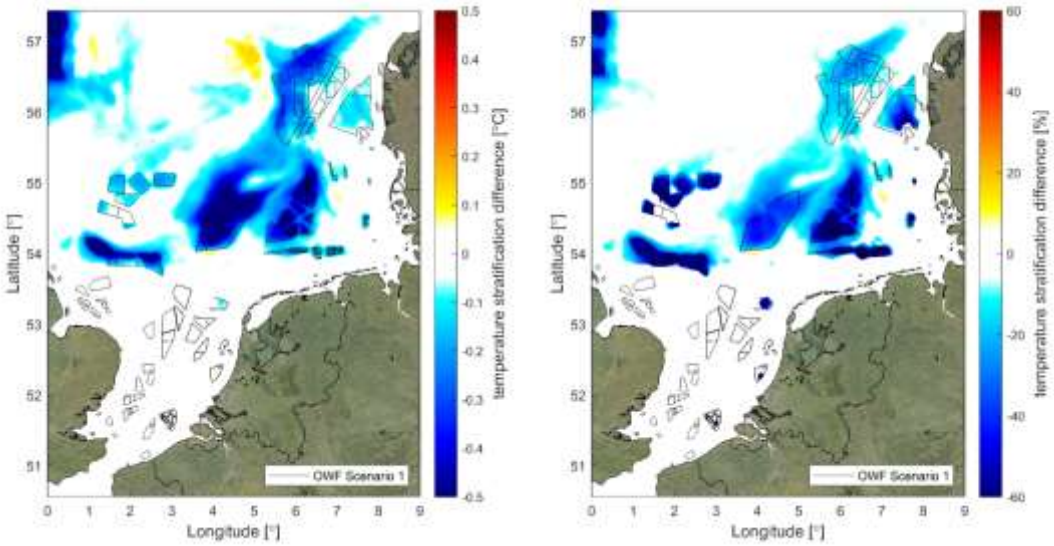

Figure 4.9 Absolute change (left) and relative change (right) in the annual mean of vertical temperature difference (scenario 1). Mean stratification differences <0.5 °C are not shown in the right chart.

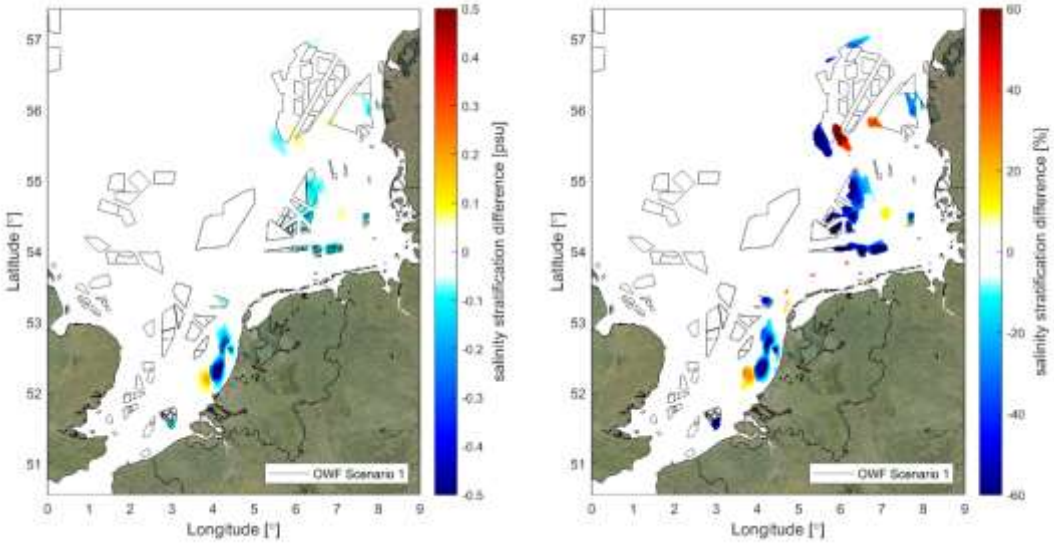

Figure 4.10 Absolute change (left) and relative change (right) in the annual mean of vertical salinity difference (2020 scenario). Mean stratification differences <0.5 psu are not shown in the right chart.

Residual currents

In Figure 4.11 the change in magnitude as well as in vector difference (to indicate any changes in direction) of the annual mean (residual) currents at the surface is presented. These figures show reductions of residual currents by more than 0.03 m/s at the surface, primarily inside the OWFs. Outside the OWFs both increases and decreases in magnitude occur, with some increases along the OWF areas of more than 0.03 m/s. There appears to be less circulation around 54°-55° latitude in the central North Sea.

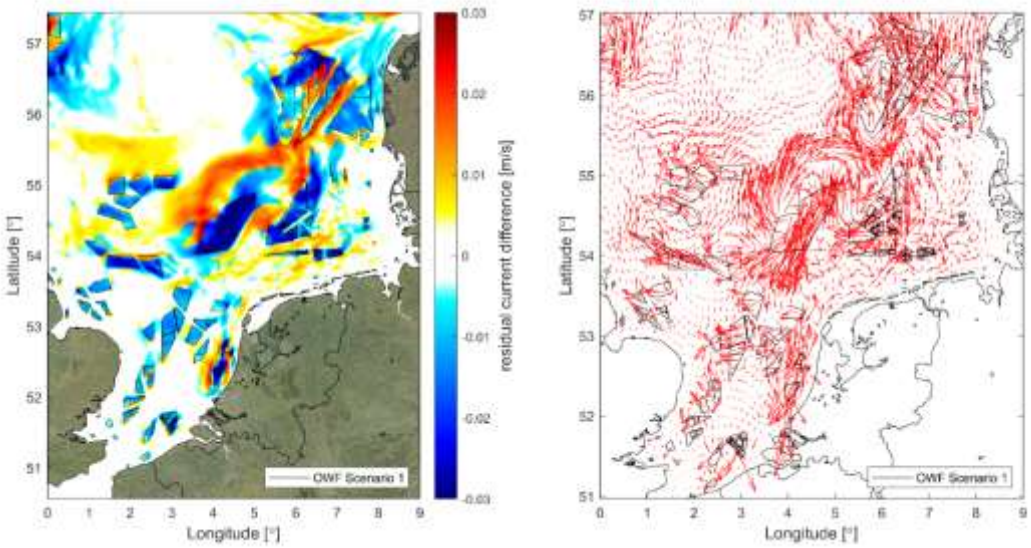

Figure 4.11 Absolute change in annual residual velocity in the top layer (2007) – magnitude (left) and vectors (right).

M2 tide

In Figure 4.12 the spatial pattern of the change in M2 tidal amplitude and phase lag is shown. In most parts of the northern and central North Sea, the impact on the amplitude is negligible with a magnitude of less than 1 cm. In the southern North Sea, primarily along the Belgian, Dutch and German coasts, a more significant reduction in amplitude of up to 1 cm is present. The largest impact on the phase lag is present around the amphidromic points. Note however that the resulting impact on tidal water levels is limited there because of small local tidal amplitudes.

Further away from the amphidromic points the largest increase in phase lag is present to the west of Texel and off the German and southern Danish coast, whereas south of Norway a decrease in the M2 phase is present.

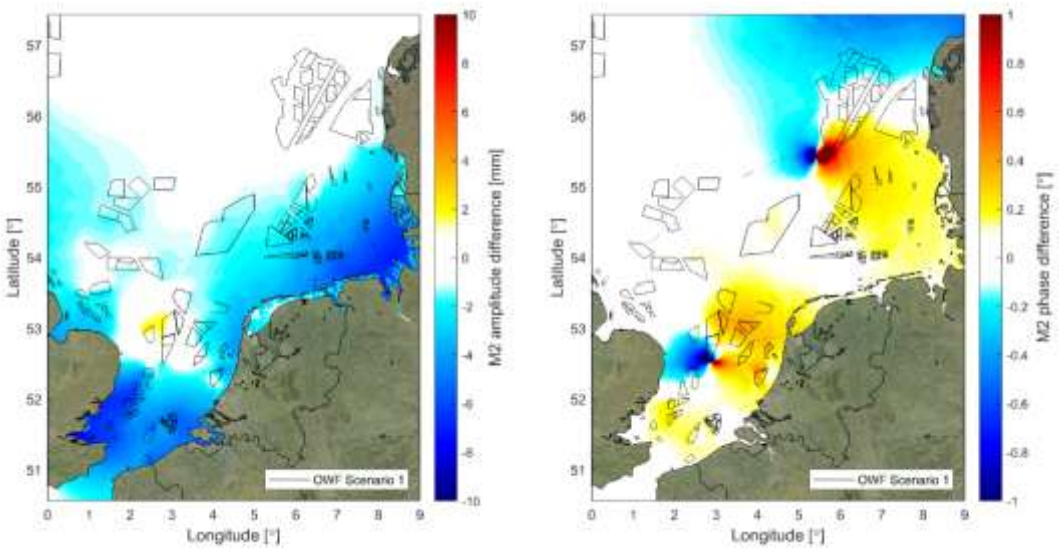

Figure 4.12 Change in M2-tide (2007) – amplitude (left) and phase lag (right).

4.2.2.3 Results of Scenario 2 compared to Scenario 1

In this section, the results of Scenario 2 are presented. Because the OWFs in scenario 1 and scenario 2 coincide for a large part, their impact compared to the reference simulation is similar. Therefore, the differences between scenarios 1 and 2 (i.e., the effect of the additional OWFs in scenario 2) is assessed in this section.

Temperature and salinity

In Figure 4.13 the change in the annual mean of the sea surface temperature and sea surface salinity is presented. This shows that the presence of additional OWFs has a relatively limited impact. In and around the additional OWFs, the mean temperature decreases by around 0.1 °C. Surface salinity shows hardly any changes larger than 0.1 psu.

In Figure 4.14 the change in the annual mean of the vertical temperature difference is shown. There, a larger impact is present than in the surface values, which implies that the lower part of the water column is more affected, due to enhanced vertical mixing. Changes in vertical temperature stratification are found in and around the additional OWFs.
In a relative sense, the change in temperature stratification can be more than 50% in some areas.

In Figure 4.15 the change in the annual mean of the vertical salinity difference is shown. The impact of additional OWFs on salinity stratification is very limited. Only in the OWF to the north of the Wadden Sea, a change of 0.5 psu can be observed.

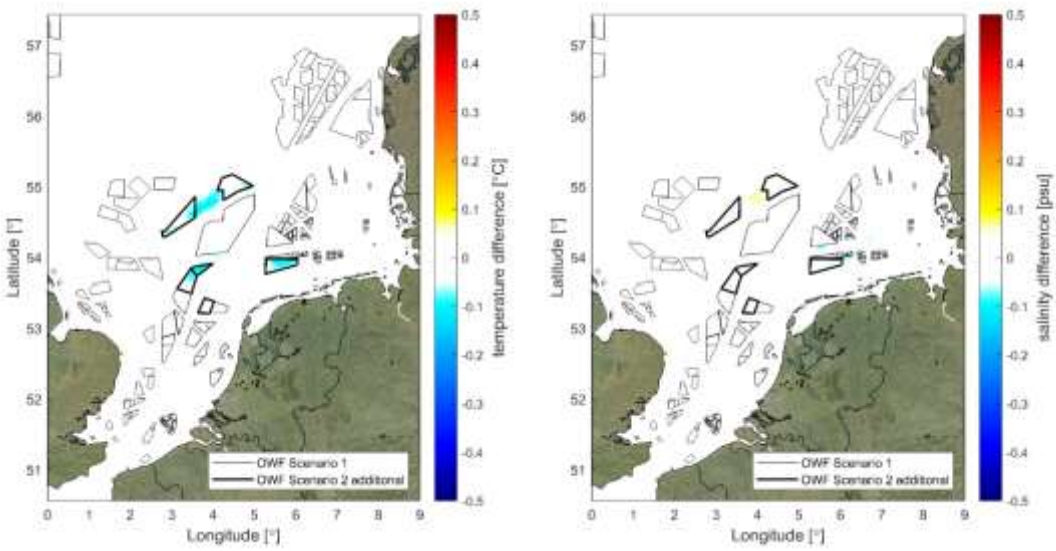

Figure 4.13 Change in the annual mean of sea surface temperature (left) and sea surface salinity (right) – scenario 2 compared to scenario 1.

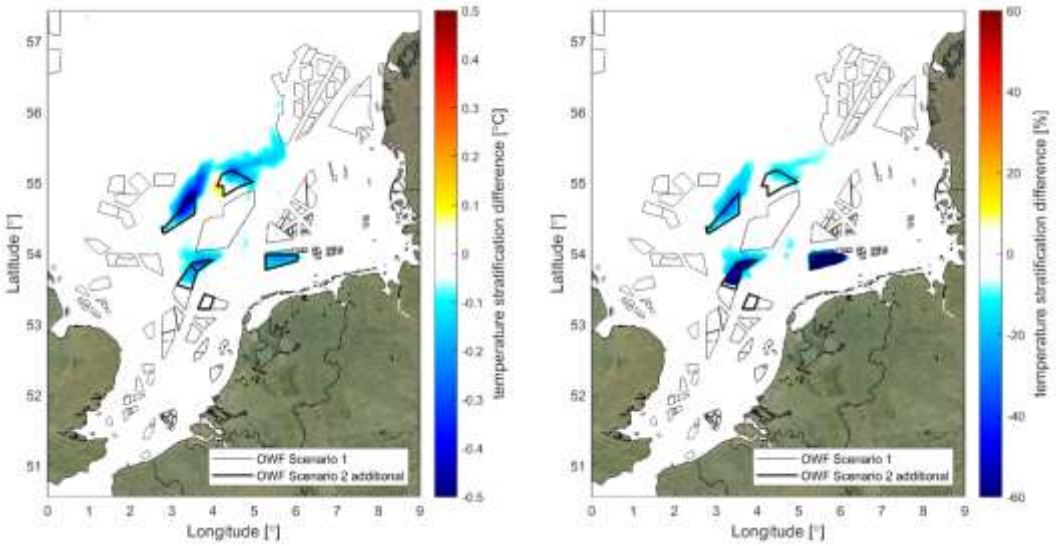

Figure 4.14 Absolute change (left) and relative change (right) in the annual mean of vertical temperature difference - scenario 2 compared to scenario 1. Mean stratification differences <0.5 °C are not shown in the right chart.

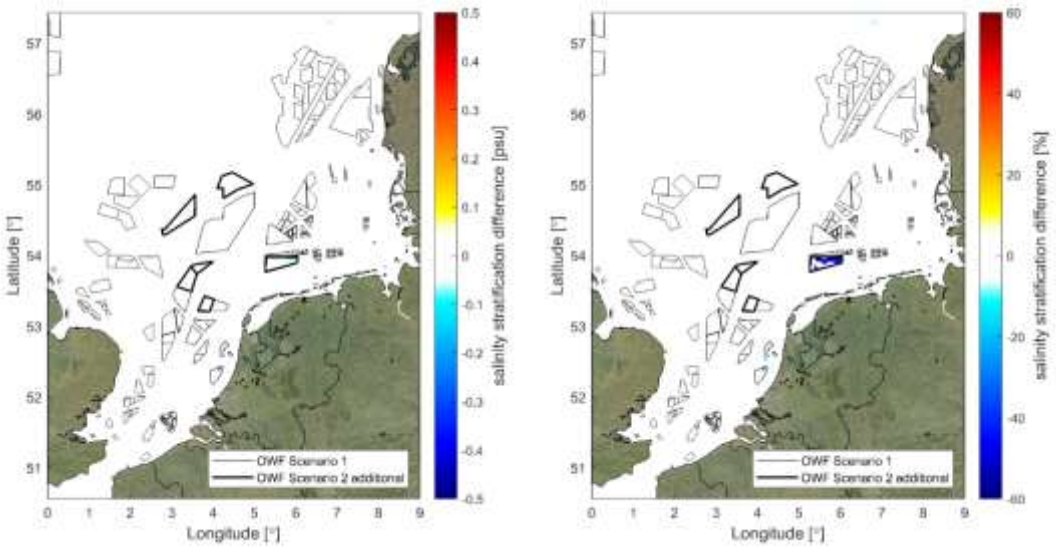

Figure 4.15 Absolute change (left) and relative change (right) in the annual mean of vertical salinity difference - scenario 2 compared to scenario 1. Mean stratification differences <0.5 psu are not shown in the right chart.

Currents

In Figure 4.16 the change in the magnitude as well as in the vector difference of the annual mean (residual) currents at the surface is presented for the year 2007. The largest impact of the additional OWFs can again be found in and around the additional OWFs.

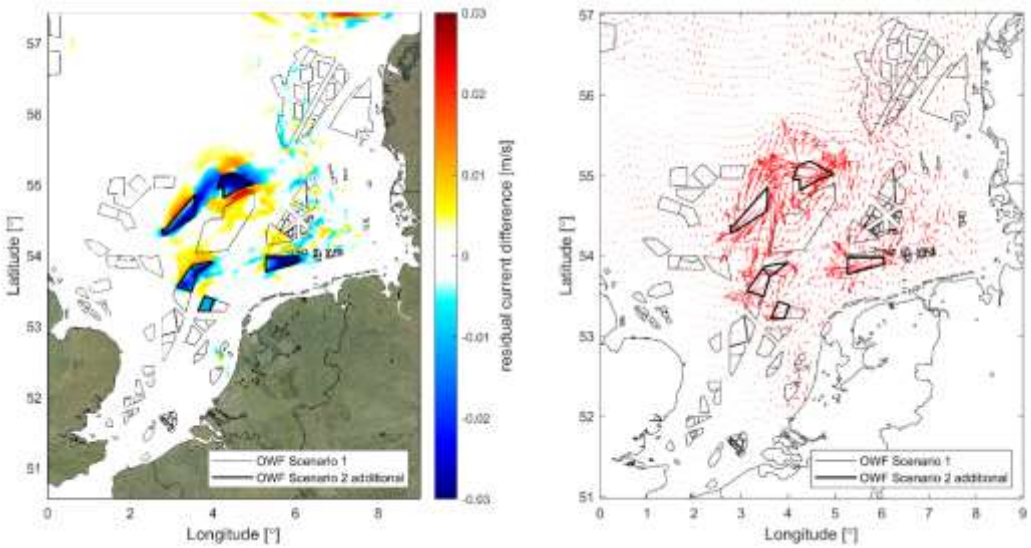

Figure 4.16 Absolute change in annual residual velocity in the top layer (2007) – magnitude (left) and vectors (right) - scenario 2 compared to scenario 1.

M2 tide

In Figure 4.17 the spatial pattern of the change in M2 tidal amplitude and phase lag is shown. The impact of the additional OWFs on the amplitude and phase is negligible (<1mm amplitude and <0.1°).

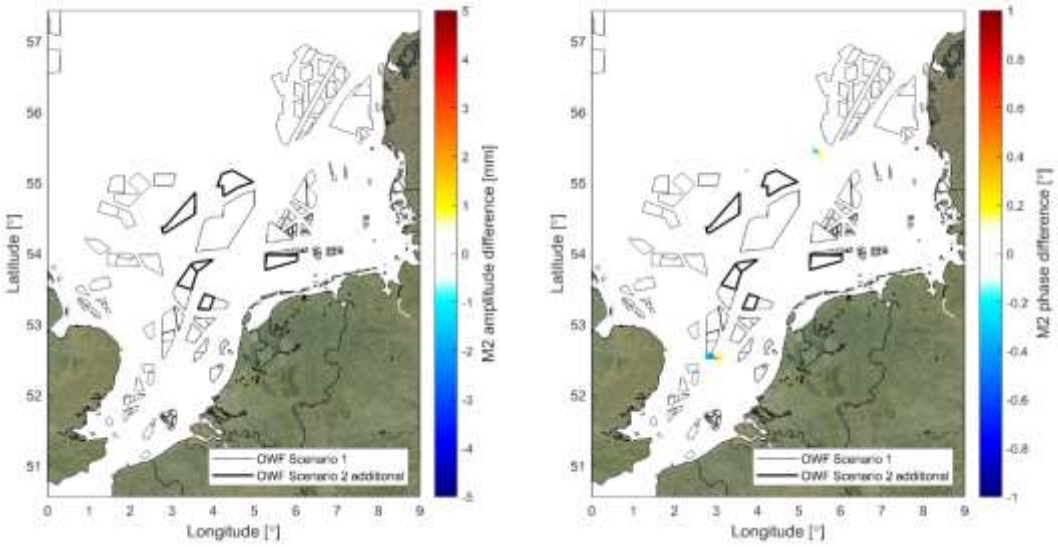

Figure 4.17 Change in M2-tide (2007) – amplitude (left) and phase lag (right) - scenario 2 compared to scenario 1.

4.2.2.4 Comparison of temperature stratification time series

In addition to the previously presented maps of mean temperature stratification, its temporal variation is assed in a number of locations at the edge of offshore wind farms in the scenarios (see Figure 4.18). Figure 4.19 and Figure 4.20 show the amount of temperature stratification in 2007 for stations F3PFM and NLO2. In the scenario computations, OWFs have can have an impact on the hydrodynamic conditions through two mechanisms: the enhanced production of turbulent kinetic energy due to the presence of piles in the water column and the reduction of wind speed due to the presence of the wind turbines in the atmospheric boundary layer.

In the legend, the duration of the temperature stratification is shown, defined as the number of days for which the vertical temperature difference is above 0.5°C (plotted as a dashed line). Both scenarios have a significant impact on the amount and duration of temperature stratification. At station F3PFM, the duration of stratification drops from 155.8 days in the reference scenario to 133.4 and 139.0 days in scenarios 1 and 2. At station NL02, the duration of stratification drops from 156.8 days in the reference scenario to 131.9 and 130.5 days in scenarios 1 and 2.

At the other stations plotted in Figure 4.18, hardly any change in the amount and duration of temperature stratification is noticeable, in both scenarios. In stations NOORDWK70 and EURPFM this is because there is hardly any temperature stratification in the reference scenario. Stations ANSRA, AUKFPFM, UKO5 and A12 are in areas with seasonal temperature stratification but are further away from OWFs included in the scenarios.

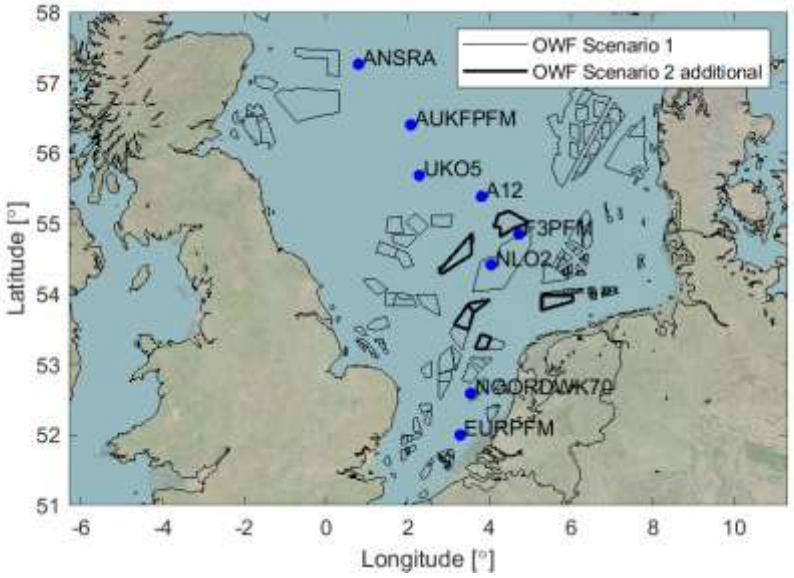

Figure 4.18 Locations of stations with plotted stratification and OWF scenarios.

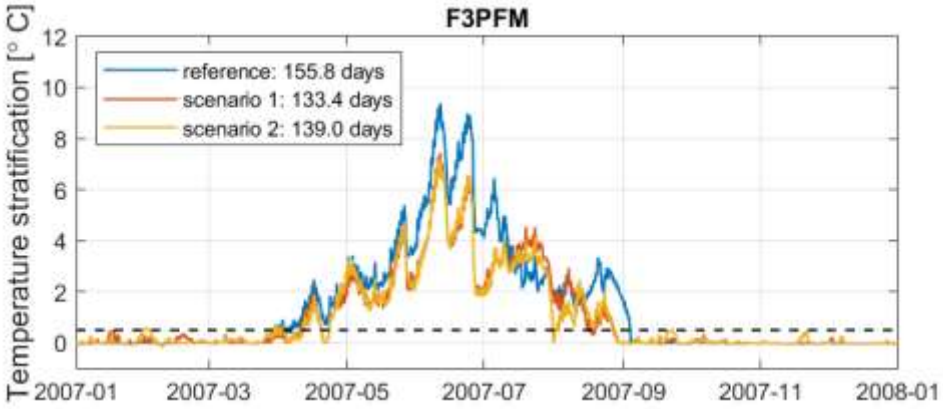

Figure 4.19 Temperature stratification at platform F3 for different modelled scenarios.

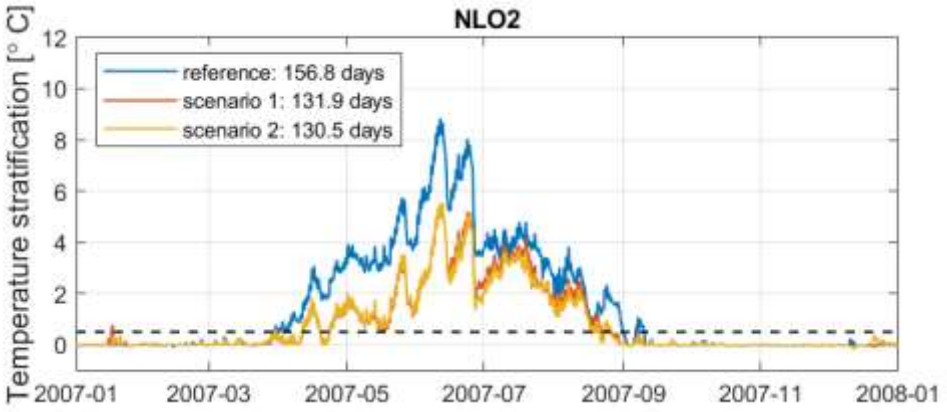

Figure 4.20 Temperature stratification at station NLO2 for different modelled scenarios.

4.3 Wave model

This section describes the model setup for the wave modelling and its results for the different scenarios. The wave model used for this analysis is equal to the one used for the 2021 Wozep study (Zijl et al, 2021). We refer to this report for further details on the wave model. Changes in wave patterns can result in changes in total bed shear stress. This will in turn affect sediment dynamics. Direct effects of changes in bed shear stress (e.g. on species composition of the seabed) are not assessed in this study.

4.3.1 Modelling approach

The wave model was run in non-stationary mode for the period from 2006 to 2008, with a timestep of 1 hour. The numerical settings and boundary conditions were applied in the same way as in the 2021 study.

The effects of the wind farms in scenario 1 and 2 were again modelled by adjusting the wind forcing - a 10% reduction of wind speeds applied uniformly across the areas designated for future wind farm development in the scenario model runs. This uniform reduction in wind speeds inside wind farm contours is illustrated in Figure 4.21.

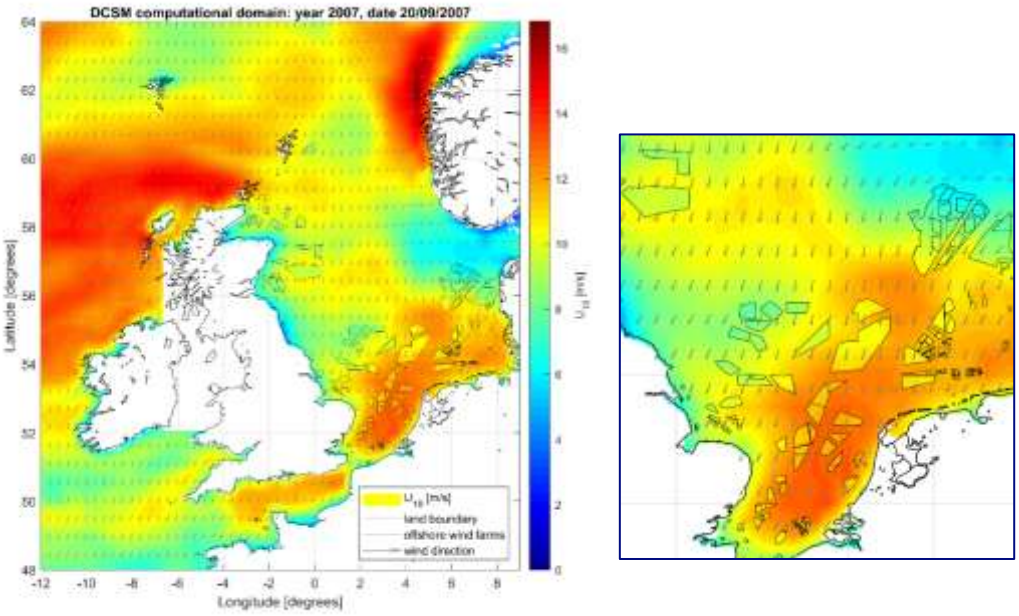

Figure 4.21 Plot of the modified wind speed field in scenario 2 for one time step. Left figure shows the wind forcing over the model domain, and the right figure is zoomed in on the Dutch North Sea.

4.3.2 Results

The results of wave modelling for the base scenario (without OWFs) are illustrated with a map of significant wave heights for one time step of the simulations in Figure 4.22. The results of wave modelling for the scenarios 1 and 2 are presented in terms of instantaneous absolute and relative differences in significant wave height between the base scenario and a future scenario in Figure 4.23 (scenario 1) and Figure 4.24 (scenario 2). In these figures the plot is zoomed in on the part of the North Sea where wind farms are located – outside of this area there are no changes to wave heights between the scenarios.

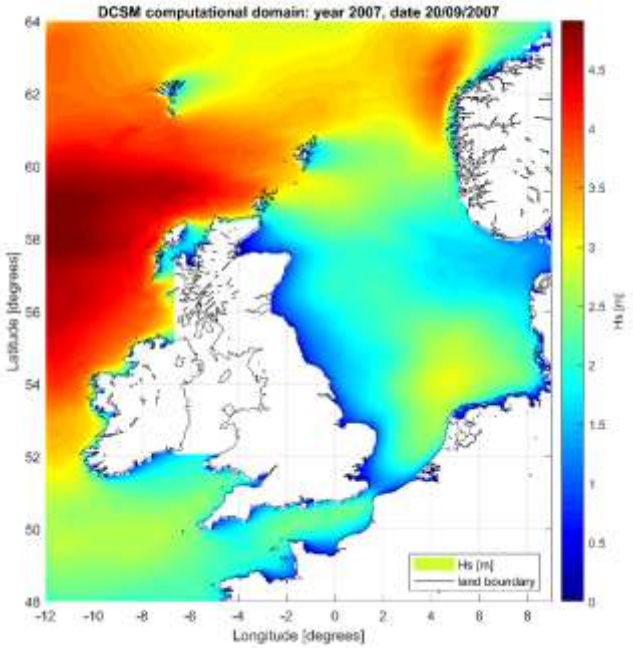

Figure 4.22 Significant wave height (H_S) in the base scenario (without OWFs) on 20.09.2007.

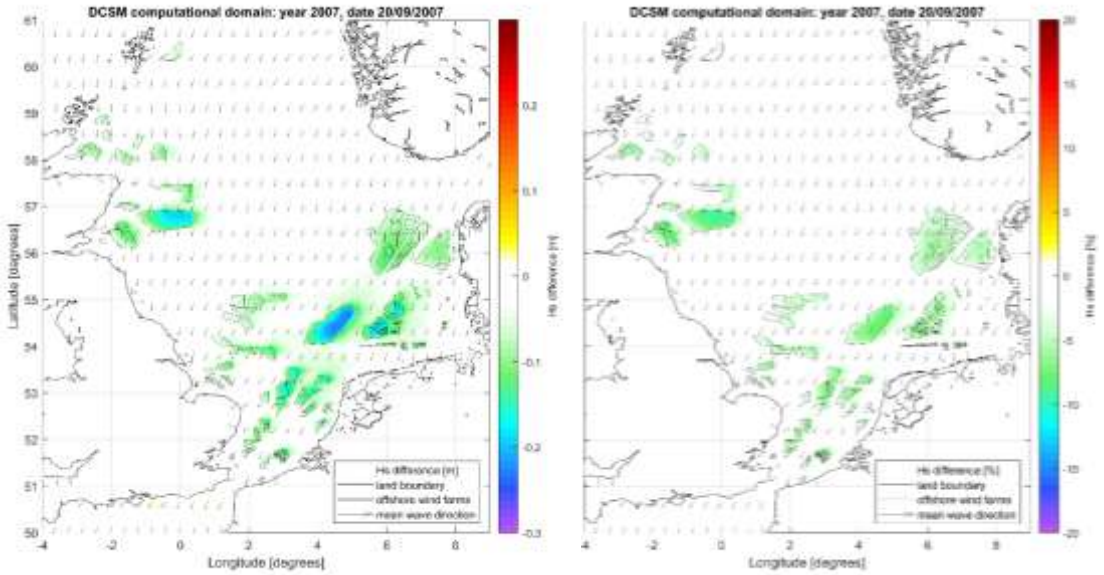

Figure 4.23 Absolute (left) and relative (right) differences in significant wave height (H_s) between the base scenario and scenario 1, on 20.09.2007.

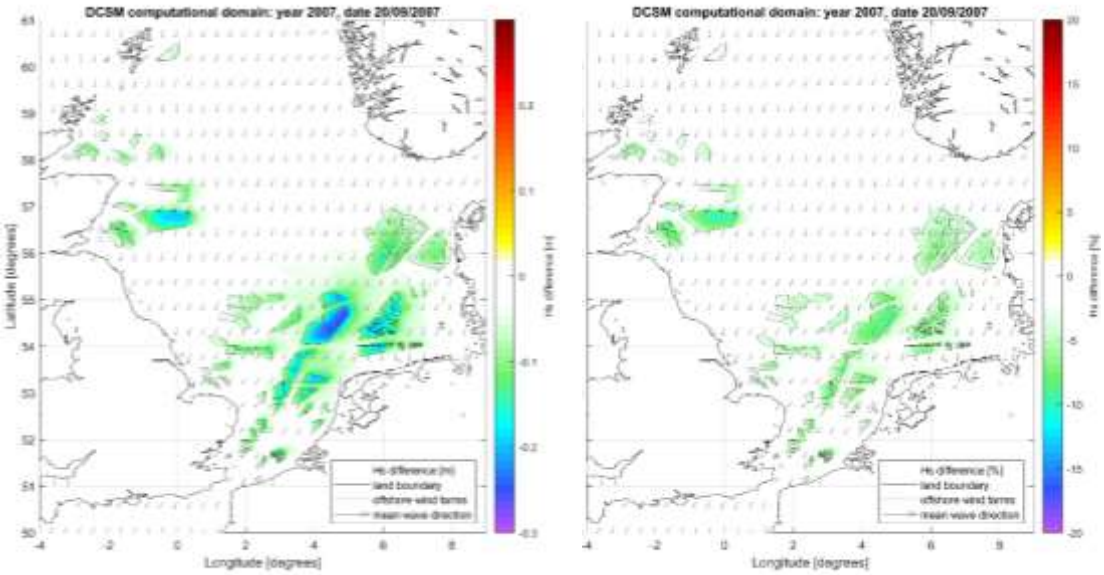

Figure 4.24 Absolute (left) and relative (right) differences in significant wave height (H_s) between the base scenario and scenario 2, on 20.09.2007.

The plots of difference in wave heights clearly demonstrate the reduction in wave height due to the presence of the wind farms; this decrease in significant wave heights can reach up to 8% reduction within the wind farm contours. The reduction in wave height depends on the direction of the waves and the wind with respect to the clusters of wind farms and the magnitude of wave height (and wind speed). The areas with wave height reduction due to the presence of wind farms can extend well beyond the wind farm contours, with visible wave height reduction wakes. In areas with dense clusters of wind farms (e.g. in the Dutch North Sea, and especially in scenario 2) these wakes can reach neighbouring wind farm contours; in these cases, global wave height reduction zones are visible, encompassing a group of wind farms and stretching over large distances.

In the present schematization, wave height reduction beyond the wind farm contours is caused by the reduction in local wind-induced wave generation inside the wind farms. Atmospheric wake effects are not resolved in the present model. Further improvement to the schematization of the wind forcing conditions in and around the wind farms can lead to a more accurate estimate of wave height reduction.

For the purposes of the present study, the wave model results are further used for the fine sediment modelling.

4.4 Fine sediment model

This section shows the scenario results for SPM concentrations, both near the surface and near the bed. For interpretation, also figures on bed shear stress (and differences between scenarios) are shown, as bed shear stress steers resuspension. Mixing over the water column is another important steering factor, notably for near-surface SPM. These are presented in section 4.2 and the discussion on sediment fluxes in Chapter 3.

For the reference scenario, absolute values are presented. For scenario 1 the difference with the reference is shown and for scenario 2 the difference with 1. Results are available as year-averages and summer and winter averages. Many of the results are presented in both absolute effects (in change in mg/l) as well as relative effect (change in %). In areas that are very turbid an increase of a few mg/l might be not much in relative terms and in very clear water even a tiny increase in absolute terms can be large in relative terms. To interpret the importance of the effects, both are required.

4.4.1 Year-average effects

Figure 4.25 shows the year average bed shear stress and changes herein due to the OWF scenarios. Inside OWFs, computed bed shear stress was lower, higher or equal to surroundings, depending on the region. In the West most parks show an increase in bed shear stress, in the East a decrease and in the centre the effect is negligible. Outside OWFs generally equal to less bed shear stress is computed (except for Dover Strait). Along the Dutch coast this is probably related to the decrease in M2 amplitude, see the hydrodynamic model results in Section 4.2.

Figure 4.26 and Figure 4.27 show the year average near-bed and near-surface SSC and changes herein due to the OWF scenarios. Overall, SSC values decrease near the shores of the Netherlands, Germany and Denmark, but increase farther offshore towards the UK. This is observed both near the bed and near the surface, although inside wind farms surface SSC increases in many (but not all) OWFs due to additional mixing.

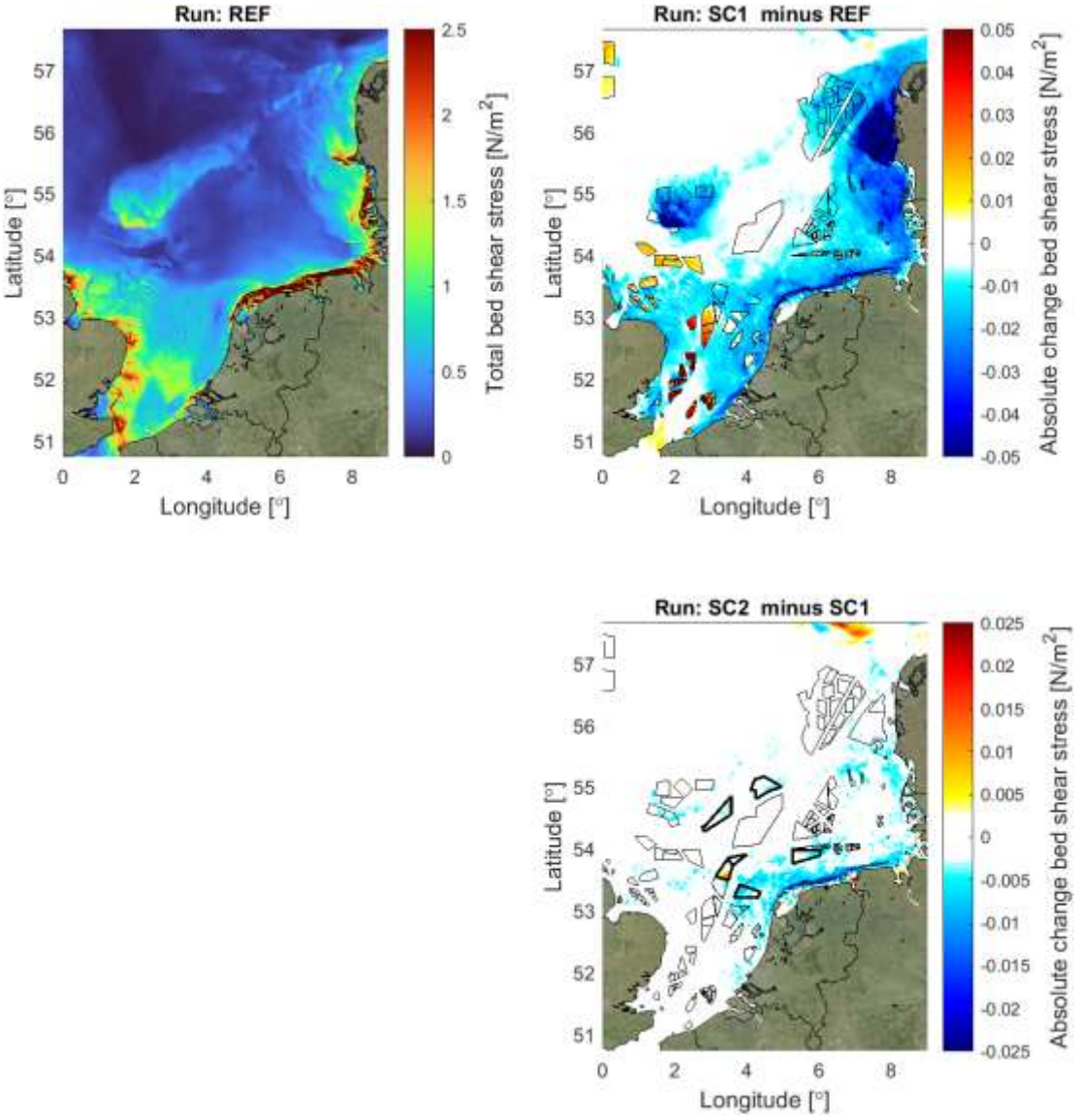

Figure 4.25 Year-average bed shear stress changes (2007) for future wind farm scenarios 1 and 2. Upper-left panel shows the total bed shear stress [N/m^2] in the simulation without wind farms (average of 2007, including the effect of waves). Upper-right panel shows the bed shear stress change [N/m^2] when the wind farms of scenario 1 are added. Thin black contours indicate the wind farms in scenario 1. Bottom-right panel shows the bed shear stress change [N/m^2] for scenario 2 compared to scenario 1. The additional wind farms compared to scenario 1 are indicated with thick black contours.

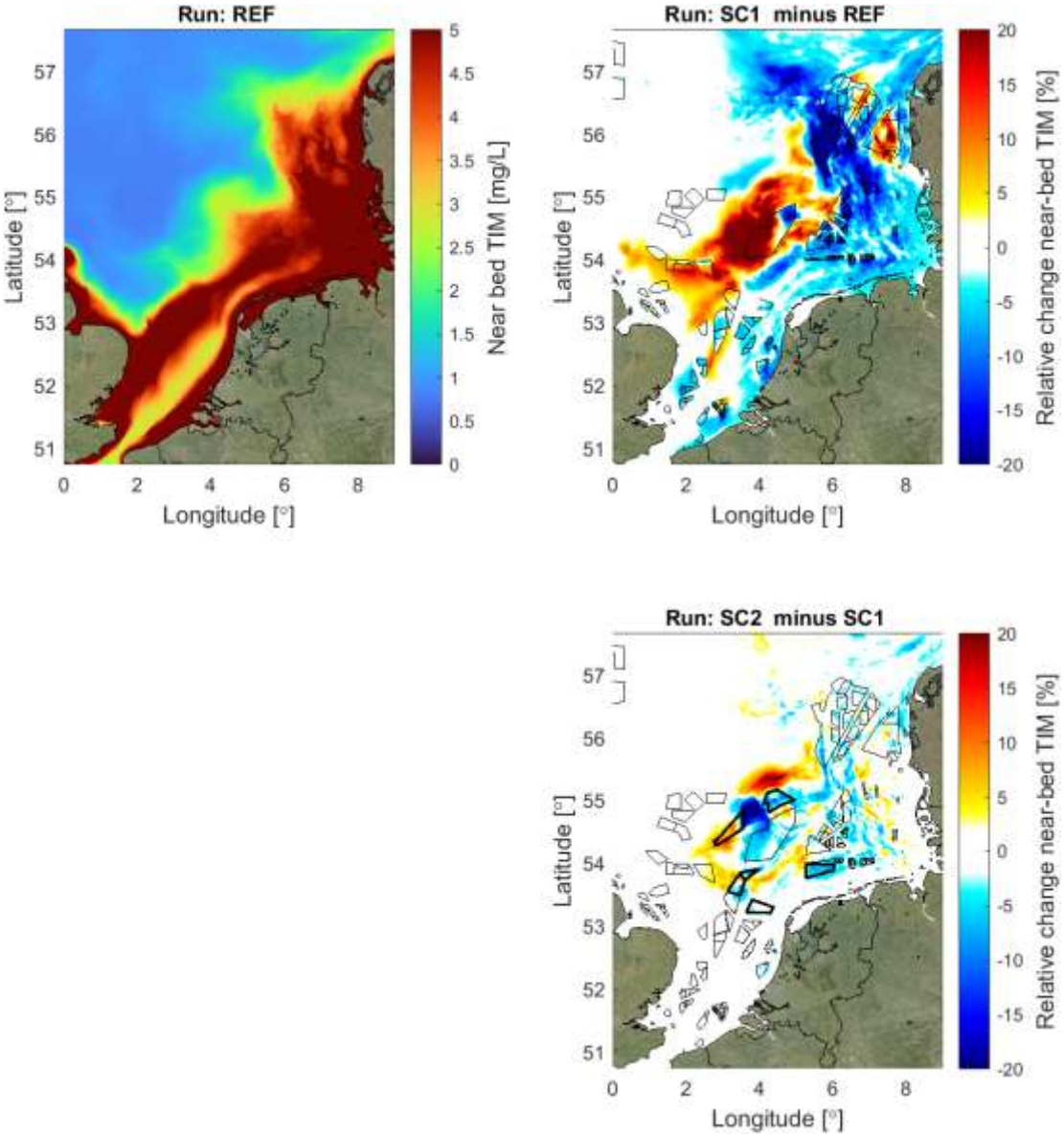

Figure 4.26 Changes in year-average, near-bed total inorganic matter (TIM) for future wind farm scenarios 1 and 2. Upper-left panel shows the near-bed TIM [mg/L] (average of 2007) in the simulation without wind farms. Upper-right panel shows changes in near-bed TIM [%] when the wind farms of scenario 1 are added. Thin black contours indicate the wind farms in scenario 1. Bottom-right panel shows the change in near-bed TIM [%] for scenario 2 compared to scenario 1. The additional wind farms compared to scenario 1 are indicated with thick black contours.

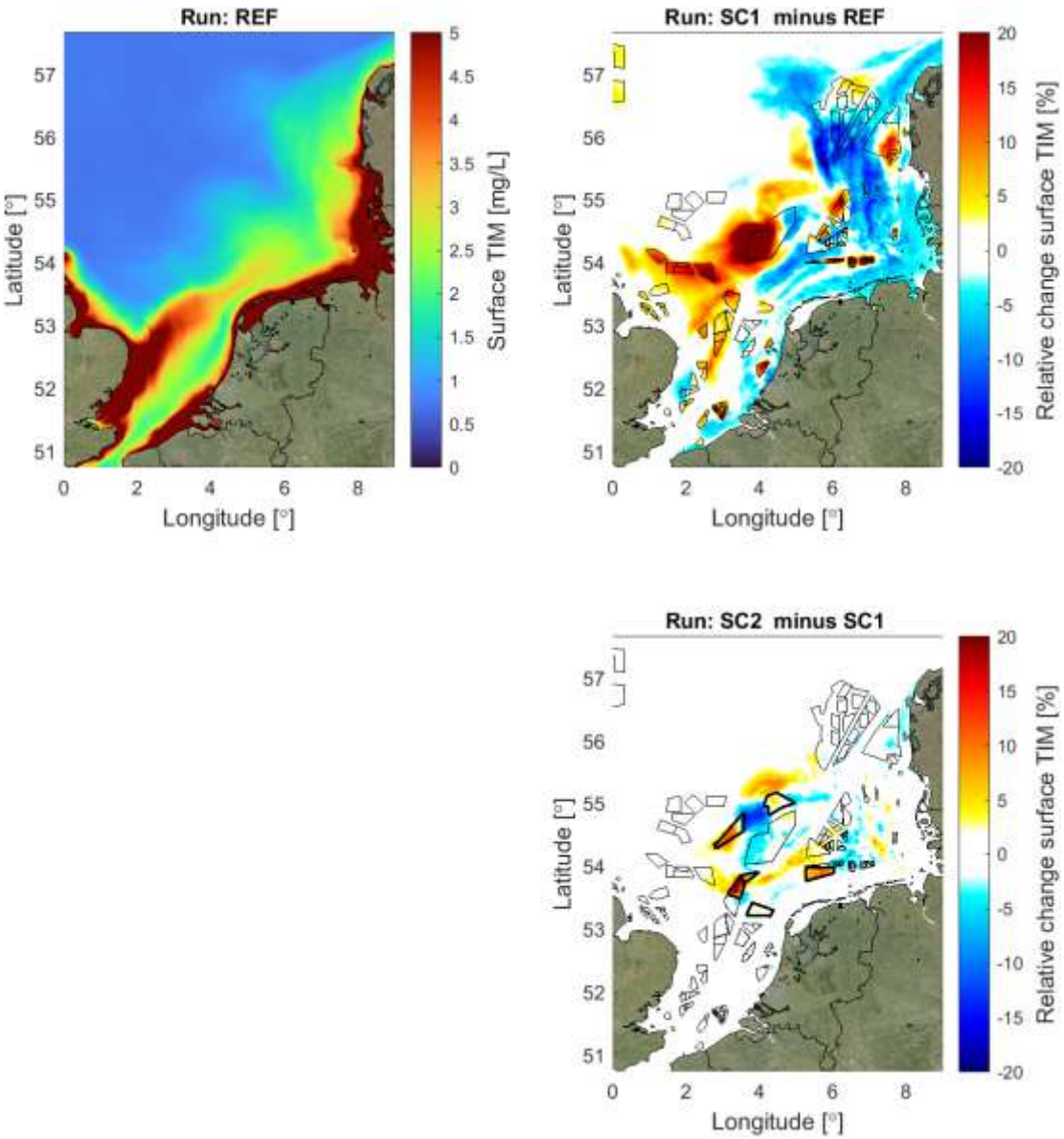

Figure 4.27 Changes in year-average, surface total inorganic matter (TIM) for future wind farm scenarios 1 and 2. Upper-left panel shows the surface TIM [mg/L] in the simulation without wind farms (average of 2007). Upper-right panel shows the change in surface TIM [%] when the wind farms of scenario 1 are added. Thin black contours indicate the wind farms in scenario 1. Bottom-right panel shows the change in surface TIM [%] for scenario 2 compared to scenario 1. The additional wind farms compared to scenario 1 are indicated with thick black contours.

4.4.2 Seasonal effects

Apart from year-average results, also seasonally average results are available of bed shear stress (Figure 4.28, Figure 4.29 and Figure 4.30), surface SSC (Figure 4.31, Figure 4.32 and Figure 4.33) and bottom SSC (Figure 4.34, Figure 4.35 and Figure 4.36). These results are not separately discussed herein for brevity.

Near-bed changes are quite persistent over the seasons, although absolute changes vary with hydrodynamic forcing, with higher bed shear stress and SSC values in winter. How much of this change is also observed near the surface, depends on the amount of stratification. In stratified conditions the near-surface response of SSC is different. Therefor for surface SSC seasonal differences in the effects of OWFs are more pronounced.

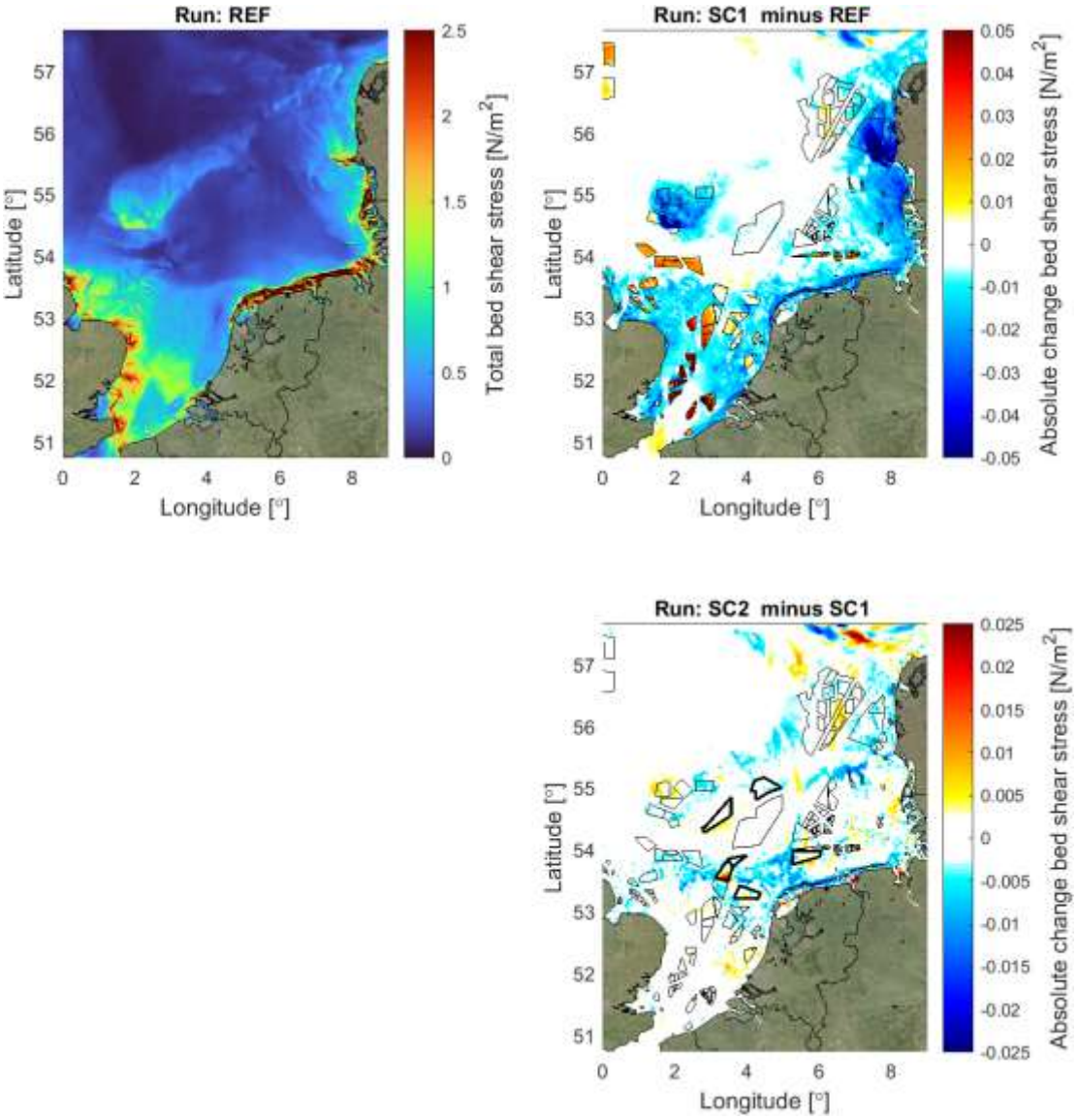

Figure 4.28 Bed shear stress changes for future wind farm scenarios 1 and 2 – average of March-May 2007 . Upper-left panel shows the total bed shear stress [N/m^2] in the simulation without wind farms (average of 2007, including the effect of waves). Upper-right panel shows the bed shear stress change [%] when the wind farms of scenario 1 are added. Thin black contours indicate the wind farms in scenario 1. Bottom-right panel shows the bed shear stress change [%] for scenario 2 compared to scenario 1. The additional wind farms compared to scenario 1 are indicated with thick black contours.

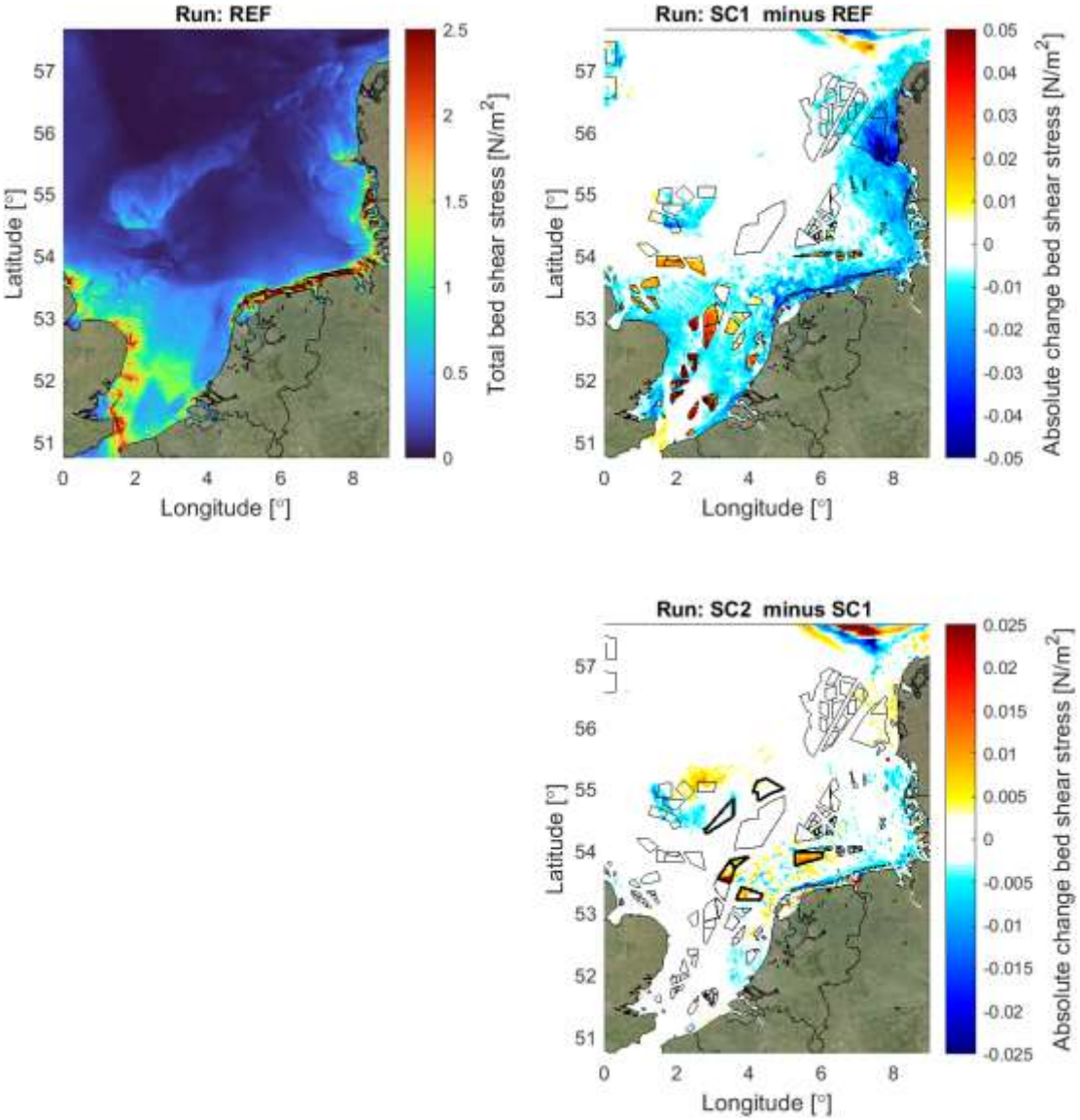

Figure 4.29 Bed shear stress changes for future wind farm scenarios 1 and 2 - average of June-August 2007. Upper-left panel shows the total bed shear stress [N/m^2] in the simulation without wind farms (average of 2007, including the effect of waves). Upper-right panel shows the bed shear stress change [%] when the wind farms of scenario 1 are added. Thin black contours indicate the wind farms in scenario 1. Bottom-right panel shows the bed shear stress change [%] for scenario 2 compared to scenario 1. The additional wind farms compared to scenario 1 are indicated with thick black contours.

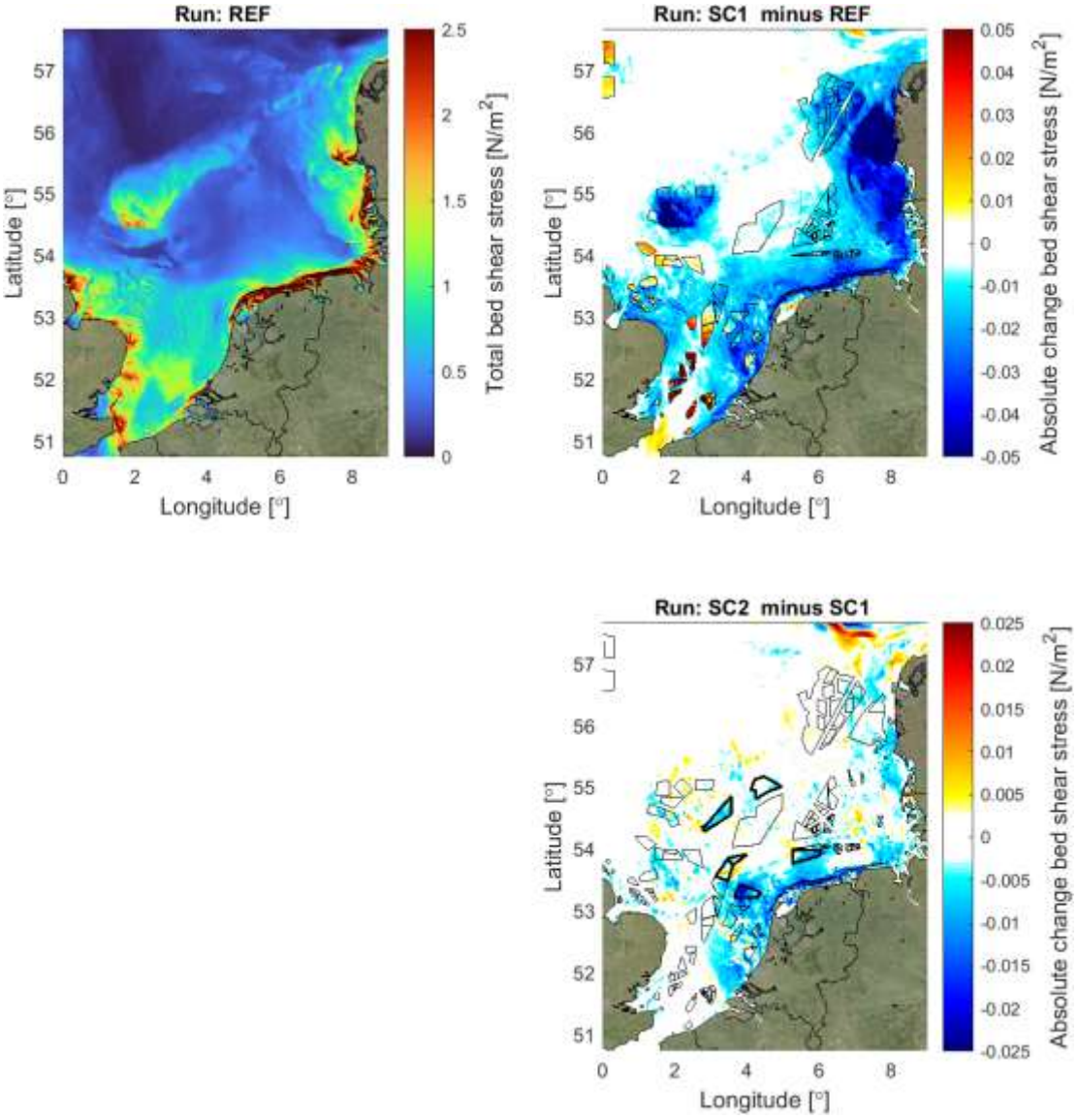

Figure 4.30 Bed shear stress changes for future wind farm scenarios 1 and 2 - average of September-December 2007. Upper-left panel shows the total bed shear stress [N/m^2] in the simulation without wind farms (average of 2007, including the effect of waves). Upper-right panel shows the bed shear stress change [%] when the wind farms of scenario 1 are added. Thin black contours indicate the wind farms in scenario 1. Bottom-right panel shows the bed shear stress change [%] for scenario 2 compared to scenario 1. The additional wind farms compared to scenario 1 are indicated with thick black contours.

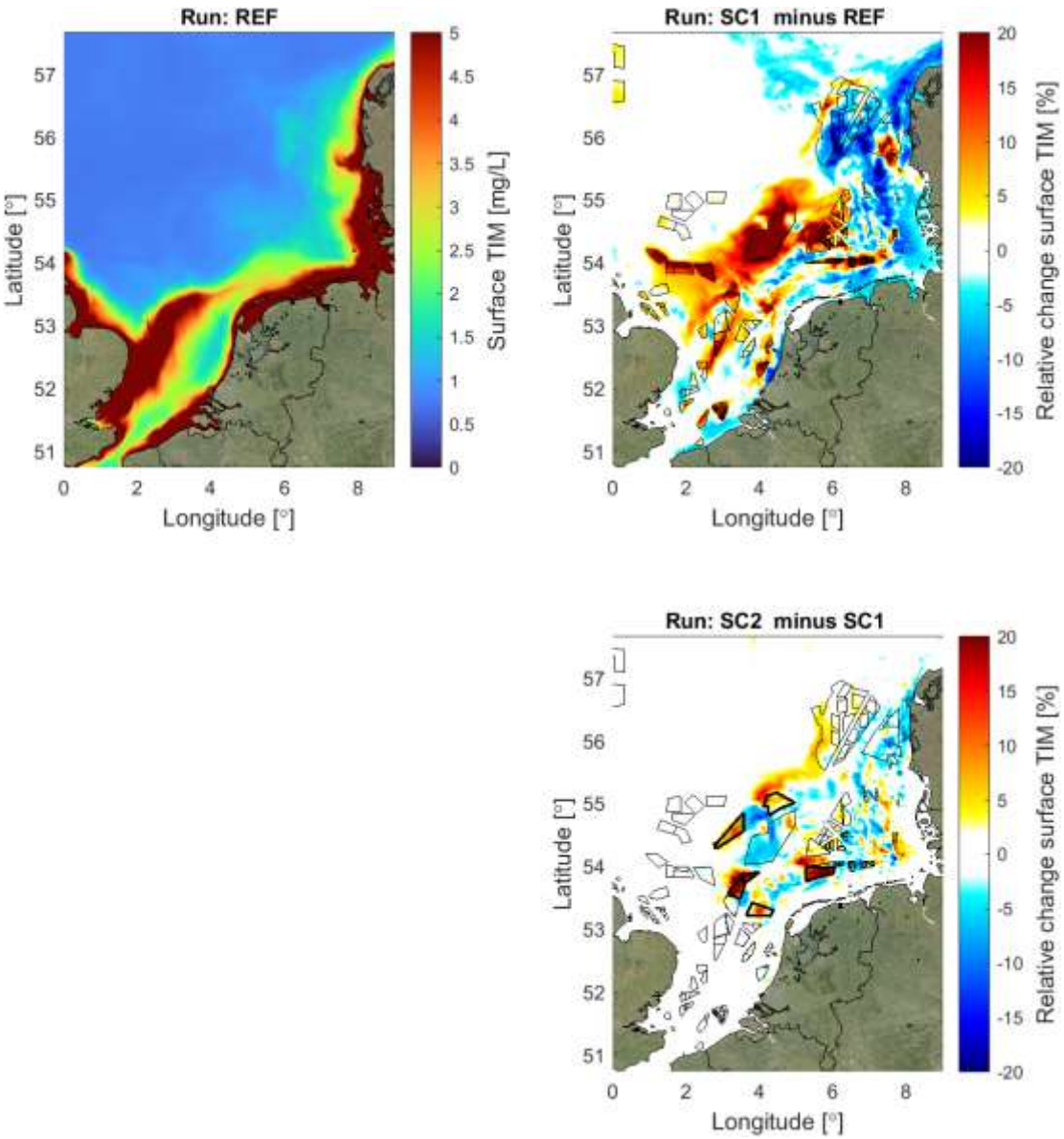

Figure 4.31 Change in surface total inorganic matter (TIM) for future wind farm scenarios 1 and 2 - average of March-May 2007. Upper-left panel shows the average, surface TIM [mg/L] in the simulation without wind farms. Upper-right panel shows the change in surface TIM [%] when the wind farms of scenario 1 are added. Thin black contours indicate the wind farms in scenario 1. Bottom-right panel shows the change in surface TIM [%] for scenario 2 compared to scenario 1. The additional wind farms compared to scenario 1 are indicated with thick black contours.

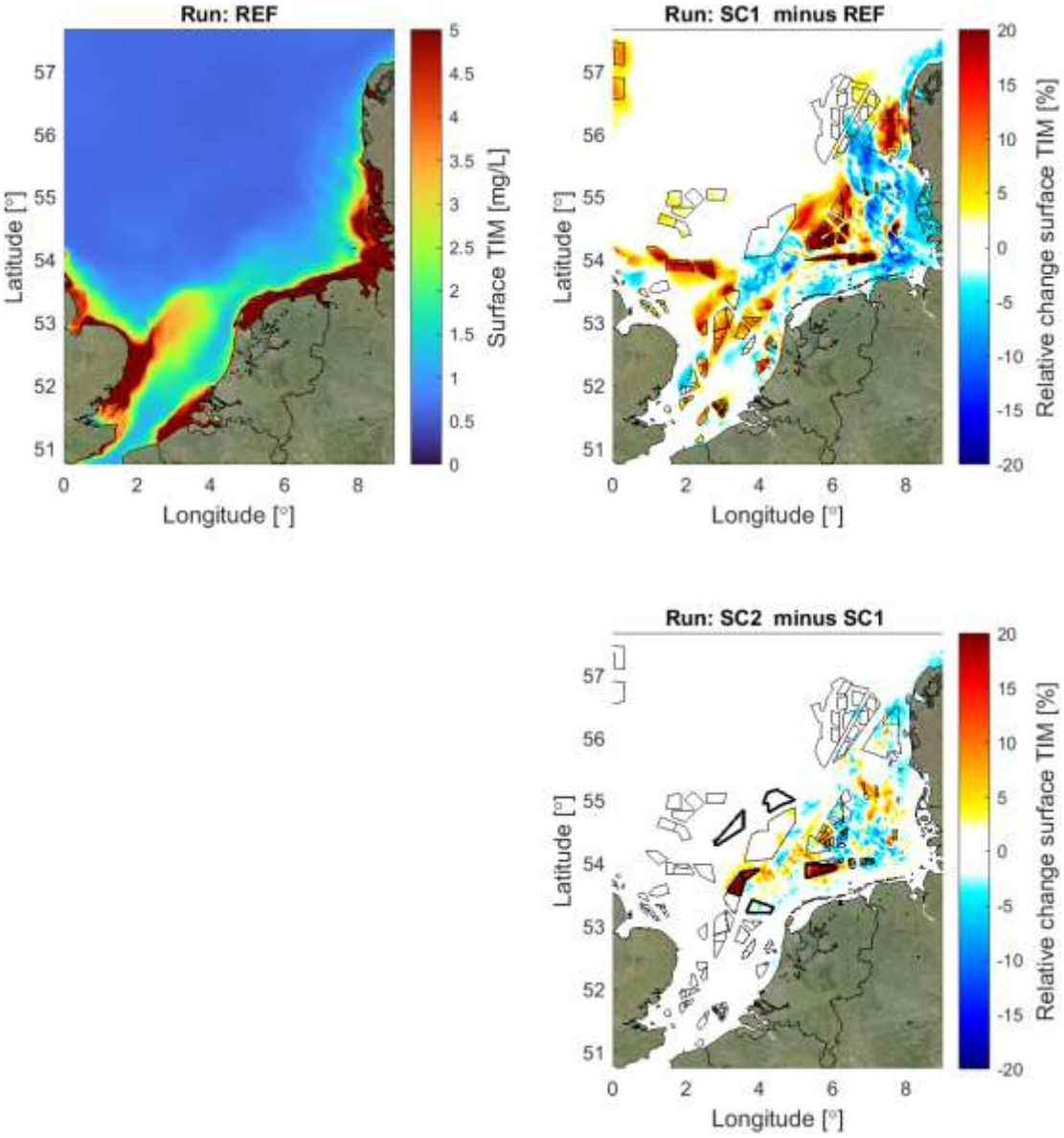

Figure 4.32 Change in surface total inorganic matter (TIM) for future wind farm scenarios 1 and 2, average of June-August 2007. Upper-left panel shows the average, surface TIM [mg/L] in the simulation without wind farms. Upper-right panel shows the change in surface TIM [%] when the wind farms of scenario 1 are added. Thin black contours indicate the wind farms in scenario 1. Bottom-right panel shows the change in surface TIM [%] for scenario 2 compared to scenario 1. The additional wind farms compared to scenario 1 are indicated with thick black contours.

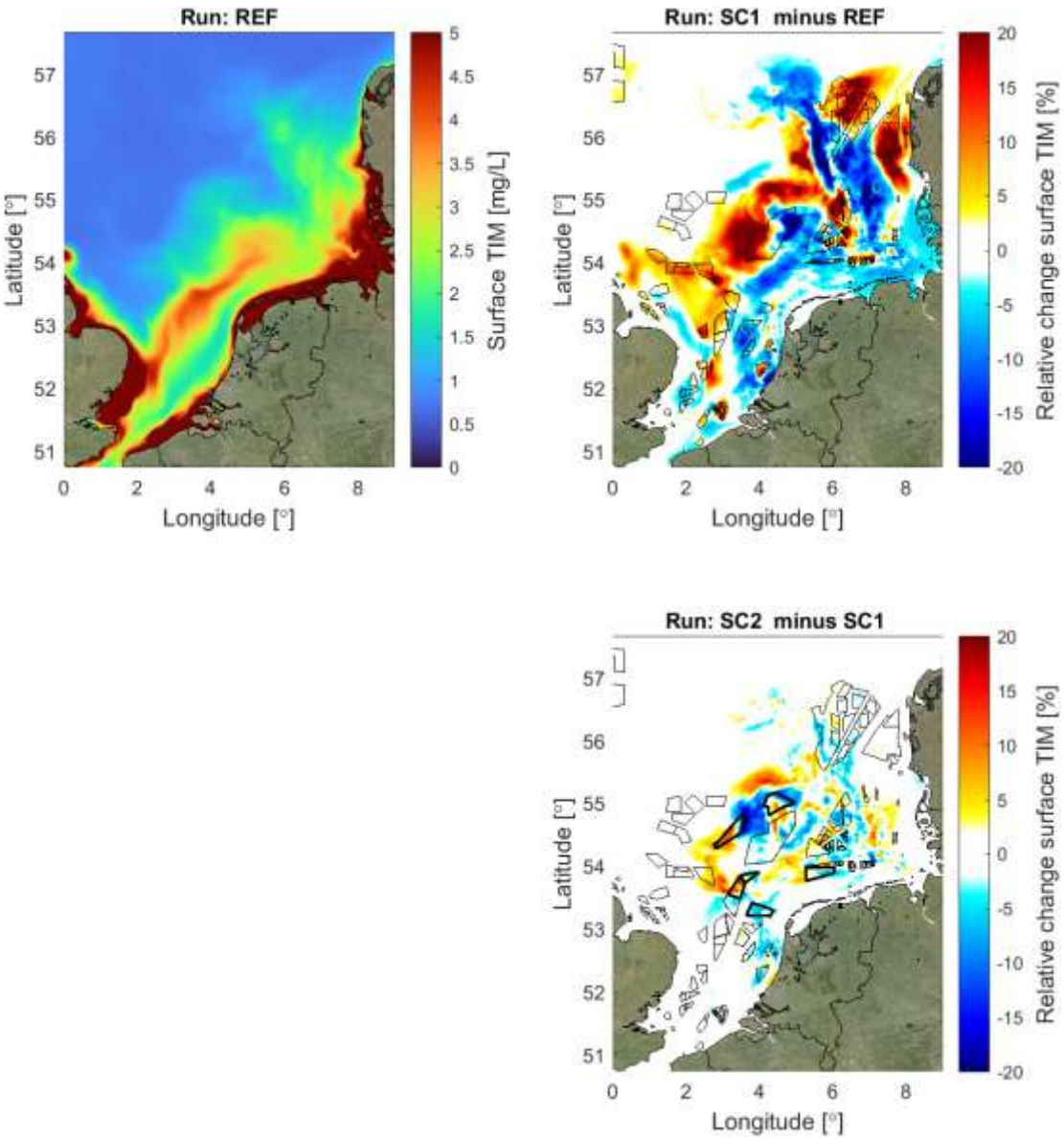

Figure 4.33 Change in surface total inorganic matter (TIM) for future wind farm scenarios 1 and 2, average of September-December 2007. Upper-left panel shows the average, surface TIM [mg/L] in the simulation without wind farms. Upper-right panel shows the change in surface TIM [%] when the wind farms of scenario 1 are added. Thin black contours indicate the wind farms in scenario 1. Bottom-right panel shows the change in surface TIM [%] for scenario 2 compared to scenario 1. The additional wind farms compared to scenario 1 are indicated with thick black contours.

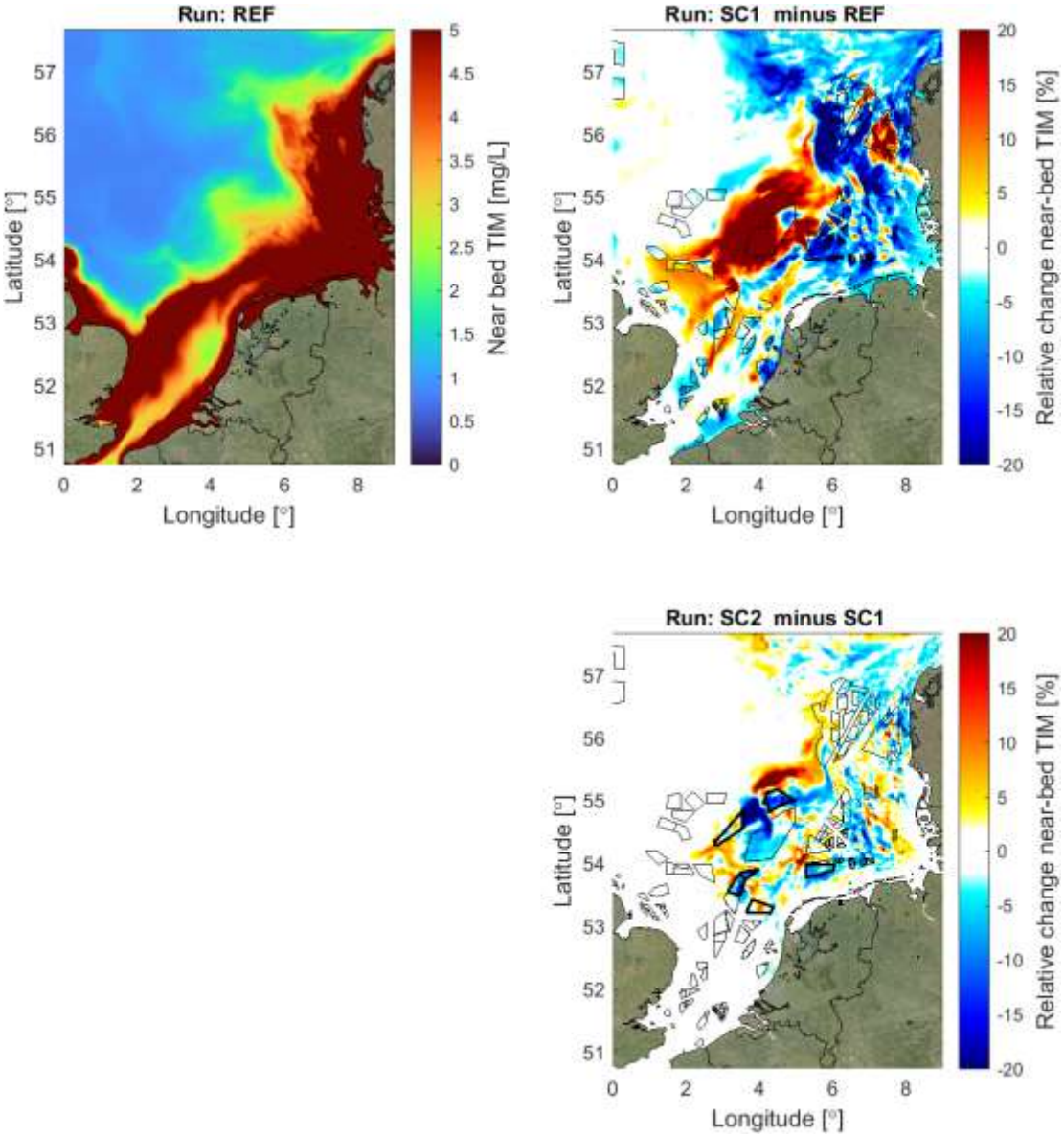

Figure 4.34 Change in near-bed total inorganic matter (TIM) for future wind farm scenarios 1 and 2, between March-May 2007. Upper-left panel shows the average, near-bed TIM [mg/L] in the simulation without wind farms. Upper-right panel shows the change in near-bed TIM [%] when the wind farms of scenario 1 are added. Thin black contours indicate the wind farms in scenario 1. Bottom-right panel shows the change in near-bed TIM [%] for scenario 2 compared to scenario 1. The additional wind farms compared to scenario 1 are indicated with thick black contours.

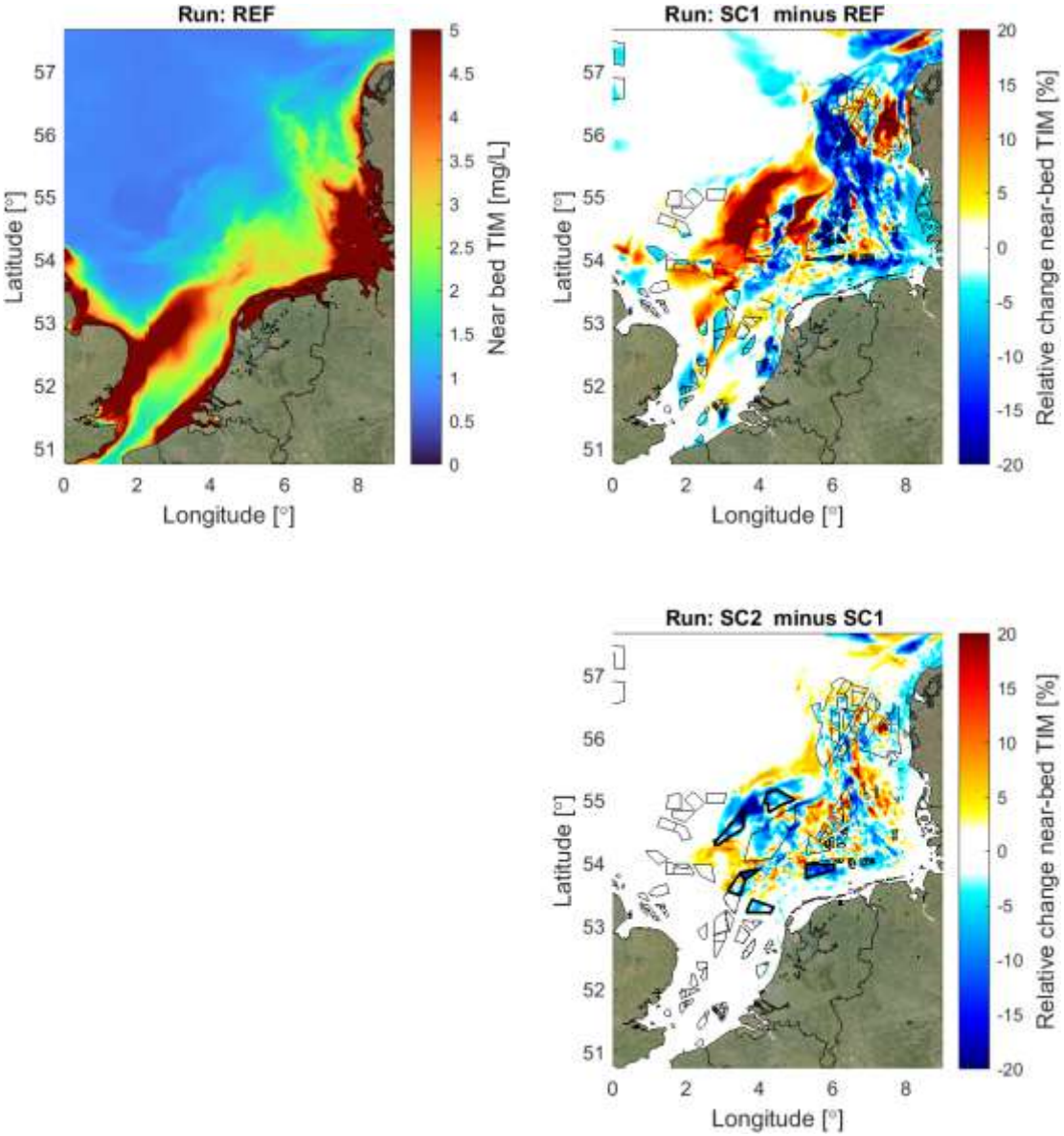

Figure 4.35 Change in near-bed total inorganic matter (TIM) for future wind farm scenarios 1 and 2, between June-August 2007. *Upper-left panel shows the average, near-bed TIM [mg/L] in the simulation without wind farms. Upper-right panel shows the change in near-bed TIM [%] when the wind farms of scenario 1 are added. Thin black contours indicate the wind farms in scenario 1. Bottom-right panel shows the change in near-bed TIM [%] for scenario 2 compared to scenario 1. The additional wind farms compared to scenario 1 are indicated with thick black contours.*

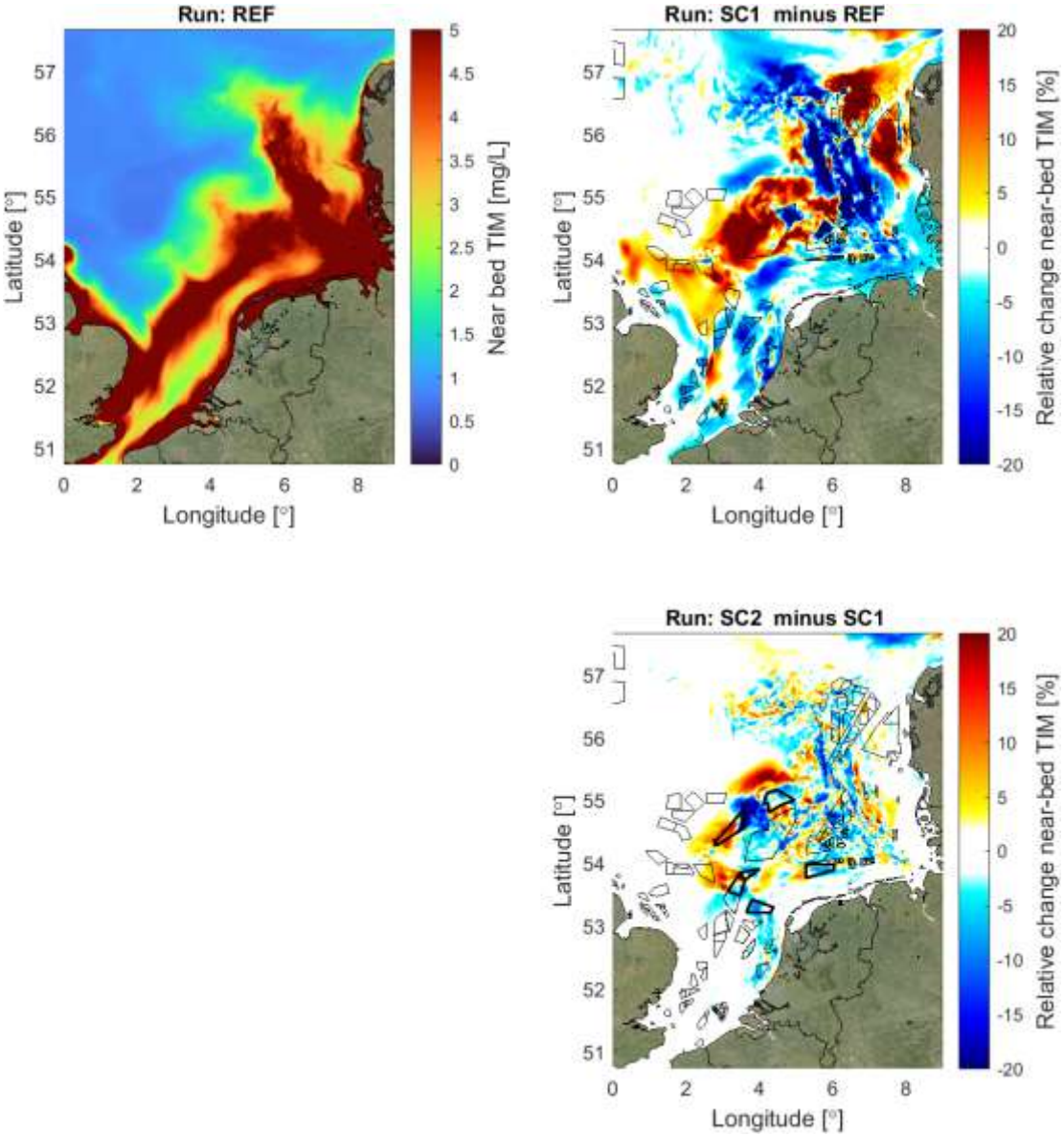

Figure 4.36 Change in near-bed total inorganic matter (TIM) for future wind farm scenarios 1 and 2, between September-December 2007. Upper-left panel shows the average, near-bed TIM [mg/L] in the simulation without wind farms. Upper-right panel shows the change in near-bed TIM [%] when the wind farms of scenario 1 are added. Thin black contours indicate the wind farms in scenario 1. Bottom-right panel shows the change in near-bed TIM [%] for scenario 2 compared to scenario 1. The additional wind farms compared to scenario 1 are indicated with thick black contours.

4.4.3 Discussion fine sediment results

Although results for the new OWF scenarios, using the further calibrated and validated fine sediment model are on details different from the original OWF2050 scenario, the type and order of magnitude impacts on SSC are similar.

Typically, computed impacts can be well understood qualitatively from changes in bed shear stress, mixing, residual flows etc., but quantitatively this is very difficult as these changes all interact and often work in opposite direction. For example, if bed shear stress decreases less sediment tends to be suspended in the water column, but if vertical mixing increases surface

SSC may still increase. Fortunately, the numerical model is available to compute the effects of all these changes and their interactions, and quantification of the overall net effect on SSC is still possible.

At the scale of the North Sea and averaged over time, concentration enhancing and concentration reducing effects of OWF partly cancel out. But at regional scales persistent changes occur, of which the reduction of SSC concentration and fluxes in the Dutch coastal zone is a remarkable one. A decrease of 5% (SSC) to 10% (mud flux at Callantsoog) is substantial, also compared to other human activities in this zone such as sand mining and maintenance dredging.

In the next section the consequences of these changes in SSC on ecology are discussed.

4.5 Ecological model

4.5.1 Effects of OWF on primary production and chlorophyll-a

In this section, the water quality results of Scenario 1 and Scenario 2 are presented. A quantitative comparison is made for both scenarios to the reference scenario without any offshore wind farms. This also allows a qualitative comparison of Scenario 1 with Scenario 2. Therefore, difference maps between scenarios and the reference situation (without OWFs) are plotted for yearly average phytoplankton primary production, integrated over the entire water column, and near-surface chlorophyll a concentrations. It must be noted than an increase/decrease in primary production does not necessarily manifest itself in an increase/decrease in near-surface chlorophyll-a. Primary production is indeed calculated as the net autotrophic organic carbon production by phytoplankton, based on temperature conditions, nutrient and light availability, while chlorophyll-a (proxy for phytoplankton biomass) is the resultant of phytoplankton primary production and phytoplankton mortality. Moreover, primary production results are integrated over the entire water column, while chlorophyll-a results are shown for the near-surface layer only.

Figure 4.37 shows the difference in yearly average primary production of scenario 1 (left) and scenario 2 (right) with the reference simulation. Because the OWFs in scenario 1 and scenario 2 coincide for a large part, their impact compared to the reference simulation is very similar. Both subfigures display a patchiness in primary production and difference in primary production varies with the different OWFs. Three OWF areas can be distinguished within both subfigures for primary production. Firstly, the OWFs off the east coast of Scotland, the OWFs off the coast of Zuid- and Noord Holland as well as the OWFs located in the German Bight show a distinct decrease in primary production within the OWFs and a distinct increase outside of the immediate boundaries of the OWFs. Secondly, search area 6/7 (large OWF located in the central Dutch North Sea) shows an increase in primary production within the windfarm. Lastly, the OWFs located off the west coast of Denmark show a distinct patchiness with increases and decreases in primary production that cannot be seen to that extent in the other OWFs. This coincides with the area where changes in residual currents are extremely variable in space as well. These effects of OWFs on primary production are significant (Figure 4.38), with local increases with respect to the scenario without OWFs of more than 40% (e.g. in search areas 6/7 and around OWFs from the German Bight and off the Scottish coast). In areas such as Borssele or the German Bight the presence of OWFs can lead to local decreases in yearly average primary production of 60% or more directly within the windfarms.

Figure 4.37 and Figure 4.38 can also be used to compare the difference between Scenario 1 and Scenario 2. Additional OWFs in the North of the Dutch EEZ lead to very little difference (very slight overall increase) in primary production between Scenario 1 and Scenario 2. Other

additional OWFs (in the western part of the Dutch EEZ and German Bight) lead to a decrease in primary production in Scenario 2 with the decrease being most pronounced in the German Bight.

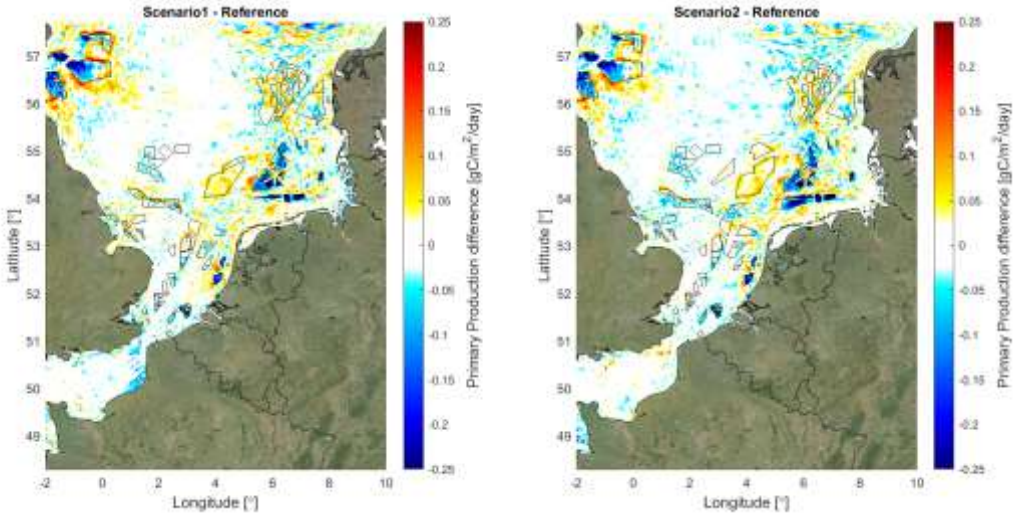

Figure 4.37 Absolute difference in the yearly average primary production simulated for scenario 1 (left) and scenario 2 (right) with respect to the "Reference" run.

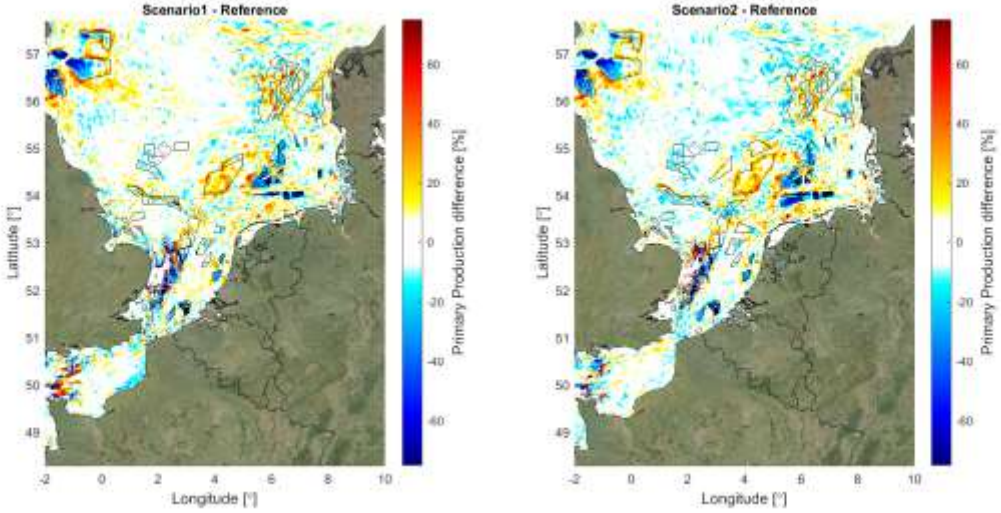

Figure 4.38 Relative difference in the yearly average primary production simulated for scenario 1 (left) and scenario 2 (right) with respect to the "Reference" run.

Figure 4.39 shows the difference in near-surface chlorophyll-a of scenario 1 (left) and scenario 2 (right) with the reference simulation. As illustrated for primary production, the impact of the scenarios compared to the reference simulation is not very different. Both subfigures display a patchiness in the differences in near-surface chlorophyll-a.

The OWFs off the east coast of Scotland as well as the OWFs off the coast of Zuid- and Noord Holland show a distinct decrease in near-surface chlorophyll-a within the OWFs and a distinct increase outside of the immediate boundaries of the OWFs. The increase in near-surface chlorophyll-a outside of the OWF is especially distinct for the OWF off the coast of Noord Holland. This coincides with the pattern seen for those OWFs in primary production. Similarly, while there was a clear increase in primary production in the search area 6/7, the same is true for near-surface chlorophyll-a. However, while all OWFs located in the German

Bight displayed a decrease in primary production, the same cannot be said for near-surface chlorophyll-a. The OWFs located near to the coast in the German Bight show a strong decrease in near-surface chlorophyll-a, while the OWFs located more in the central German Bight display a patchiness in the near-surface chlorophyll-a response compared to the reference simulation. This shows that the decrease in primary production is most likely mainly in the subsurface and deeper layers due to reduced light availability, while near-surface phytoplankton still grows in similar amounts than without OWFs near the surface. Lastly, The OWF off the coast of Denmark also show a less patchy response in near-surface chlorophyll-a than for primary production. The OWF close to the Danish coasts displays a clear increase in near-surface chlorophyll-a, while the OWFs located further away from the Danish coast display a decrease in chlorophyll-a. While absolute differences are very small for OWFs that are far offshore (these locations displaying low chlorophyll-a levels), the differences relative to the reference run are significant (Figure 4.40). For example, the presence of OWFs in search area 6/7 leads to local increases in simulated yearly average near-surface chlorophyll-a concentrations of ~20%, within and around the OWFs. In areas such as the Scottish coast and in the Southern German Bight, simulated near-surface chlorophyll-a within OWFs is 20-25% or more, lower than without OWFs, and displays sharp increases around the windfarms. Figure 4.39 can also be used to compare the difference in near-surface chlorophyll-a between Scenario 1 and Scenario 2. Similar to primary production, the additional OWFs north of search area 6/7 and search area 3 (southwest of search area 6/7, show hardly any difference in near-surface chlorophyll-a between Scenario 1 and Scenario 2. The additional OWFs search area 4 and the section between Lagelander-North and search area 3 show a decrease of primary production in Scenario 2 with the decrease being most pronounced in Search area 4, located in the German Bight. The response of those OWFs in terms of near-surface chlorophyll-a coincides with the response of primary production. The additional OWF 3 displays an increase in near-surface chlorophyll-a which is not displayed in the primary production.

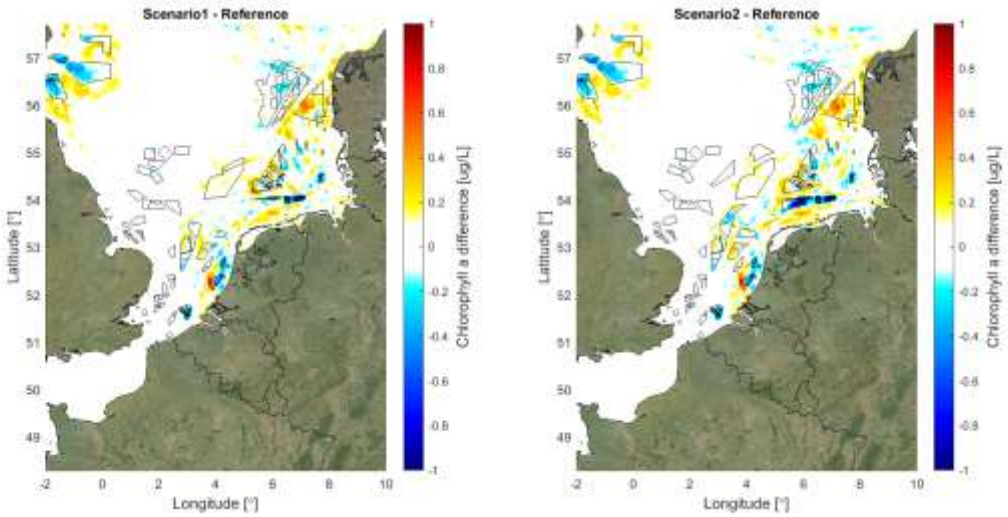

Figure 4.39 Absolute difference in the yearly average near-surface chlorophyll-a simulated for scenario 1 (left) and scenario 2 (right) with respect to the "Reference" run.

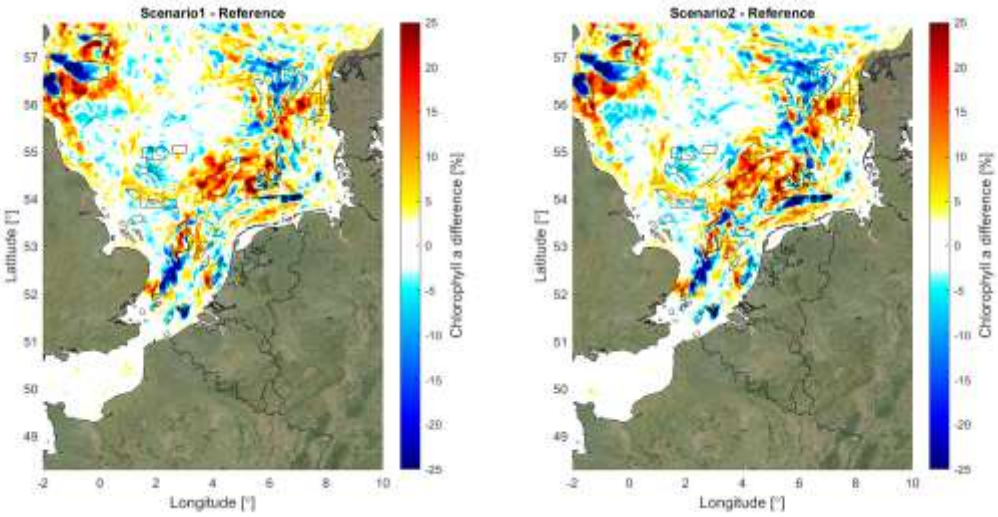

Figure 4.40 Relative difference in the yearly average near-surface chlorophyll-a simulated for scenario 1 (left) and scenario 2 (right) with respect to the "Reference" run.

4.5.2 Effects of mussel growth on primary production and chlorophyll-a

In this section, the additional effect of mussel growth on pillars on the water quality is presented. A quantitative comparison is made for both scenarios with and without mussel growth. It must be noted that for both scenarios the chosen colour scale is very small (25 times smaller than previous plots for primary production, 10 times smaller for chlorophyll-a). This illustrates that the impact of mussel growth on primary production and near-surface chlorophyll-a is very small. Both scenario 1 and 2 show only very slight decreases in primary production (Figure 4.41) and near-surface chlorophyll-a due to mussel growth (Figure 4.42).

The model results show a decrease in yearly average near-surface chlorophyll-a concentrations in OWFs in the Rhine ROFI and near the Danish coast. However, according to present results, the effects of mussel growth on pillars within OWFs on yearly average primary production and chlorophyll-a concentrations are at least one order of magnitude smaller than the effects resulting from changes in hydrodynamics (e.g. residual currents, vertical mixing) and sediment dynamics.

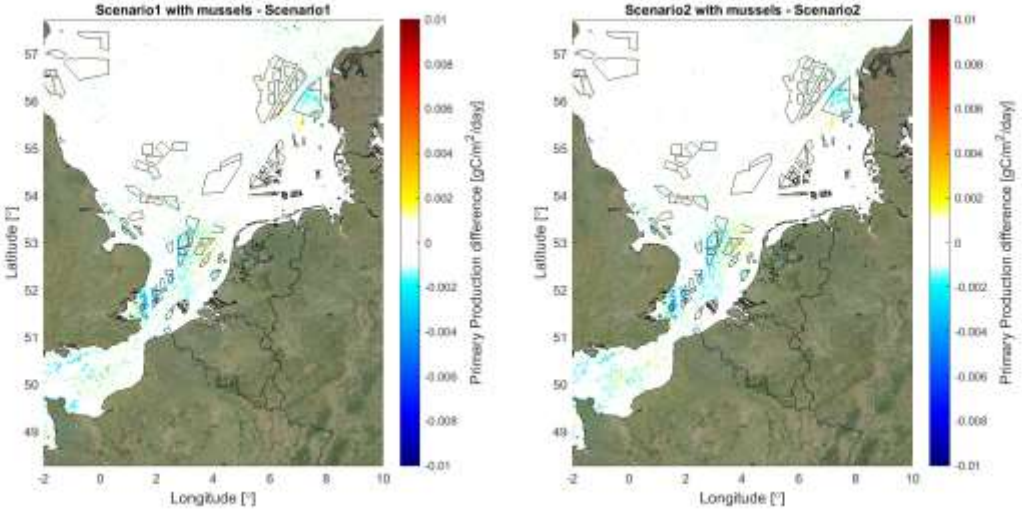

Figure 4.41 Absolute difference in the yearly average primary production simulated for scenario 1, with and without mussel growth on OWF pillars (left) and scenario 2, with and without mussel growth on OWF pillars (right).

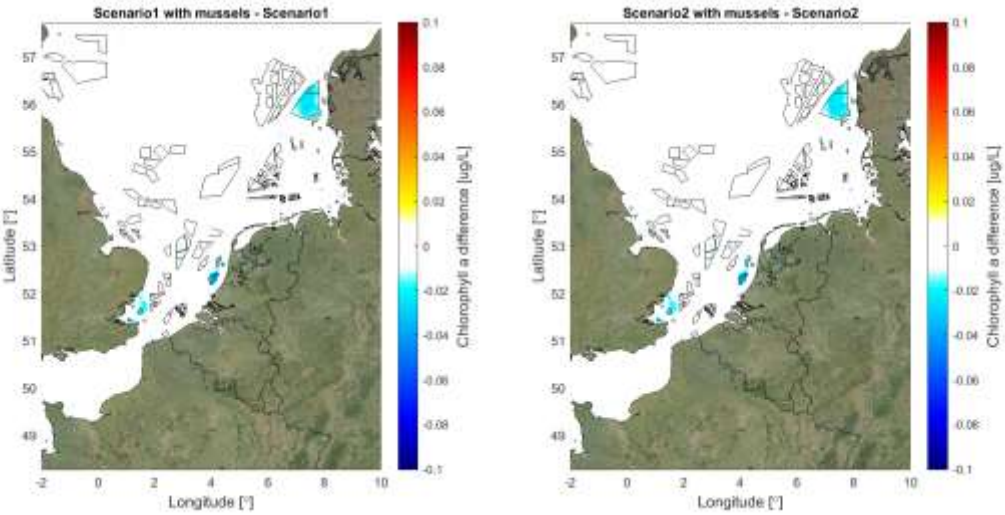

Figure 4.42 Absolute difference in the yearly average near-surface chlorophyll-a concentrations simulated for scenario 1, with and without mussel growth on OWF pillars (left) and scenario 2, with and without mussel growth on OWF pillars (right).

4.5.3 Discussion Ecological model

4.5.3.1 Future model improvements

Improvements in the coupled hydrodynamic-sediment-ecological model
We identified different steps to be addressed in a next stage to improve the coupled sediment-ecological model, listed here as bullet points.

- A shift from a σ-layer vertical representation to a z-σ-layer representation will improve the representation of vertical mixing at the offshore boundaries and therefore the representation of nutrients in-flowing into to the study area.
- The settling of particulate organic matter should be simulated using two independent processes, sedimentation and re-suspension, in a way consistent with the representation of inorganic particulate matter dynamics. This is not possible with the Delft3D FM release used in the present report but was made possible in a newer version. This will allow for a better representation of spatial differences in nutrient accumulation, re-mobilization or burial. It will also make it easier to include possible feedbacks between sediment and water quality processes (e.g. flocculation) if it is judged relevant in the future.
- After these two steps are carried out, the coupled model should be validated, and if needed, re-calibrated. One point of attention should be to check if the changes in phytoplankton parameterization made in the present report are consistent with parameter values from the literature and allow for a good representation of phytoplankton dynamics over multiple years (here these were adjusted to reproduce 2007 dynamics). Another point of attention should be the simulation of O_2 dynamics, more specifically identifying the reasons for the underestimation of near-surface concentrations during the growing season.

Representation of mussels and other grazers
The effect of the colonization of OWF pillars by grazing communities (e.g. blue mussels) should also be further investigated and validated. In (Van Kessel et al. 2022) and in the present report, first steps have been made to represent the growth of mussels near the surface, using DEB modelling. The parameterization is however initially based on the ones used to simulate blue mussel bed communities from the Oosterschelde, where environmental

conditions are very different from the open North Sea and adjusted to simulate a stable average yearly biomass at the FINO1 location (assuming observed biomasses in 2005, 2006 and 2007 by Krone et al. (2013) correspond to an inter-annual equilibrium). It can however be expected that near-surface mussel communities behave differently in OWFs located in further offshore, stratified areas than in FINO1.

Recently, (Stechele et al. 2022) published a paper on individual mussel growth in Belgian offshore wind farms using a DEB module. In doing so, they updated DEB parameters for blue mussels to fit the offshore environment of the Belgian North Sea. Currently, the DEB mussel parameters for D-Water Quality are based on parameterization of mussel cultivation in the Oosterschelde. Thus, an important step in the calibration of mussel growth on pillars in offshore environments is to compare the DEB parameters from (Stechele et al. 2022) with the current D-Water Quality set of mussel DEB parameters and if needed replacing the current set of mussel DEB parameters.

Mussels growing on pillars have a limited availability of space. They are constrained by the circumference of the pillar which will allow only a limited number of individuals. Once the space is occupied then the mussels will not be able to spread as would be the case on the seabed. The constraint in space may need to be taken into account for example by limiting the maximum biomass density that can grow on a pillar or by simulating maximum number of mussel individuals. Within the model and given the model resolution, the fact that the mussels are settled on pillars also means that only a fraction of the food available within the grid cell actually reaches them. It also means that, even if at the resolution of a grid cell food is still available, the very localized high density of mussels might deplete the food reaching the vicinity of the pillars. A method should be defined to better represent the food availability in the vicinity of the pillars.

At the moment, we assume that the mussels colonize the top 5m of OWF pillars. In reality, the depth at which mussels can grow might also differ depending on the conditions at the different OWFs. 1D-V models could be setup for different OWFs to check if the maximum depth at which the mussels grow can be explained by food availability alone, or if being able to simulate this maximum depth would require to account for the effect of competition with other colonizing species.
Parallel to this, it is necessary to conduct a literature study on growth of mussels in different environments to attempt to broaden our understanding of the different between windfarm locations.

Finally, besides mussel communities, in the next stage of the project, the addition of zooplankton in the model will allow for quantifying the contributions of attached grazers and pelagic grazers in carbon transfers through the marine food chain, and their changes due to the presence of OWFs.

Further model validation
At the moment, the modelling work has focused mostly on the simulation of individual years (mostly 2007, but also 2017). For a more thorough validation of the simulated processes, their set-up and parameterization, it would be valuable to assess more years, including ones with more extreme conditions. This would allow to better evaluate the model's reliability for the simulation of changes in water quality indicators/variables for different conditions. When data becomes available, the ecological effects of OWFs should also be validated.

4.5.3.2 Effect of offshore wind upscaling on North Sea water quality and ecology

The effect of OWFs on the ambient water quality and ecology seems to depend on their location and not on the size of the OWF. Also, effects of OWFs on hydrodynamics and sediment dynamics clearly translate into effect on water quality and ecology.
Turbulent, shallow locations (such as off the coast of Zuid- and Noord Holland and the German Bight) show a decrease in primary production which is most likely due to the additional light limitation caused by the increase in resuspension as a result of increased turbulent kinetic energy along the pillars. In contrast, stratified, deeper locations (such as Search Area 6/7) show an increase in primary production which is most likely caused by the additional nutrient availability as a result of the earlier breakdown of stratification caused by the increased turbulent kinetic energy through the pillars and reduction of wind speed due to the wind turbines. This is despite the fact that in this area the annual average concentration of fine sediment in the top layer of the water is substantially increased (see Figure 4.27). The explanation for this is that the increased turbulence and subsequent reduction by the monopiles in this area is strong enough to mix more nutrients into the photic zone, but not strong enough to mix additional fine sediment into the top layers. The increased fine sediment concentration in the top layer is caused by a substantial increase during the mixed period (autumn, winter, early spring). As soon as stratification sets in in early April, the concentrations of fine sediment in the top layers drop to the same concentration as in the reference scenario. As the timing of the spring bloom is linked to the onset of stratification, it appears that the growing period of the algae is not affected by increased fine sediment (Figure 4.43).

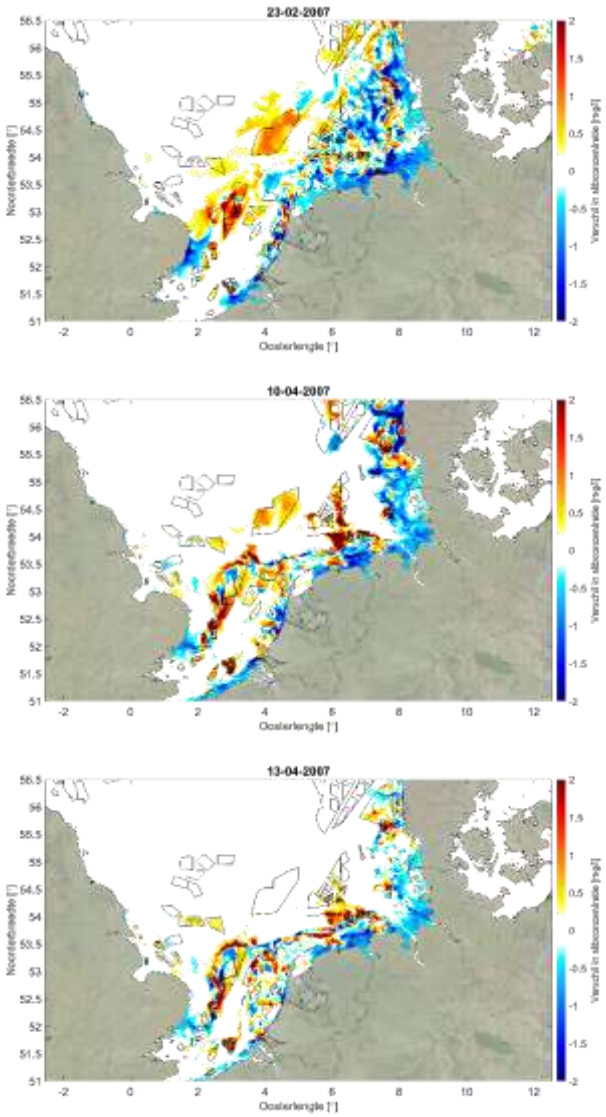

Figure 4.43 3 snapshots (daily average differences in fine sediment concentrations) of scenario 1 in winter (February, top), and in early spring, just before (middle) and just after (bottom) onset of stratification. The bottom situation (no difference between scenario 1 and reference lasts all through summer until break-up of stratification

It appears that in other areas such as the German Bight, where we see also a reduction in stratification, the local stratification is not strong enough to keep any additional sediment in the near-bed layers. The net effect on primary production in those areas is negative.

Even though the representation of mussel growth on pillars should be refined, according to present results, the effects of mussel growth on pillars within OWFs on yearly average primary production and chlorophyll-a concentrations are at least one order of magnitude smaller than the effects resulting from changes in hydrodynamics (e.g. residual currents, vertical mixing) and sediment dynamics.

A decrease in primary production does not always translate into a decrease in chlorophyll-a. Different species have different chlorophyll-a to carbon ratios and species can also adjust their chlorophyll content depending on the light availability. Thus, a decrease in primary

production caused by e.g. increased turbidity does not necessarily result in a decrease in chlorophyll-a, since light-limited communities typically have higher chlorophyll-a to carbon ratios. In the future, it would be interesting to extract those data to test that hypothesis. Consequently, the use of chlorophyll-a as a proxy for biomass should be re-evaluated. Depending on the needs for research on carbon transfers to higher trophic levels, primary production as well as carbon biomass might be more useful indicators to study the effects of OWFs.

Future scenario analysis should also investigate changes in temporal patterns due to the presence of OWFs. The increase in sediment concentrations might for example lead to a shift in the timing of the spring bloom, with optimal light conditions occurring later in the year, as was shown by Zijl et al. (2022). The timing of the spring bloom is also an important factor for development of species higher up in the food chain.

5 General conclusions and steps forward

5.1 Model performance

The modelling suite as a whole has been much improved in comparison to the earlier studies (Zijl et al. 2021, Van Kessel et al. 2022). The model can now be run completely coupled. This is due to the fact that certain technical issues have been solved, but fundamentally because the bias in the SPM concentrations has been substantially reduced and validation with observations indicates that these are in the right order of magnitude. However, there are still some questions regarding the parameterisation of SPM in the model and its suitability to correctly predict the impact of the turbines on dynamics. The model results show a strong non-linearity between increase of bottom shear stress (a few percent increase) and increases in SPM concentrations (tens of percent). An increase in average bottom shear stress can be inferred from the mass balance of kinetic energy and is easily explicable (flow energy is dissipated in turbulent energy due to the wakes). However, the increased turbulence is localized in the wakes behind the pillars and is not uniform over the area of the OWFs (in nature). Given the strong non-linearity as presently observed, it would be sensible to look at the smaller-scale processes within wind farms in much more detail.

The other issue that has been improved since Van Kessel et al. (2022) is the growth rate of the mussels. In the first trials of having mussels growing on the turbine poles the mussels were not restricted in their growth and ended up with an unrealistically high filtration rate. Recalibration of some of the DEB parameters significantly lowered their impact. However, the DEB model still requires further investigation. The model is currently forced with observed densities on turbines in the German bight. This may not be representative for all areas

In the currently used model we still applied z-layers throughout the domain. Tests in other projects have already indicated that the use of z-σ layers can significantly improve the fluxes of water, SPM and nutrients through the channel and via the northern links to the Atlantic Ocean. This is caused by the fact that using only z-layers in the deeper waters of the Atlantic results in very ‘thick’ layers that do not accurately represent the pycnocline (the layer where the density gradient is greatest) in the Atlantic. This has repercussions for the transport of water, SPM and solutes into the North Sea.

There is also work ongoing, investigating the impact of the wakes of the wind farms. Technical advances have been made allowing a coupling between DSCM-FM and the KNMI model “HARMONIE”, through which also impacts of OWFs on the larger scale wind fields can be calculated and in the near future a first test will be carried out on HARMONIE scenarios carried out in the WINS50 project (https://wins50.nl/), to assess the impact on waves and other ecosystem effects. In the present study we include a reduction of wind within the farms of 10%. This is for current wind farms likely a right order of magnitude, but for future wind farms which may be larger or have different energy densities this may differ. At present no wakes behind wind farms are considered. We currently do not know how much impact this may have. It is certainly dependent on the atmospheric stability. Wakes in a stably stratified atmosphere dissipate much less quickly than in a well-mixed, turbulent atmosphere (Hasager et al. 2015).

5.2 Effects of wind farms

The major effects of wind farms that we have identified earlier (changes in nutrient availability in the top layers of water as well as impacts of changes in SPM dynamics on light availability) are still considered valid. The results show that effects are spatially variable and appear to relate mostly to two factors: effects through SPM and effects of changes in vertical mixing. OWFs extract kinetic energy from the flow and transform this into turbulence. This results in a small but significant large-scale change in flow characteristics that works cumulatively throughout the Lagrangian path of the water – hence slowly increasing in importance from south west to north east. The other effect is enhanced turbulence within the OWFs, resulting in enhanced SPM concentrations and in enhanced nutrient mixing. Depending on stratification, one of these two will be dominant. This has impacts on primary production throughout the North Sea. In deeper, seasonally stratified areas the effect of more mixing and hence more nutrients being available is dominant. In these areas spring blooms are delayed due to the fact that the onset of the spring bloom is linked to the onset of stratification (Sharples et al. 2006). Also, an increase of SPM and hence a decrease in light availability can have such an effect (Wilson and Heath 2019). In the previous study we saw that particularly in the German Bight the delay in spring bloom was most pronounced due to the interactive effect of reduced stratification and increased SPM in the top layers. How this works out in the current scenarios still needs further investigation. Both processes occur, but the impact of increased SPM in the top layers appears to be more dominant than in the previous studies. Possibly a third effect is that enhancing mixing in the OWFs, together with a local restriction on primary production due to light, leads to more nutrients and more production downstream of the OWFs. This is a compensating mechanism leading to less severe North Sea-averaged production. Due to the importance of SPM dynamics in the North Sea and the relative balance with the effects of changes in nutrient dynamics due to increased mixing, it is very important to get more insight into the fundamental processes governing SPM (through observations as well as through more small-scale models).

The current study also confirmed the impact of the presence of wind farms on the along coast transport of fine sediment. This appears to be determined by the presence of wind farms throughout the southern part of the North Sea, not just the two farms that happen to be closest to the coast. The largest impact is on the Callantsoog transect, but the most relevant is the transport across the Texel transect, which is directly indicative of the import of fine sediment into the Wadden Sea. This may need further attention in the future, particularly in cumulation with effects on sandmining and coastal defence, which may have similar impacts.

The impact of the presence of large amounts of mussels in the upper layers of the water column still needs further investigation. Mussels remove algal biomass by filtration, but the quick remineralisation of nutrients due to digestion may also boost local primary production. However, the latter can only take place if 1) nutrients are limiting primary production and 2) mussels do not ‘over graze’ the system, i.e. remove algae at a faster rate than primary production can replenish (Troost et al. 2010, Filgueira et al. 2015). The potential biomass is clearly sufficient to have a moderate effect on algae, but the net effect (also taking the impact of zooplankton grazing more explicitly into account) needs further investigation.

5.3 Spatial differences

Based on the new scenarios we do see some differences with the earlier upscaling scenario (Zijl et al. 2021). However, the spatial delineation of areas in the North Sea reacting differently to the presence of windfarms remains roughly the same as indicated in Zijl et al (2021) and Van Duren et al (2021). The main differences that came to light in this study are the relative magnitude of the impact of increased mixing (boosting primary production in areas that show stable stratification in summer) and increased SPM concentrations in the top

of the water layers. The latter appears to be relatively more important, indicating a relatively stronger reduction of primary production in the Holland Coast and in the German Bight than was modelled before. This appears to be a consequence of the fact that in the earlier models we could not couple the SPM model directly to the ecological model. We applied an SPM field from an older (well calibrated) model and simulated the impact of the wind farms with a proportional increase or decrease, as resulted from the SPM model.

5.4 Future work

5.4.1 Model improvement and processes to be added

Future work will be done with the new z-σ parameterisation of the depth layers in the DCSM-FM model. We already know this is likely to improve validation of nutrient distribution and hence primary production. Current work on the assessment of the impact of wind wakes behind wind farms will continue.

We also have still limited validation of the impacts of the wind farms. As identified in section 5.1, this is urgently needed. Recently in a parallel NWA project measurement data on changes in currents and mixing have been collected in a Belgian wind farm and also more data are becoming available from other sites. Further validation, particularly on farm effects will be taken up in future work. At present we have to rely on data collected in wind farms abroad, which is not desirable. A dedicated measurement programme should be part of the multi-year planning of Wozep (which will be within the MONS programme (Monitoring-Onderzoek-Natuurversterking-Soortbescherming, https://www.noordzeeloket.nl/omgeving/noordzeeoverleg/mons-onderzoeks-monitoringprogramma/)), as Wozep is going to be an integral part of this research and monitoring programme.

5.4.2 Coupling with the top-down approach

One of the ultimate questions in this project is how changes in the food web caused by bottom-up processes ultimately have an impact on top predators, such as birds, fish and marine mammals, etc.. This requires improving our ability to assess this is to gain insight into how the ratio in carbon fluxes throughout the food web may change between benthic food webs and pelagic food webs. A first step has been taken within the Wozep project last year to assess the efficiency transfer of energy between trophic levels in the food web and the differences between benthic and pelagic food webs (Van der Meer and Van de Wolfshaar 2023). Many seabirds that feed on fish tend to feed on fish species that depend on zooplankton as a food source. Due to the changes in primary production in combination with the increase in biomass of benthic filter feeders on the turbine supports, this ratio may change. Although essentially benthic, the mussels on turbines tend to grow in the upper layers of the water column (Degraer et al. 2013, Slavik et al. 2018), where primary production takes place, rather than on the seabed, where filter feeders depend on food mixed down through water layers. In the current model we can model the growth of shellfish explicitly, but zooplankton is not currently explicitly modelled in our current set-up. In 2023 we will start developing DEB models for one or more selected zooplankton species and have these ‘growing’ in the model in direct competition with each other. Although this is still an oversimplification of the complex food web interactions, it can give a first indication if absolute carbon fluxes and ratios are likely to change.

A big missing link in the bottom-up top-down approach is currently fish. It is not feasible to include higher trophic levels such as fish into the D3D modelling framework. However, using the knowledge of potential orders of magnitude change in food availability there are individual based modelling systems (IBMs) for fish available that can be used to investigate potential shifts in certain species of interest. One such system is OSMOSE (https://osmose-

model.org/). This model assumes opportunistic predation based on spatial co-occurrence and size adequacy between a predator and its prey. It represents fish individuals grouped into schools, which are characterized by their size, weight, age, taxonomy and geographical location (2D model), and which undergo major processes of fish life cycles (Van de Wolfshaar et al. 2021, Hill Cruz et al. 2022). This model is currently proposed as a tool to get more insight in how changes at the base of the food web propagate through the system to higher trophic levels.

6 References

Agatova, A. I., N. M. Lapina, and N. I. Torgunova. 2008. Organic Matter of the North Atlantic. Oceanography 48(2):182-195.

Cronin, K., R. Plieger, S. Gaytan Aguilar, J. R. de Lima Rego, and M. Blaas. 2013. MoS2-II: Deterministic Model Calibration: Updates of the ZUNO-DD Hydrodynamic and SPM model. Deltares, Delft.

Degraer, S., R. Brabant, and B. Rumes. 2013. Environmental impacts of offshore wind farms in the Belgian part of the North Sea: Learning from the past to optimise future monitoring programmes., Royal Belgian Institute of Natural Sciences, Brussels.

Deltares. 2021. Demonstration of the updated Bays Eutrophication Model. Boston: Massachusetts Water Resources Authority. 2021-02.

Filgueira, R., L. A. Comeau, T. Guyondet, C. W. McKindsey, and C. J. Byron. 2015. Modelling Carrying Capacity of Bivalve Aquaculture: A Review of Definitions and Methods. Encyclopedia of Sustainability Science and Technology. Springer, New York.

Gwee Simin, R. 2018. Modelling primary production in the North Sea: Applying a light-dependent model on MERIS images between 2002-2012. Utrecht University MSc thesis.

Hasager, C. B., P. Vincent, R. Husson, A. Mouche, M. Badger, A. Peña, P. Volker, J. Badger, A. Di Bella, A. Palomares, E. Cantero, and P. M. F. Correia. 2015. Comparing satellite SAR and wind farm wake models. Institute of Physics Publishing.

Hendriks, E., U. Braeckman, E. Zing Ong, J. Dujardin, J. Vanaverbeke, P. Hablützel, M. Perneel, and K. Langedock. 2022. NWA windfarms measurement campaign. Unpublished data set.

Hill Cruz, M., I. Frenger, J. Getzlaff, I. Kriest, T. Xue, and Y.-J. Shin. 2022. Understanding the drivers of fish variability in an end-to-end model of the Northern Humboldt Current System. Ecological Modelling **472**:110097.

Krone, R., L. Gutow, T. J. Joschko, and A. Schröder. 2013. Epifauna dynamics at an offshore foundation – Implications of future wind power farming in the North Sea. Marine Environmental Research 85:1-12.

Letscher, R. T., J. K. Moore, Y.-C. Teng, and F. Primeau. 2015. Variable C : N : P stoichiometry of dissolved organic matter cycling. Biogeosciences 12:209-221.

Seitzinger, S. P., J. A. Harrison, E. Dumont, A. H. W. Beusen, and A. F. Bouwman. 2005. Sources and delivery of carbon, nitrogen, and phosphorus to the coastal zone: An overview of Global Nutrient Export fromWatersheds (NEWS) models and their application. Global Biogeochemical Cycles 19:GB4S01.

Sharples, J., O. N. Ross, B. E. Scott, S. P. R. Greenstreet, and H. Fraser. 2006. Inter-annual variability in the timing of stratification and the spring bloom in the North-western North Sea. Continental Shelf Research **26**:733-751.

Slavik, K., C. Lemmen, W. Zhang, O. Kerimoglu, K. K., and K. W. Wirtz. 2018. The large scale impact of offshore windfarm structures on pelagic primary production in the southern North Sea. Hydrobiologia **in press**.

Stechele, B., D. van der Zande, A. Alvera-Azcárate, D. Delbare, G. Lacroix, and N. Nevejan. 2022. Biological site suitability for exposed self-regulating cultivation of blue mussel (Mytilus edulis): A Belgian case study. Aquaculture Engineering 98:102264.

Swart, D. H. 1974. Offshore sediment transport and equilibrium beach profiles. Technical University of Delft, Delft.

Troost, T. A., J. W. M. Wijsman, S. Saraiva, and V. Freitas. 2010. Modelling shellfish growth with dynamic energy budget models: An application for cockles and mussels in the Oosterschelde (southwest Netherlands). Philosophical Transactions of the Royal Society B: Biological Sciences **365**:3567-3577.

Van de Wolfshaar, K. E., U. Daewel, S. S. Hjøllo, T. A. Troost, M. Kreus, J. Pätsch, R. Ji, and M. Maar. 2021. Sensitivity of the fish community to different prey fields and importance of spatial-seasonal patterns. Marine Ecology Progress Series **680**:79-95.

Van der Meer, J., and G. Aarts. 2021. Individual-based modelling of seabird and marine mammal populations. C002/21, Wageningen Marine Research, IJmuiden.

Van der Meer, J., and K. E. Van de Wolfshaar. 2023. Ecological efficiency differences between benthic and pelagic food chains. Wageningen Marine Research, IJmuiden.

Van Duren, L. A., F. Zijl, V. T. M. van Zelst, L. M. Vilmin, J. Van der Meer, G. M. Aarts, J. Van der Molen, K. Soetaert, and A. W. Minns. 2021. Ecosystem effects of large upscaling of offshore wind on the North Sea - Synthesis report. 11203731-004-ZKS-0010, Deltares, Delft.

Van Kessel, T., V. T. M. van Zelst, J. Hanssen, L. M. Vilmin, and L. A. van Duren. 2022. Environmental effects of large-scale implementation of offshore wind farms. Further analyses. . 11208071-001-ZKS-0006, Deltares, Delft.

Van Leeuwen, S., P. Tett, D. Mills, and J. van der Molen. 2015. Stratified and nonstratified areas in the North Sea: Long-term variability and biological and policy implications. J. Geophys. Res. **120**:4670-4686.

Vroom, J., R. van Weerdenburg, B. Smits, and P. Herman. 2020. Modellering slibdynamiek voor de Waddenzee: Kalibratie voor KRW slib. Deltares, Delft.

Wilson, R. J., and M. R. Heath. 2019. Increasing turbidity in the North Sea during the 20th century due to changing wave climate. Ocean Science **15**:1615-1625.

Zijl, F., and S. C. Laan. 2022. Model results of effects of Offshore Wind Farms for MSFD; OWF 2024. 11208613-002-ZKS-0001, Deltares, Delft.

Zijl, F., S. C. Laan, A. Emmanouil, V. T. M. van Zelst, T. Van Kessel, L. M. Vilmin, and L. A. Van Duren. 2021. Potential ecosystem effects of large upscaling of offshore wind in the North Sea. Final report model scenarios. 11203731-004-ZKS-0015, Deltares, Delft.

Deltares is een onafhankelijk kennisinstituut voor toegepast onderzoek op het gebied van water en ondergrond. Wereldwijd werken we aan slimme oplossingen voor mens, milieu en maatschappij.

Deltares

www.deltares.nl